

ACOUSTIC FATIGUE PROCEDURE VALIDATION AND APPLICATION ON
CAVITY WALL

A THESIS SUBMITTED TO
THE GRADUATE SCHOOL OF NATURAL AND APPLIED SCIENCES
OF
MIDDLE EAST TECHNICAL UNIVERSITY

BY

ZEYNEP KÜDEN

IN PARTIAL FULFILLMENT OF THE REQUIREMENTS
FOR
THE DEGREE OF MASTER OF SCIENCE
IN
MECHANICAL ENGINEERING

SEPTEMBER 2019

Approval of the thesis:

**ACOUSTIC FATIGUE PROCEDURE VALIDATION AND APPLICATION
ON CAVITY WALL**

submitted by **ZEYNEP KÜDEN** in partial fulfillment of the requirements for the degree of **Master of Science in Mechanical Engineering Department, Middle East Technical University** by,

Prof. Dr. Halil Kalıpçılar
Dean, Graduate School of **Natural and Applied Sciences**

Prof. Dr. M.A Sahir Arıkan
Head of Department, **Mechanical Engineering**

Prof. Dr. Mehmet Çalışkan
Supervisor, **Mechanical Engineering, METU**

Examining Committee Members:

Assoc. Prof. Dr. M. Bülent Özer
Mechanical Engineering, METU

Prof. Dr. Mehmet Çalışkan
Mechanical Engineering, METU

Prof. Dr. Yusuf Özyörük
Aerospace Engineering, METU

Assoc. Prof. Dr. M. Metin Yavuz
Mechanical Engineering, METU

Prof. Dr. K. Melih Güleren
Aeronautics and Astronautics, Eskişehir Technical University

Date: 02.09.2019

I hereby declare that all information in this document has been obtained and presented in accordance with academic rules and ethical conduct. I also declare that, as required by these rules and conduct, I have fully cited and referenced all material and results that are not original to this work.

Name, Surname: Zeynep Kden

Signature:

ABSTRACT

ACOUSTIC FATIGUE PROCEDURE VALIDATION AND APPLICATION ON CAVITY WALL

Küden, Zeynep
Master of Science, Mechanical Engineering
Supervisor: Prof. Dr. Mehmet Çalışkan

September 2019, 123 pages

Acoustic loading formed due to boundary layer fluctuation, engine efflux and separated aerodynamic flow cause vibration that may result in fatigue failure of the structure. The subject of this thesis deals with the analytical acoustic fatigue procedure composition and validation in addition to critical wall stress analysis of representative weapon bay. It is aimed to feed the design process of the projects during its preliminary stages from structural point of view.

The thesis can be discussed into two section. Firstly, analytical procedure on acoustic fatigue is composed by Engineering Science Data Unit documents. Verification is achieved via Finite Element Method by assuming single degree of freedom theory; since, fatigue damage is usually dominated by one mode, although acoustically induced vibration usually consists of several response modes. Analytical method covers the extraction of dynamic characteristics, response under unit loading, acoustic loading generation and dynamic stress response of the simple-geometry structures. Obtained stress levels are used to predict endurance life of the structure with simplified equations. Secondly, critical wall stress response analysis of cavity shape structure, represents weapon bay of an aircraft, with different boundary conditions is carried out. These boundary conditions arise from different housing cases of the internal members of the aircraft. Effects of changes in the internal rib structures' location on the

structural response is investigated for different Mach numbers and controlling methods, spoiler and swept rear wall alike, applied to reduce the pressure fluctuation generated due to the flow over cavity.

Keywords: Acoustic Fatigue, Cavity Acoustics, Mile's Equation, Aerodynamic Noise, Weapon's Bay

ÖZ

AKUSTİK YORULMA PROSEDÜRÜ DOĞRULAMASI VE KAVİTE DUVARI UYGULAMASI

Küden, Zeynep
Yüksek Lisans, Makina Mühendisliği
Tez Danışmanı: Prof. Dr. Mehmet Çalışkan

Eylül 2019, 123 sayfa

Sınır tabaka dalgalanmaları, motor ve ayrık akış gibi gürültü kaynaklarının yarattığı akustik yük yapılar üzerinde titreşime ve buna bağlı olarak yorulma hasarlarına neden olabilir. Bu tez çalışması akustik yorulma analitik prosedürünün çıkarılması ve doğrulanması ile birlikte temsili silah yuvası kritik duvar analizlerini kapsamaktadır. Tasarım aşamasındaki bir projede akustik yük altındaki bir parçanın tasarıma yapısal bakış açısından girdi vermesi hedeflenmektedir.

Tez iki ana başlık altında ele alınabilir. Öncelikle, akustik yorulma analitik prosedürü ESDU dokümanları referans alınarak oluşturulmuştur. Akustik yük altında titreşen yapı birden fazla modu tahrik edebilir ancak akustik yorulma hasarı baskın olan bir modun hakimiyetinde olarak kabul edilir. Bu nedenle tek serbestlik derecesine dayandırılarak kurulan analitik prosedür aynı kabul koşulları altında sonlu elemanlar metodu ile doğrulanmıştır. Doğrulanmış bu analitik prosedür, yapının dinamik karakteristiğinin çıkarılması, birim yükleme altında frekans cevabı, ölçüm sonuçlarından elde edilen ses basınç seviyelerinden güç spektrumlarının çıkarılması ile dinamik stres sonuçlarının karmaşık olmayan bir yapı için elde edilmesini kapsar. Elde edilen bu stres seviyeleri, yapının dayanım ömrünün basitleştirilmiş denklemlerle ön görülmesinde kullanılır. İkinci bölüm, bir hava aracının silah yuvasını temsil eden jenerik bir kavitenin kritik olan duvarının stres analizlerinin farklı sınır koşulları

altında gerekleřtirmesini kapsamaktadır. Farklı sınır kořulları, uak i elemanlarının farklı yerleřtirilmesinin sonucu olarak doęan ve tasarıma girdi saęlaması iin gerekleřtirilen analizlerdir. İ kaburga elemanlarının yerleri ile deęiřen farklı sınır kořulları altında farklı Mach sayıları ve akustik yk azaltmak amalı kullanılan spoyler ve arka duvara aı verilmesi kontrol metotlarının yapıya etkisi incelenmiřtir.

Anahtar Kelimeler: Akustik Yorulma, Kavite Akustięi, Mile's Denklemi, Aerodinamik Grlt, Silah Yuvası

To my mother...

ACKNOWLEDGEMENTS

First of all, I would like to express my gratitude to my academic advisor Prof. Dr. Mehmet alıřkan for his guidance and encouragements provided me during the thesis study and my graduate education. I would also like to thank Assoc. Prof. Mehmet Bülent Özer for his suggestions, contributions and valuable feedbacks.

I would like to express special thanks to my dear friend Damla Özonur for sharing my all good and stressful times, as well as her emotional support and understanding during my endless academic works. I also want to thank Esra Karařın, Ezgi Karařın, Büřra Bulut, Gamze Sarıyıldız and Yeliz Yıldız for being there for me, for their invaluable support and to whose friendships I know I can always rely on. Moreover, I want to thank Aysu Özden for her unwavering support, and good times amidst the struggles of the thesis life. We have not shared only the laboratory that we worked on but also all our happy and stressful moments throughout the thesis period. I would like to thank Enes Erkan Kısa, Tuğberk Keeciođlu and Kerem Doruk Katlıođlu for their laid-back attitude any time I got stressed. They always bring me up and thanks to them this study has been successfully ended up.

Last but not least, I would like to express grateful thanks to my parents, Emine and Burhan, and to my dear brother and sisters Özgür, Özge and Joanna without whom none of these have been possible. They have always been on my side by providing all kinds of support throughout this demanding period of my life. I am lucky to have them.

TABLE OF CONTENTS

ABSTRACT	v
ÖZ	vii
ACKNOWLEDGEMENTS	x
TABLE OF CONTENTS	xi
LIST OF TABLES	xiv
LIST OF FIGURES	xvi
LIST OF ABBREVIATIONS	xix
LIST OF SYMBOLS	xx
CHAPTERS	
1. INTRODUCTION	1
1.1. General Definitions	1
1.2. Source of Acoustic Loading, Sonic Fatigue and Cavity Acoustics.....	3
1.3. Objective and Scope	7
2. LITERATURE SURVEY	11
2.1. Acoustic Fatigue	11
2.2. Cavity Acoustics.....	15
3. ACOUSTIC FATIGUE METHODOLOGY AND PROCEDURE.....	21
3.1. Structural Response	21
3.1.1. Acoustically Excited Structures.....	24
3.1.1.1. Damping in Acoustically Excited Structures	26
3.2. Spectrum Loading and Sound Pressure Levels	27
3.3. Theoretical Estimation of Response Levels and Stress Predictions.....	29

3.4. Life Assessment under Random Acoustic Loading.....	31
3.5. Random Vibration Fatigue and Cumulative Damage Prediction.....	32
4. VALIDATION STUDIES ON FLAT PLATE	35
4.1. General Assumptions Regarding the Analysis.....	36
4.2. Analytical Method and Design Guideline.....	37
4.3. Finite Element Method and Design Guideline.....	45
4.3.1. FEM Relevant Parameters.....	47
4.3.1.1. Mesh Size.....	47
4.3.1.2. Material Definitions.....	47
4.3.1.3. Properties	48
4.3.1.4. Boundary Conditions	48
4.3.1.5. Loading Conditions	48
4.3.1.6. Frequency Range of Interest.....	49
4.3.1.7. Monitoring Results	50
4.3.2. Frequency Response Analysis.....	51
4.3.3. Random Vibration Analysis	52
4.4. Flat Plate Application by both Analytical and FEM Method	54
4.4.1. Analytical Method of Flat Plate Application	54
4.4.2. Finite Element Method Flat Plate Application.....	63
4.5. Comparison of Analytical and Finite Element Method	78
5. CAVITY STUDIES	83
5.1. Cavity Rear Wall Analysis.....	86
6. CONCLUDING REMARKS AND FUTURE WORK.....	105
6.1. Concluding Remarks.....	105

6.2. Future Work	108
REFERENCES.....	113

LIST OF TABLES

TABLES

Table 1.1. Main Procedure for Acoustic Fatigue [6]	8
Table 4.1. Analytical Guideline of Acoustic Fatigue Process	38
Table 4.2. Geometrical Properties and Dimensions	55
Table 4.3. Material Properties	56
Table 4.4. Natural Frequency of Simply Supported Edge Condition (ESDU 87002 Figure 1 [37])	56
Table 4.5. Natural Frequency for Fixed Edge Condition (ESDU 87002 Figure 2,4,6,8 [37])	57
Table 4.6. Frequency Information of the Structure	58
Table 4.7. Rectangular Plate All Edges Fixed, Uniform Pressure Over Entire Plate [41]	59
Table 4.8. Parameters needed for nomograph 1 in ESDU 72005 [31]	62
Table 4.9 Mesh Size Comparison	66
Table 4.10. Conformity of the items for meshing	68
Table 4.11. Damping Definition .bdf file of NASTRAN	68
Table 4.12. Total Effective Mass Fraction	70
Table 4.13. Modal Effective Mass Fraction	71
Table 4.14. Example of Generic SPL Spectrum for 2 Different Flight Cases	73
Table 4.15. Spectra $G_p(f)$ for Validation Analysis - .bdf file of NASTRAN	74
Table 4.16. Frequency Extraction FREQI Card	74
Table 4.17. Stress Value for Element 865	75
Table 4.18. Comparison of Analytical Method with FEM	78
Table 5.1. Mach Number 0.5 PSD values for Envelope	92
Table 5.2. Mach Number Effect Analysis Result Summary at Rear Wall at 0.85 Mach Number	100
Table 5.3. Spoiler Effect Analysis Result Summary at Rear Wall at 0.85 Mach Number	100

Table 5.4. Swept Rear Wall Effect Analysis Result Summary at Front Wall at 0.85 Mach Number.....	100
Table 5.5. Principal RMS Stress Values for Mach Number at Rear Wall.....	101
Table 5.6. Principal RMS Stress Values for Spoiler at Rear Wall at 0.85 Mach Number	101
Table 5.7. Principal RMS Stress Values for Swept Rear Wall at Front Wall at 0.85 Mach Number.....	101
Table 5.8. Summary of RMS Stress Results for Spoiler Effect at Front Wall at 0.85 Mach Number.....	102
Table 5.9. Principal RMS Stress Values for Swept Rear Wall at Front Wall at 0.85 Mach Number.....	103
Table 6.1. Principal RMS Stress Values Comparison at Front Wall	107
Table 6.2. % Reduction Rate Values at Front Wall	107
Table 0.1. Frequency Ranges Corresponding to Center Frequency for a 1/3-Octave Bandwidth	117
Table 0.2. Comparison of FREQ _i Selection Sensitivity Analysis Number of Frequency Extracted	120

LIST OF FIGURES

FIGURES

Figure 1.1. Main Cavity Flow-Based Sources for Aviation Industry – Weapon Bay & Landing Gear [3].....	5
Figure 1.2. Representative Cavity Flow [4].....	6
Figure 2.1. Open and Closed Flow Types over Cavities [19]	16
Figure 2.2. Pressure Spectra measured for tested Mach Numbers [22].....	17
Figure 2.3. Sketch of flow over a cavity with spoiler [25]	19
Figure 2.4. Sketch of swept and chamfered cavity rear wall [25]	20
Figure 3.1. Main weapon bay keel sonic fatigue test & IAR Rack Development Vibration Test [17]	22
Figure 3.2. Input Output Relation for a Structure.....	23
Figure 3.3. Excitation of A Simply Supported Beam by Normal Incidence Sound Wave [28]	25
Figure 3.4. Comparative Fatigue Data for Sinusoidal and Random Loading [33]....	33
Figure 3.5. Available Data for Plain and Integrally Machined Specimen [34]	33
Figure 4.1. Simplified Flat Plate Geometrical Representation	37
Figure 4.2. Aerospace Structures’ Construction Design Representation [38].....	39
Figure 4.3. Classification of Dynamic Environment	52
Figure 4.4. Panel of Wing Trailing Edge Simplified Representation	55
Figure 4.5 Low Range Stress Nomograph [31]	61
Figure 4.6. Finite Element Model Mesh of Flat Plate	66
Figure 4.7. First 3 Modes of the Flat Plate	67
Figure 4.8. Frequency Response - Maximum Stress Location and Critical Element	69
Figure 4.9. Cumulative RMS stress -Element 865	70
Figure 4.10. Unit Pressure Excitation for Frequency Response Analysis.....	72
Figure 4.11. Fully Fixed Boundary Condition.....	73
Figure 4.12. RMS Stress Results of Elements 865 @ Z1	76
Figure 4.13. XY Plot log-log Scale Results of Stress Response	77

Figure 4.14. XY plot in lin-log Scale Results of Stress Response.....	77
Figure 5.1. Measured local SPL spectra on the cavity rear wall for the empty bay case. Rossiter mode predictions are also known: $M=0.85 \alpha = \beta = 0$ [23]	84
Figure 5.2. Measured local SPL spectra on the cavity front wall for the empty bay case. Rossiter mode predictions are also known: $M=0.85 \alpha = \beta = 0$ [23].....	84
Figure 5.3. Measured OASPL as a function of Cavity Location (x/L) for the empty bay case: $M=0.85 \alpha = \beta = 0$ [23].....	85
Figure 5.4. Generically constructed layout – main noise sources location generically	86
Figure 5.5. Probable rib and spar location of generic UCAV	87
Figure 5.6. Probable rib and spar locations of generic UCAV	87
Figure 5.7. Selected Boundary Condition 1	88
Figure 5.8. Selected Boundary Condition 2.....	88
Figure 5.9. Selected Boundary Condition 3	88
Figure 5.10. Parent and store models installed in the TWT working section on the TSR during the March 2012 tunnel entry [23]	89
Figure 5.11. Digitized Mach Number vs Literature Mach Number [23] SPL Plot at Rear Wall	90
Figure 5.12. Digitized Rear Wall Slope Effect vs Literature Rear Wall Slope Effect [23] SPL Plot at Front Wall at 0.85 Mach Number	90
Figure 5.13. Digitized Spoiler Effect vs Literature Spoiler Effect [23] SPL Plot at Rear Wall at 0.85 Mach Number	90
Figure 5.14. PSD Envelope Extracted by Center Frequencies $M=0.5$	91
Figure 5.15. PSD Extracted per Frequency by Using Digitized Frequencies $M=0.5$ 92	
Figure 5.16. Frequency response of the representative rear wall under unit loading and determination of the critical element – Element 323 for Boundary Condition 1.....	97
Figure 5.17. CRMS on Element 323 for 0.5 Mach number and Boundary Condition 1	97
Figure 5.18. PSD envelopes obtained by Nastran for 0.5, 0.7 and 0.85 Mach number cases	99

Figure 5.19. Digitized Spoiler Effect vs Literature Spoiler Effect [23] SPL Plot at Front Wall at 0.85 Mach Number	102
Figure 0.1. PSD response of system with different output extraction log-log scale	120
Figure 0.2. First 3 Mode of Simply Supported Flat Plate (552.6 Hz first mode)	121
Figure 0.3. Frequency Parameter for Plates with all Edges Simply Supported [37]	122
Figure 0.4. Frequency Parameter for First Symmetric – Symmetric Mode (Plates with all Edges Simply Fixed) [37]	123
Figure 0.5. Frequency Parameter for First Symmetric – Antisymmetric Mode (Plates with all Edges Simply Fixed) [37]	124
Figure 0.6. Frequency Parameter for First Antisymmetric- Symmetric Mode (Plates with all Edges Simply Fixed) [37]	125
Figure 0.7. Frequency Parameter for First Antisymmetric- Antisymmetric Mode (Plates with all Edges Simply Fixed) [37]	126

LIST OF ABBREVIATIONS

ABBREVIATIONS

AGARD	Advisory Group for Aerospace Research and Development
APU	Auxiliary Power Unit
CFD	Computational Fluid Dynamics
CRMS	Cumulative RMS Stress
DES	Detached Eddy Simulation
DSG	Design Service Goal
ESDU	Engineering and Science Data Unit
ESPM	Equivalent Static Pressure Method
FE	Finite element
FEA	Finite Element Analysis
FEM	Finite Element Method
Hz	Hertz
PSD	Power Spectral Density
RAAM	Random Acoustic Analysis Method
RMS	Root Mean Square
SDOF	Single Degree of Freedom
SEA	Statistical Energy Analysis
SF	Scatter Factor
SPL	Sound Pressure Level
SPSD	Sound Pressure Spectral Density
TBL	Turbulent Boundary Layer
TSR	Two Sting Rig
TWT	Transonic Wind Tunnel
UCAV	Unmanned Combat Aerial Vehicle
WTT	Wind Tunnel Test

LIST OF SYMBOLS

SYMBOLS

ρ	Density [kg/m ³]
E	Young's Modulus [Pa]
ν	Poisson Ratio
P_{RMS}	RMS Value of Fluctuating Sound Pressure [Pa]
f_n	Fundamental or Critical Frequency of the Panel/Structure [Hz]
S_{rms}/σ_{rms}	Root Mean Square Stress [Pa]
V_s	Velocity Parameter for Plate Material
K_{mn}	Natural Frequency Parameter for Simply Supported Plate in (m,n) th Mode
K	Natural Frequency Parameter for Fixed Edge
n, m	Mode Number in y and x Directions
$\sigma_{unitload}$	Maximum Unit Load Stress [Pa]
N_f	Safe Life Number of Cycles to Failure [cycles]
$t_{exposure}$	Exposure Time in Hours [hr]
$S_j(\omega)$	Power Spectral Density of the Response
$H_{ja}(\omega)$	Frequency Response Function
$S_a(\omega)$	Power Spectral Density of the Input Source
λ	Wave Length [m]
v	Speed of Sound [m/s]
U_∞	Freestream Velocity [m/s]
M_∞	Mach Number
ξ_{mat}	Damping of Material

CHAPTER 1

INTRODUCTION

1.1. General Definitions

The technical terms that will be mentioned many times throughout the thesis should be defined clearly.

Acoustic related technical terms cover all definitions as acoustic environment, acoustic/sonic fatigue, sound pressure, sound pressure level (SPL), 1-Hz, 1/3 Octave and 1-Octave bandwidth level etc. Acoustic environment for an aircraft can be defined as the environment that the level of pressure varies for different flight cases across the whole frequency domain in the volume surrounding any exposed surface. The acoustic fatigue caused by this acoustic environment is the accumulation of damage due to repeated loading in response to acoustic energy.

Although sound pressure is confused with sound pressure levels, they are correlated two distinct terms. Sound pressure is the difference between the pressure due a noise source and the ambient pressure of the environment that the noise generated as a function of time and space. It can be either a randomly varying or deterministic variable and is normally expressed as a set of root mean squared (RMS) value across the frequency domain. On the other hand, sound pressure level is expressed as a power of sound pressure relative to threshold of human hearing level which is taken as 0 dB representing $2 \cdot 10^{-5} Pa$. There are different bandwidth levels to express these sound pressure levels. 1-Hz Bandwidth level is used for SPL level in the frequency domain averaged in 1-Hz frequency interval. 1/3-Octave bandwidth level is used for SPL level in the frequency domain averaged in predefined frequency segments and identified by a center frequency, where each segment represents a step 1/3 of an octave. 1-Octave Bandwidth level is used for SPL level in the frequency

domain averaged in predefined frequency segments and identified by a center frequency, where each segment represents doubling of frequency. Apart from sound pressure level, pressure spectrum level can be defined as the pressure levels relating to the energy in each this specific bandwidth levels.

Technical terms about structural response and fatigue calculations can begin with the basic damage definition. It is the ratio of required life cycles to the predicted life cycles according to linear damage accumulation rule, which is known as Miner's rule. When the damage gets equal to unity, the failure will be initiated. Damage calculation requires some information as exposure time, root mean square stress or some indicative stress etc. Exposure time is the duration that is used in the fatigue life calculations which represents the time that the aircraft component is exposed to the acoustic excitation. Root mean square stress (S_{rms}) is randomly varying stress values in a RMS; where, RMS is the square root of the arithmetic mean of a set values which have been squared.

Dynamic characteristics of the structure should be investigated for the response of the structure before damage calculations. The first term to be defined under this heading is mode of vibration, mode shape or eigen vector which is the specific pattern of vibration of the structure in terms of displacements at its natural frequency. Undamped natural frequencies can be defined as the frequencies of the structure that are directly dependent on the way mass and stiffness are distributed within the structure. In the analytical calculations section of the thesis, natural frequency range which represented as f_{n1} and f_{n2} (lower and upper bounds of natural frequencies) will be used for the structure. It is the range of frequencies over which a particular natural frequency may exist due to different boundary conditions.

S_{rms} -N data is used for the fatigue calculations in the scope of this thesis. S_{rms} -N is defined as random vibration material fatigue properties. One should be aware is that typical Wöhler's S-N material fatigue curve and random S_{rms} -N data curves represent different manners. S-N is against constant amplitude stress. Before fatigue

calculation concerns, random vibration analysis should be carried out. Random loading can be defined as power spectral density (PSD) which is typically used to characterize broadband random signals and it is a measure of power of a signal within a specified frequency band. One another term that should be defined is the joint acceptance function which is described as the degree of spatial correlation between distributed input excitation and structure.

The Engineering and Science Data Unit (ESDU) Library is used throughout the thesis as a major source. This library provides validated information in engineering design and analysis for use by or under the supervision of qualified engineers [1].

1.2. Source of Acoustic Loading, Sonic Fatigue and Cavity Acoustics

Acoustical energy, caused by the aerodynamic or thermodynamic variation, has become a potential cause of failures of structural component in aviation industry. To assess the structural damage against high intensity noise, characteristics of the probable noise sources should be considered. These sources can be considered as engine-based noise sources and aerodynamic flow noise.

- ✓ Engine Based Noise Sources
 - Jet Exhaust Noise
 - Shock-Cell Noise
 - Propeller Noise
 - Fan and Compressor Noise
- ✓ Aerodynamic Flow Noise:
 - Boundary Layer Noise
 - Flow over cavities

Although engine is usually taken as the main noise source, airflow over the aircraft can induce significant structural vibration. Examples of aerodynamic flow excitations include fluctuating pressures in boundary layers. Aerodynamic surfaces exposed to acoustic loading resulted with acoustically induced vibration which cause

acoustic fatigue with the accumulation of losses in the structure. The most critical failure of aerodynamic noise source is the resonant acoustic response of cavity with one side exposed to aerodynamic flow [2]. Flow and geometrical parameters effects on the representative weapon bay cavity wall will be examined in the scope of the dissertation.

Determination of fluctuating acoustic pressure as an input loading is the first step of the sonic fatigue failure calculations. The following steps will be prediction of structural response in terms of dynamic characteristics of the structure, stress amplitude against acoustic loading and prediction of fatigue life for a particular structure, whatever its material composition, for a given stress distribution [2].

In order to design the structures and equipment that resist and respond enough against the randomly fluctuating loading, resulting from turbulent boundary layer (TBL), cavity resonance or propulsion system noise, random vibration considerations should be understood assimilatingly. Problem is usually mechanical vibration characterized by very high intensity acoustic excitation at its predominant resonant frequency. Therefore, dynamic characteristic of the component, exposed to acoustic excitation directly, influence the stress patterns of the structure. Stress results of random vibration may result in low stresses in comparison with static stresses arising in the structure; however, very large number of stress reversals can be induced, which makes the acoustic fatigue phenomena a current issue that needs to be looked upon.

The aeroacoustic analysis of flow over cavity which is presented in aviation industry as fuselage opening, landing gear, and weapon bay, is an essential topic. Understanding the behavior of flow and the ways to control flow over cavity are challenging subjects to figure out. Computational and experimental techniques are applied to provide prediction of cavity noise.

Studies about flow over cavity are mostly about internal weapon bay of a combat aircraft which is often termed as “*an urban legend*” or “*flight clearance nightmare*” in the literature. It is because, highly energetic unsteady flow field inside the cavity is generated during store release phases of operation especially for modern high-performance aircraft. Not only structural but also functional problems are encountered. Unsteady flow field may cause inaccuracies in guidance of certain projectiles as well as structural fatigue-induced failures on the cavity structure itself and equipment inside. Therefore, physical phenomena behind the fluid-structure interaction which may result in high intensity unsteady pressure fluctuations and acoustic loads is crucial for the design of a cavity [3].

Prediction of structural response against random pressure fields is of interest in air-vehicle development, especially for acoustic fatigue problems and vibration requirements as stated before.



Figure 1.1. Main Cavity Flow-Based Sources for Aviation Industry – Weapon Bay & Landing Gear [3]

Focusing on flow generated sound in aviation industry, sound generation mechanisms of cavities should be investigated. Noise is generated due to vortex shedding at the upstream edge of cavity when flow passes through it. Shear layer formation and pressure changing are the base of flow phenomena over cavity. In terms of acoustics, what happens around cavity is the right topic to be curious about the cause – effect relationship between shear layer and acoustic –frequency fluctuations in the cavity.

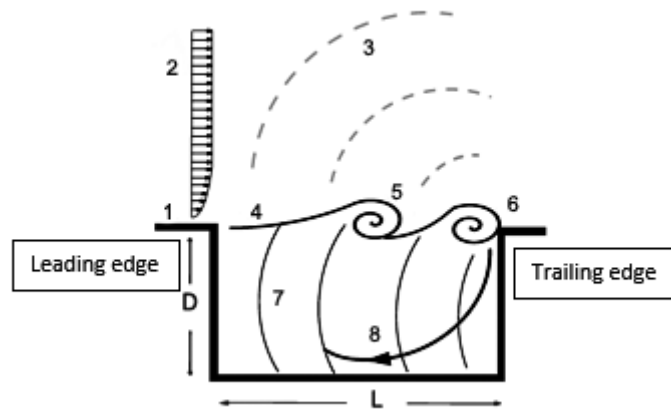


Figure 1.2. Representative Cavity Flow [4]

Figure 1.2 shows cavity flow with, (1) boundary layer, (2) mean flow, (3) acoustic wave, (4) shear layer, (5) vortex generation, (6) vortex-wall interaction, (7) pressure oscillation and (8) recirculation [4]. Feedback mechanism works between vortex generation and acoustic wave produced by vortices. Growth of acoustic waves is greatest when the characteristic frequency of vortex shedding is proportional with or close to a natural acoustic frequency of the cavity [4]. This complex phenomenon is simplified to obtain Rossiter formula (Rossiter 1964) which will be explained in detail in Chapter 5.

When it comes to the structural concerns in aviation industry about acoustic loading and sonic fatigue; it is presumed that structure in the flow field subjected to pressure fluctuations can be categorized as low frequency (<100 Hz) and high frequency (>100 - 2000 Hz). Low frequency vibrations can be visualized by global models and associated with performance and stability of an aircraft; whereas high frequency vibrations typically related to high cycle fatigue problems as sonic fatigue. It requires special attention in order to protect equipment from severe acoustic environment within the internal weapon bay (IWB). Realization of coupling mechanism of structural vibration and aeroacoustic loading is significant to evaluate

the design of cavity-geometry parameters. Random vibration phenomena will be used for structural response processes and basic fatigue life estimation procedure will be used analytically for design purposes in this study scope.

1.3. Objective and Scope

The aim of this thesis is to define acoustic fatigue analysis procedure. Two different techniques are presented for preliminary design and detail design stages of the projects. Comparison and advantages-drawback of the methods are included throughout the thesis and summarized in discussion part in Chapter 6. Analytical procedure can be used especially on the phase of concept design of the projects and finite element method is aimed to be used for more severe analysis in the detailed design stages.

Firstly, analytical procedure is generated based on the Engineering Science Data Unit (ESDU) library items. ESDU provides a large amount of design data using the results published in the open literature. Analytical procedure needs to be established for the simplest model, which is taken as flat plate for the scope of the dissertation. The procedure includes prediction of natural frequencies, root mean square stresses and stress reversals accumulation to appropriate engineering accuracy and compile with reliable fatigue data set, i.e., $S_{\text{rms}}-N$ curves under random acoustic loading [5]. This procedure has a great importance in concept design stages since there may be too many configurations to be checked from the structural point of view under acoustic loading when quick feedback is requested by designers. Analytical procedure presents a fast and effective way to compare the probable configurations.

“Introduction and Guide to ESDU Data on Acoustic Fatigue” [6] outlines the important factors influencing acoustic fatigue failure. Important factors affecting acoustic fatigue life of a structure subjected to pressure fluctuations is summarized as follows;

Table 1.1. Main Procedure for Acoustic Fatigue [6]

Characteristics of Noise Field	Flight plan Broadband/narrowband, random, TBL
Structural Response	Natural frequencies Eigen vectors
Critical Stresses	Predominant modes Detail design factors (stress concentration)
Fatigue damage	S_{rms} - N curve under random loading

The procedure obtained analytically is validated with finite element method (FEM) by providing the same conditions that the analytical procedure based on, to the finite element model. Important points that should be taken into consideration for FEM analysis is expressed in detail in Chapter 4 for the structures exposed to acoustic loading.

Secondly, the critical wall of cavity shaped structures is investigated. Measured sound pressure levels taken from literature are converted to required PSD form [Pa^2/Hz] and analysis is carried out finite element method. This is used to compare the stress response of the generic cavity wall with different palliative methods and dynamic loads under 0.5, 0.7 and 0.85 Mach numbers. Different

boundary conditions are investigated for each case to supply information on the selection of internal members' location in Chapter 5.

This thesis exploits multidisciplinary theories, including the flow induced dynamic loading, extraction of dynamic characteristic, stress response of the structure and basic fatigue life prediction, together to support analysis activities at the design stage of the projects.

CHAPTER 2

LITERATURE SURVEY

In this section of the thesis both acoustic fatigue and cavity acoustic related studies are presented from the literature.

2.1. Acoustic Fatigue

Sound pressure waves may cause deterioration and failure of panels due to the resultant high-cycle stresses when the amplitudes are sufficiently high. This phenomenon is known as sonic fatigue and is an essential topic for aviation industry. The sonic-fatigue failure theories inherited from late 1950's need enhancement of techniques. Many investigations leading to practical solutions are undertaken to prevent components from sonic fatigue failures. Design criteria for many types of structures were developed under U.S Air Force sponsorship and by Industry [7].

In the scope of this thesis a design guidance is tried to be implemented to the procedure for the preliminary acoustic fatigue analysis on structures subjected to acoustic pressure loading. ESDU data sheets are used as a main source to determine a road map as used in [8]. It is known that analytical process for the acoustic fatigue calculations cannot be implemented for complex structures. In [9], box-type structures are investigated for the determination of internal support structures housing. For more complex geometries, FEM is preferred as explained in-detail in Chapter 4 of this thesis.

ESDU 86025 "*Design Against Fatigue: Vibration of Structures Under Acoustic or Aerodynamic Excitation*" [10] provides a general overview on the design of structures under acoustically induced fatigue failures. It is emphasized that predominantly resonant response of structural component under radiated sound field cause structural fatigue; therefore, probable acoustic sources and their characterization

has to be determined for the assessment of acoustic damage. All the potential sources that may cause acoustic fatigue are tried to be classified in Section 1.2 as a summary and detailed information can be found in [10]. This characterization has to be considered in design process of the projects at least for the major sources for the development of design criteria of vibration and acoustics.

In [11], importance of one predominant mode is expressed as a collaborative study of all other sources found in the literature as [8], [12], [13] and [14] etc. All these sources work on acoustic fatigue in different manners and the evaluation of structural design guides eventuated in single degree of freedom model that can be used for stress prediction in the design analysis for a limited range of structural dimension [13]. The equation for single degree of freedom assumption stress is given in equation (2.1) and investigated in detail in Chapter 4.

$$\sigma_{rms}^2 = \frac{\pi f_n G_p(f_n)}{4 \delta_{mat}} \sigma_{unitload}^2 \quad (2.1)$$

Although the procedure used in the scope of this thesis based on linearity assumptions, there are many studies as [12] that investigate the improvement of the understanding of nonlinear behavior of the structures excited to high levels of vibration. The focus of [12] is the nonlinear response of simple structures; however, predictions are still based on the fundamental mode for simplification. It is proved that 1st, 3rd and 5th vibration of modes has the highest contribution into the response found from the results of acoustic progressive wave tube tests of plates. Therefore, equation (2.2) is used as the total mean square stress may be expressed as;

$$\sigma_{rms}^2 = A_1 \left(\frac{\pi f_1 G_p(f_1)}{4 \delta_{mat}} \sigma_{unitload1}^2 \right) + A_3 \left(\frac{\pi f_3 G_p(f_3)}{4 \delta_{mat}} \sigma_{unitload3}^2 \right) + A_5 \left(\frac{\pi f_5 G_p(f_5)}{4 \delta_{mat}} \sigma_{unitload5}^2 \right) \quad (2.2)$$

where A is the coefficient and $A_1 + A_3 + A_5 = 100\%$ as referenced by [12].

Experimental results from past experiences and cumulative damage theory is utilized for the acoustic fatigue-life predictions. The process includes the spectrum of acoustic loading, vibrational stress response and the life from stress versus cycles to failure curves for the materials.

Enhancing the knowledge and understanding of acoustic fatigue strength data is the main concern of the development of design criteria for vibroacoustic [11]. Focus on acoustic fatigue of selected advanced composite and metallic materials in addition to develop an analytical /computational and experimental methodology. Carbon Fiber Reinforced Plastic (CFRP) is investigated in terms of standard random vibration endurance features in addition to aeroacoustic loading studies and testing of structural element in wind tunnel. This study declares that aeroacoustic loads pose difficult types of loading conditions for the structure in terms of their spectral content. Correct prediction requires high level environmental simulation to excite the structures to the same level as they are actually exposed.

“Some Consideration of Fatigue Behavior of Aluminum Alloy Structure Under Acoustic Loading” [15] focus on fatigue performance relation with the mean stress levels and bandwidth of stress spectrum. In addition, it has been argued that the safe life approach is more preferable for the acoustic fatigue consideration rather than damage-tolerance approach. The difference between these two approaches and the reason why safe life is favored will be given in detail in Chapter 3.5.

All the sources already pointed out worked on the acoustic fatigue calculation for design process which keep the results in a conservative side and feed the designers in concept design stages. From the fatigue point of view, it is known that time history of loads is needed. Measurements of the magnitude in RMS pressure is preferable way of definition of random loads arising from jet noise or separated flow. When it comes to FEM, as used in [16], random vibration is carried out where the loading and the structural response vary with time. Random vibration is the post processing of frequency response analysis that will be explained in detail in Section 4.4. RMS value

that is resulted from frequency response analysis is equivalent to the square root of the integral of the power spectral density (PSD) output response of the structure [16].

“*Certification of the F22 Advanced Tactical Fighter for high Cycle and Sonic Fatigue*” [17] presents certification process of F22 for sonic fatigue design step by step. The process is divided into 4 steps and begin with the specification of vibration and acoustics. Although this section seems too easy to determine, it is almost the most miscellaneous process that will direct the subsequent processes. Second step is the development a detailed design which includes ground and laboratory tests to develop design allowable and margins. Step 3 is the verification of the environment. All the requirements determined in step 1 and its execution in step 2 are discussed with flight test program for vibro-acoustic concerns. Last step is the process employed for the validation of the aircraft structure. The section related to this thesis is the analysis methods presented. Two basic methods are used called “equivalent static pressure method” (ESPM) and “random acoustic analysis method” (RAAM) are presented. Miles equation is used for the RMS sound pressure response as given in equation (2.3) which is exactly the same expression given in equation (2.1) that also used in this thesis. However, an equivalent factor given in equation (2.4) is multiplied with the found response value that based on Gaussian distribution [17].

$$P_{RMS} = \sqrt{\frac{\pi}{2} SPSD f_n Q} \quad (2.3)$$

where P_{RMS} is the RMS sound-pressure response, SPSD is sound pressure spectral density, f_n fundamental or critical frequency of the panel/structure, Q is transmissibility at the resonant frequency which is approximately $1/2\xi_{mat}$ and ξ_{mat} is the damping.

$$P_{equiv_{factor}} = (0.683 (1^b) + 0.271 (2^b) 0.683 (3^b))^{\frac{1}{b}} \quad (2.4)$$

where $P_{equiv_{factor}}$ is the equivalent factor which will be multiplied by the P_{RMS} to convert an equivalent random pressure or response [17].

The fieldwork researches on acoustic fatigue analysis procedure are summarized and now cavity acoustics related sources will be presented, which is taken as representative weapon bay of high-performance aircraft.

2.2. Cavity Acoustics

In this section, a brief literature review of the basic cavity oscillation phenomenon, the major parameters affecting the flow and various previously investigated control techniques are presented.

Cavity acoustics in aviation industry is taken into consideration and the investigations are presented focusing on the complex unsteady flow field. Cavity geometric parameters and external flow properties play an important role on the physics of cavity flow. Characterization of the flow field over cavity depends on the cavity streamwise length-to-depth ratio and named as open and closed type cavities. Closed cavity (attached flow) is for the case where length-to-depth ratio is greater than 13 whereas open cavity (detached flow) is for the cases where length-to-depth ratio is smaller than 10. The values for length-to-depth ratio is between 10 and 13 is called as transitional type cavity flow [18]. The phenomena of flow characteristics difference are demonstrated in Figure 2.1.

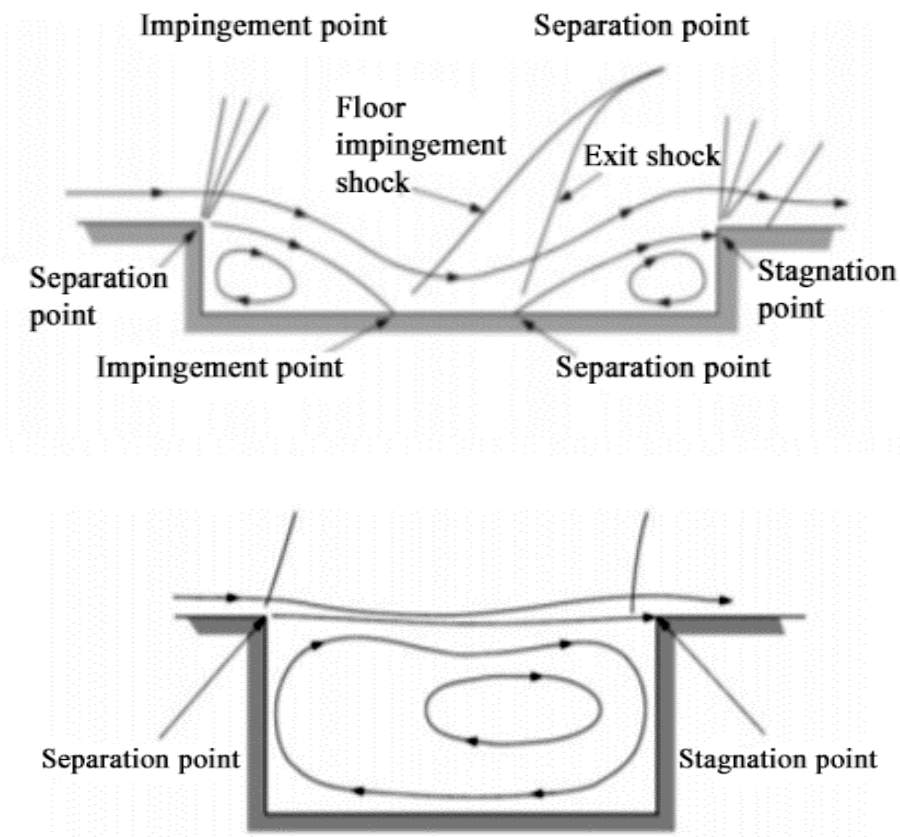


Figure 2.1. Open and Closed Flow Types over Cavities [19]

In design stages of aeronautics applications, internal weapon bay is almost the most critical component and many studies are available in literature in order to understand the complexity of the flow mechanism in different cavity configurations.

Analysis and control of aerodynamic noise is not an easy assignment since the noise generation mechanism depends on many flow and geometric specifications (L/D , L/W), incoming boundary layer thickness, mean flow Mach number, stagnation temperature, cavity configurations etc. Methods to control flow oscillations in cavities will be also examined and presented widely in the literature.

Most of the investigations are related to length-to-depth ratio of the cavity since the flow characteristic of the cavity is directly dependent on this ratio as shown

in Figure 2.1 also. However, in the content of this thesis, effect of Mach number will be investigated since there are many other design restrictions that play roles on determination of the cavity length-to-depth sizes as drag concerns, size and mission of the combat, low observability, system housing etc.

Higher the Mach number as a flow parameter resulted with higher noise levels throughout the spectrum and tonal frequencies are increased with the increment in Mach number as found in [18] [20] [21] and [22]. Higher Mach number triggers to nonlinear interactions and higher order harmonics. Especially for the open type cavities where feedback mechanism is dominant, these nonlinear interactions resulted with increase in SPL values in the cavity as studied in [22] and shown in Figure 2.2. Subsonic flow at Mach number 0.19, 0.29, 0.39, 0.58 and 0.73 over a shallow cavity with length-to-depth ratio 6 is studied experimentally and resulted with increased SPL values and shift in Rossiter modes overall the spectrum [22].

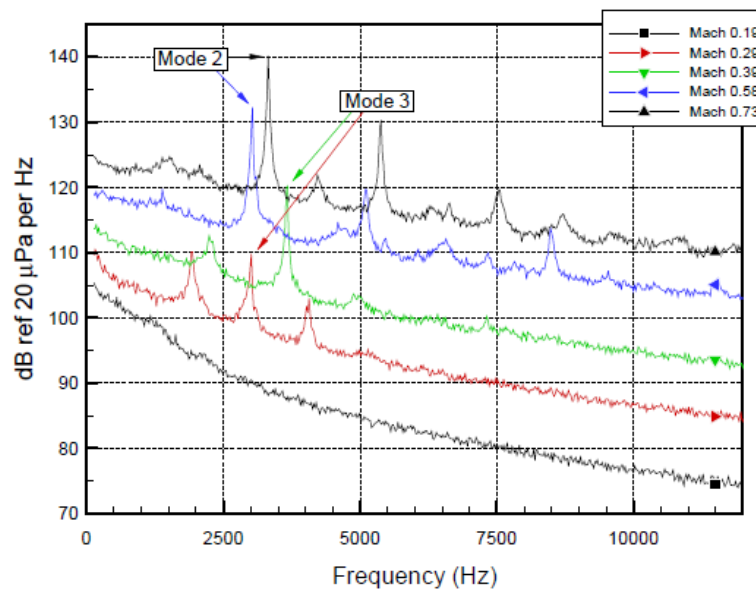


Figure 2.2. Pressure Spectra measured for tested Mach Numbers [22]

Mach-number effect on dynamic loading on the structure is studied in [23] and the loading from this study is used in Chapter 5 of this thesis. The Mach-number effect can be checked in Figure 5.11.

Unsteadiness of cavity flow is a critical issue and the solution to the problem can be either stiffening the structure, not favorable in aviation industry, or to control the flow over cavity to reduce dynamic loads in terms of structural strength.

A great number of palliatives are investigated to suppress the flow induced resonance in cavity flow. Controlling approaches are divided into two as passive and active methods. Passive control systems do not require energy addition into the cavity flow; however, active control systems require energy to attenuate the noise and dynamic loads of the structure.

Examples of passive controlling methods as spoilers, baffles, static or oscillating fences, leading edge ramps and rods, provide reduction of amplitude of cavity tones. It is important to consider all design conditions for the selection of control methods since they may increase drag or may reinforce the cavity acoustic feedback mechanism of under off-design conditions. Before giving the methods and their effects on aerodynamic noise and dynamic loading, the idea behind controlling method that disrupts the acoustic resonance and reduce sound pressure levels will be expressed depending on [24] as follows:

- ✓ Modification of downstream reattachment point by lifting the shear layer
- ✓ Thickening the shear layer and so changing of shear layer stability
- ✓ Low frequency excitation of shear layer at off-resonance condition
- ✓ High frequency excitation which resulted in mean flow alteration and change stability characteristics
- ✓ Cancellation of feedback acoustic wave
- ✓ Oblique shock flow deflection and reduction of longitudinal speed [24].

Active control methods, as mass injection into the cavity, are out of scope of this thesis and are not found feasible for the high-performance aircraft. It is because increasing the complexity is not favored. On the other hand, passive controlling

methods have to be investigated in detail because they may contradict with other design requirements of the aircraft as expressed before.

Two passive controlling methods' effect on the critical wall of the cavity is investigated in Chapter 5. Spoiler and swept rear wall are chosen since their feasibility and effectiveness are relatively higher than other controlling methods as expressed in [25] and [26] and shown in Figure 2.3 and 2.4.

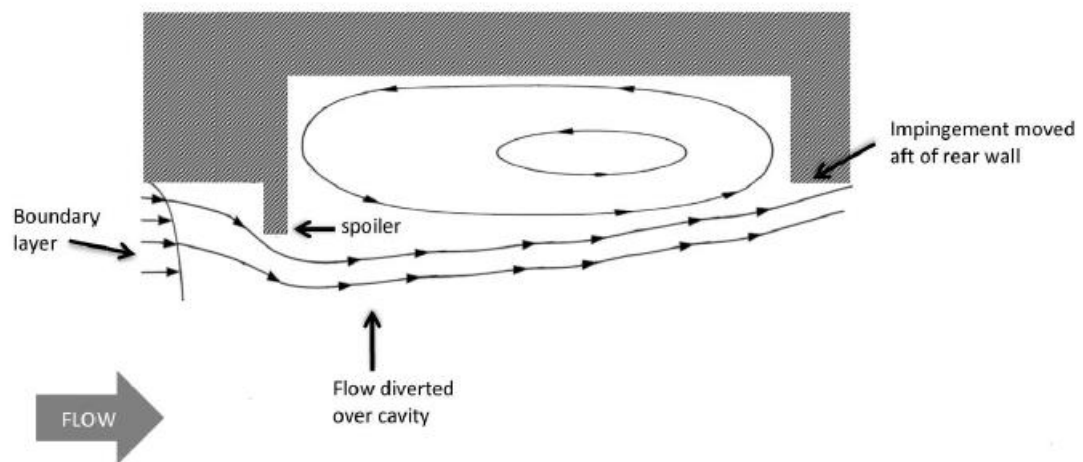


Figure 2.3. Sketch of flow over a cavity with spoiler [25]

Rear wall of the cavity is regarded as the source of the modal pressure fluctuations within the resonant cavities. That's why there exists many studies that modifies the shape of this structure to affect modal generation process and reduce the intensities of the modal peaks. A number of options are available for the rear wall modifications studied in [25] which covers swept rear wall and chamfered cavity rear wall as shown in Figure 2.4.

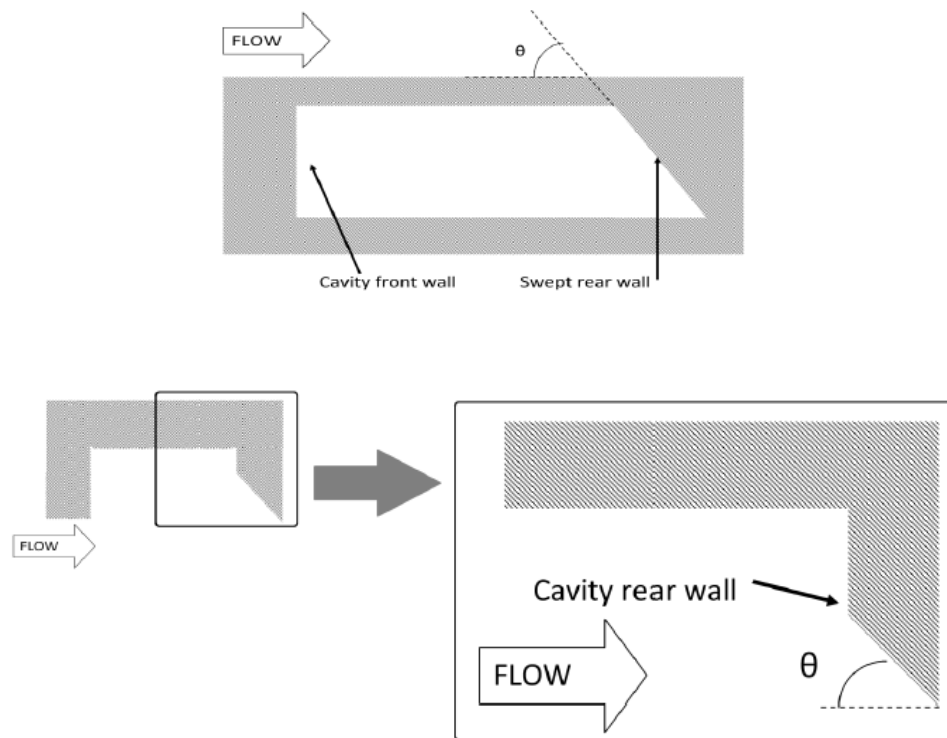


Figure 2.4. Sketch of swept and chamfered cavity rear wall [25]

The swept-rear wall controlling method is investigated in Chapter 5 in terms of structural response in addition to spoiler effect as described before. Acoustic measurements obtained experimentally from [23] are used as an excitation force (acoustic loading). Details are included in Chapter 5.

CHAPTER 3

ACOUSTIC FATIGUE METHODOLOGY AND PROCEDURE

In order to design any structure in engineering, the first consideration comes to mind is its ability to withstand the environment in which it is projected to operate. Experience on many different aerospace vehicles has shown that high frequency-low amplitude pressure fluctuations associated with random acoustic loading can cause structural fatigue or lead to unacceptable expenses for maintenance and inspection [17] not to mention malfunctioning. In order to avoid from fatigue failure for a structure exposed to high intensity noise, main objectives may be outlined into three stages as follows;

- Description of acoustic field i.e. generation of noise due to an acoustic source and its subsequent propagation.
- Determination of vibrations and resultant stresses of exposed surfaces in response to the fluctuating sound pressure.
- Prediction of life expectancy of the material and the accumulation of fatigue damage in the structure.

These steps present difficulties and it is particularly challenging to attempt to understand the necessary interrelation among concepts in acoustics, in dynamic stress analyses and in fatigue failure of the material.

3.1. Structural Response

Vibration is a mechanical phenomenon which can be unpleasant for the structures apart from those used for special functions. For many engineering systems it may cause fatigue failure since it is responsible for dynamic stresses development in the material as illustrated in Figure 3.1.

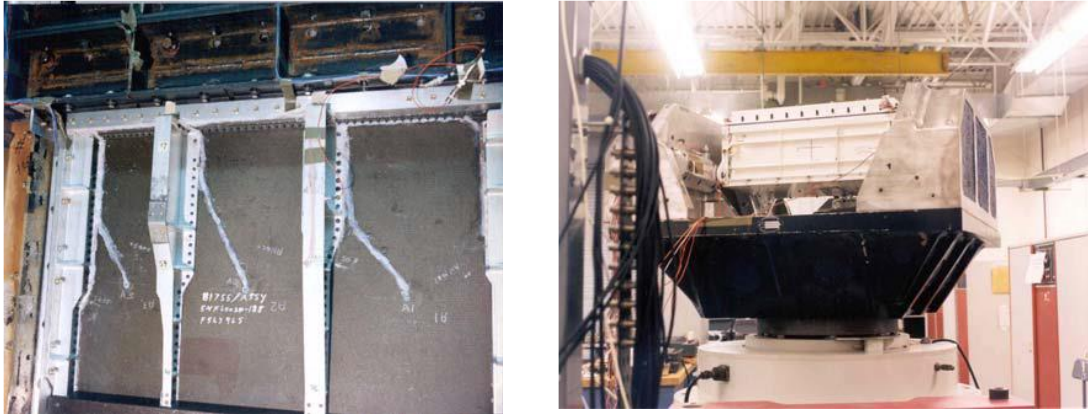


Figure 3.1. Main weapon bay keel sonic fatigue test & IAR Rack Development Vibration Test [17]

Vibration phenomena can be associated with oscillations of systems about an equilibrium state. They can occur freely at the natural frequencies of any mechanical system when a set of initial conditions are imposed on the system. Forced vibrations can take place under application of external dynamic effects. It is used to predict the natural frequencies and the response of the structure against any loading. [27]. Characteristics of a system is determined by natural frequencies and related mode shapes of the structures. If the structure is excited at one of these frequencies', resonance takes place. Resonance should be avoided since it can produce large amplitude vibrations at certain frequencies even under small driving forces. Another phenomenon is the mode shape of the structure which is usual and preferable way for characterizing of vibration responses in engineering system. For each natural frequency, structure displays a distinct form of vibration called as mode shape. These characteristics are independent of applied excitation or any other external factor, but depend on the physical characteristics of the system that are mainly inertia and elasticity as well as boundary conditions. Energy dissipation termed as damping is also involved.

Structures possess as many natural frequencies as they have a number of degrees of freedom; however, it is not possible to take all of these frequencies into consideration in design phase. Fortunately, all the natural frequencies of a structure are not needed to be calculated; since many of these frequencies will not be excited

during operation. In any case, they may produce negligibly small resonance amplitudes. This is why the analytical model of dynamic structure needs have only a few degrees of freedom, or even only one if possible. That's why structural parameters should be chosen carefully so that the correct mode of vibration is modelled.

Random vibration analogy will be used in the scope of this thesis for the stress response of the structure under acoustic loading. If a linear, time-invariant system is subjected to a random excitation, the response will also be random phenomenon of the same type. Description of a random phenomenon as a function of time does not appear particularly meaningful and does not reveal main features required for design. Time domain information has little to do with dynamical design characteristics and it is not preferable [27]. Input output relation of a structure for an acoustic analysis is summarized in Figure 3.2.

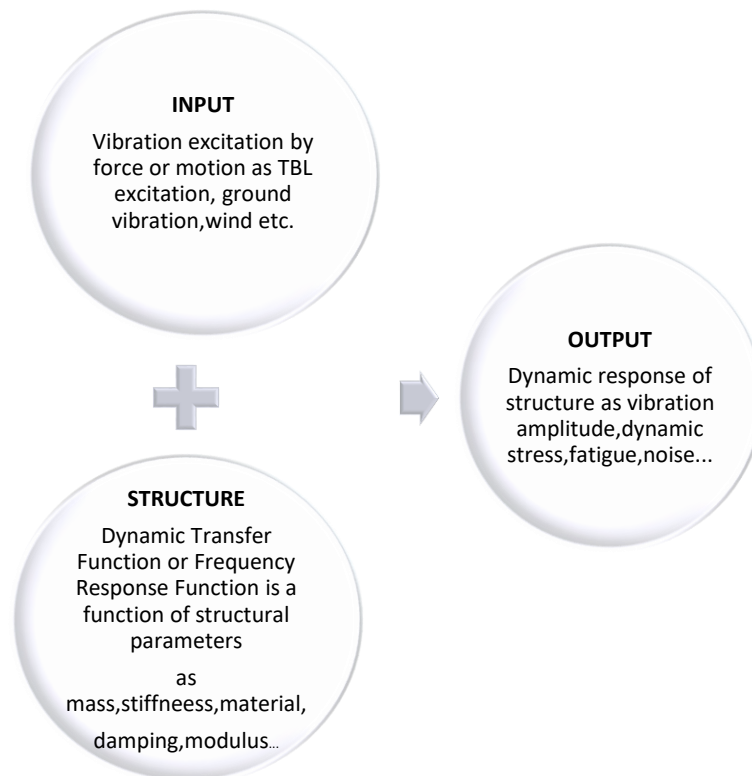


Figure 3.2. Input Output Relation for a Structure

Acoustic loads, as a matter of fact, are random in the nature and statistical methods of analysis is preferred as an efficient way. One convenient method often used to describe random vibration is called spectral analysis, Power Spectral Density, a statistical function of frequency, is often used to describe distribution of power or energy of vibration in frequency domain.

3.1.1. Acoustically Excited Structures

In order to design the structure against sonic fatigue, it should be ensured that the structural response does not include any major modes of vibration in the range of frequency that the acoustic loading exposed. However, in principle it is difficult to handle with the broadband excitation since it contains the complete the frequency range of essential modes of most aircraft structures.

When it comes to the phenomenon behind the acoustically excited structure response, unlike to mechanical excitation, actual coupling mechanism between the structural modes and the excitation field is applied for the acoustically excited structures with its particular modal characteristics. In other words, for cases of mechanical excitation, coupling efficiency is directly related with the forces; whereas for the acoustical excitation it directly depends on how well sound waves interact with the structural modes [28]. The term of ‘joint acceptance’ should be defined in order to make clear the coupling efficiency between structure and excitation. It is a measure of the effectiveness of the pressure field to excite a particular mode and corresponds to the modal participation factor or effective mass found in mechanical vibration [27]. In “*An overview of structural acoustics and related high frequency vibration activities*” [28], coupling principle under acoustic excitation is expressed very well as can be seen in Figure 3.3.

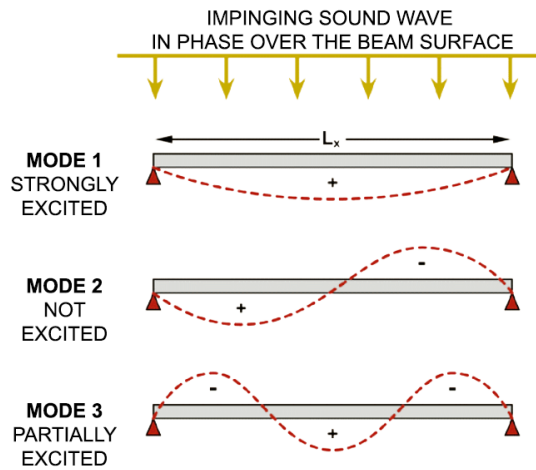


Figure 3.3. Excitation of A Simply Supported Beam by Normal Incidence Sound Wave [28]

If the sound is in phase over the structural surface, lowest order half wave structural mode shows strong coupling whereas in the case of second order mode, the energy contents of the vibrating half-waves would ‘cancel each other out’, so that the mode would not be excited at all [28].

Sound pressures are likely to be in phase over the structural surface, so that the lowest order modes are likely to be dominantly excited. Very useful and important inference is that for the plate like structures, structural response in low order modes has the greatest importance, even can be taken as one mode only. For the acoustic fatigue consideration, this simplification can be used as a reasonable assumption, however it also should be noted that, by no means all noise induced vibration consideration can be simplified as a single mode approach. For the internal equipment structural, response depends on the mechanical transmitted power as well as the resonant frequencies. For the detailed design process, further thought should be done by using Finite Element Analysis (FEA) methods rather than simplified analytical method to take the all needed modes of the structures into account. However; for the wide frequency range considerations, which is needed to include the influence of many modes, FEA might be impractical. In these cases, Statistical Energy Analysis (SEA), provides a means of assessment of vibrations and the importance of the routes through

which any vibratory power may be transmitted from a remote part of the component, is preferred. This method is not in the domain of interest of this thesis studies [28].

It can be deduced that, it is very difficult to design response characteristic into a structure. However, and the resultant stresses can sometimes be reduced by using appropriate damping materials, although this may have weight and cost penalties, as well as creating difficulties in production and reducing inspectability.

3.1.1.1. Damping in Acoustically Excited Structures

Damping, which is used to characterize energy dissipation of a vibrating system, of the structure exposed to high intensity acoustic loading is an essential topic. For the structures which is excited by the load at the resonance frequency would infinitely vibrates and diverge theoretically without damping. Increasing this parameter provides a means of reducing amplitudes of vibration and associated stresses in the structure and is represented in two different ways as viscous and structural (hysterical). These are proportional to product of the frequency and the square of the displacement amplitude and to the square of the displacement, respectively.

Structural damping is dominant in typical aircraft, although it is not possible to give exact relationship between the magnitudes of structural and acoustical damping ratios. Other sources are present but generally these make relatively small contributions to the overall damping [29]. It is crucial to state that, since the measurement techniques give total response of the structure, damping expression contains total damping from all sources.

“Introduction and Guide to ESDU Data on Acoustic Fatigue” [6] states that the RMS stress response to broadband noise pressures is inversely proportional to the square root of the modal damping; hence, an increase in damping reduces the response to acoustic loading. Damping ratio for typical aircraft skin and stringer panels vibrating in their fundamental mode is given in [8] and [31] for Aluminum 2024 as 0.017.

3.2. Spectrum Loading and Sound Pressure Levels

In order to work on structural response against acoustic loading and sonic fatigue calculations, load level should be known, preferably, with the information of the spatial distribution. Acoustic environment is represented as aerodynamic sources depend on aircraft flight conditions for this thesis. It can be obviously said that the most critical aerodynamic acoustic loads are due to flow separation and due to shock waves according to literature survey. There are still difficulties in accurate predictions of aerodynamic acoustic data. The most obvious way is making an actual flight test and measure it; however, it is not within the bounds of possibility for the early design stages of the projects. The wind tunnel tests (WTT) results can be another option to be used as an acoustic loading but it might be time consuming and too expensive. Moreover, due to a different than in flight turbulence level, WTT may not predict correctly the acoustic loads. Because of all these difficulties, numerical methods may be preferable rather than experimental methods for the determination of load.

During project development and design phases, loads estimates are obtained by empirical procedures or past experience with similar projects. Although it is widely used in concept design phases of the projects, empirical methods design guidelines has several limitations on the determination of acoustic loading. The principal assumption is related with the uniform spatial distribution of the acoustic load, means excitation is applied in phase over the structure. This assumption, simplifies the calculation procedure, but restricts the accuracy of the response and keeps the fatigue result on the conservative side.

It is clearly expressed in [27] that, using Computational Fluid Dynamics (CFD) results provides facility to make load predictions in early design process of the projects. From a good CFD simulation, load intensity, as well as spectral characteristics and spatial distributions, can be extracted. It should be pointed out that selection of turbulence models, mathematical flow models and the idealization of the

structure affect CFD results' accuracy. Hence, the correct analogy and CFD parameters should be used in the CFD simulation.

Sound pressure level values, known from the measurements or numerical analysis, have to be converted the form that will be used in the calculation process by using the expression;

$$P_{rms} = 10^{\frac{SPL}{20}} p_{ref} \quad (3.1)$$

where p_{rms} is the RMS value of fluctuating sound pressure and p_{ref} is a reference sound pressure represents the threshold of hearing given as $2 * 10^{-5} Pa$ at a frequency 1000 Hz.

As acoustic pressure is usually distributed over a range of frequencies, it is needed to use filters to separate the signal into different frequency bands. Octave Bands splits the audible spectrum into smaller segments called octaves, and provides identification of different noise levels across individual frequencies. Information outside of the specified bandwidth is rejected. Octave and one third octave bands bandwidths are commonly used for the analysis of broadband noise. An octave band is the interval between two frequencies, the higher of which twice, whereas one third octave band is obtained by splitting the octave band into three parts to create narrower bands to provide a further in-depth outlook on noise levels across the frequency composition.

For the addition of multiple noise sources' SPL values in different octave bands, bandwidth correction should be applied. ESDU item 66016 [30], ought to be used for conversion of these SPL values to the consistent units. With the summation of the noise sources in a consistent form, although acoustic excitation usually specified as a value integrated over a given frequency range and acoustically induced vibration usually consists of several response modes, usual approach for fatigue damage is usually dominated by one mode. Therefore, it is assumed that, the stress is attributable to a single response mode, which is the fundamental resonant frequency of f_n .

Consequently, the acoustic pressure at this frequency, which is known as ‘spectrum pressure level’ must be established. This single degree of freedom (SDOF) theory will be given in detail in next section.

3.3. Theoretical Estimation of Response Levels and Stress Predictions

In the preliminary design process of the projects, analytical processes for stress prediction are commonly used. It is known that, for engineering purposes considerable simplifications are needed to estimate the response of practical structures. In this sense, Mile’s equation can be used which is derived for an elastic structure under random loading and simplified by assuming single degree of freedom theory. Mile’s equation is used for predicting stress response to acoustic loading and the use of simplified analysis procedures can give adequate accuracy for design purposes. It may readily be used to investigate response trends with changes in structural geometry [6].

According to ESDU item 72005 ‘*Estimation of RMS Stress in Stiffened Skin Panels Subjected to Random Acoustic Loading*’ [31], the RMS stress for a stiffened panel under acoustic loading on one side is given approximately given as;

$$S_{rms} = \sqrt{\frac{\pi f_n G_p(f)}{4 \xi_{mat}}} S_0 \quad (3.2)$$

ξ_{mat} is the viscous damping ratio of the vibration mode of frequency at f_n , S_{rms} is the RMS stress of the panel at the location of interest, a typically the potential failure location, S_0 is the stress due to a uniform static pressure at the same location on the panel and $G_p(f)$ is the input acoustic loading in terms of pressure PSD.

This equation is derived about 1950’s but still used to estimate the fatigue life of the panel with Miner’s cumulative damage hypothesis. Derivation of the equation based on some assumptions, principally modelled by a single rectangular thin linear elastic plate. Taking the major part of the vibration response of individual plates in the panel predominantly in their fundamental fixed edge mode is an essential assumption

that has to be re-emphasized. In accordance with this assumption, procedure usage is limited for the panels where the stiffeners are sufficiently rigid in bending to give approximately fixed-edge conditions for individual plates [29]. Another critical assumption is the pressure spectrum which is taken as constant, uniformly distributed and in phase over the whole panel at the frequency of the fundamental mode f_n .

The great improvements to the response prediction of Miles' SDOF formula can be the consideration of the spatial distribution of the load, consideration of multiple modes etc. The modes of plates under acoustic pressure are assumed to be uncoupled which is reasonable assumption if the displacements are small and the structural damping is light as typically the case for metallic aircraft skin structure. Powell, [27] took Miles equation one step further by taking multiple modes into account and the total response is represented as summation of the response in each mode. Also, he introduces 'Joint acceptance' phenomena which is a measure of the effectiveness of the pressure field to excite a particular mode as defined before. Blevins [27] also extends Miles equation and studied on how different spatial distributions of acoustic load affects the response of the structure.

Coming to the theoretical process and stress prediction used in finite element analysis programs for acoustic loading which will also be used in this thesis, the techniques are all depending on the frequency response and random vibration analysis.

Although fatigue analyses traditionally done with time variation of loading, since it may be very complex and time consuming, analysts prefer to work in frequency domain which has advantages in terms of definition of discretized loads in time series form, computational time and disc storage. *Fourier Transformation* is the way that converts time history of the data to frequency domain where *Inverse Fourier Transformation* can be applied to frequency domain to back to time domain.

Structural analysis can be done both in time and frequency domains. In time domain analysis, time history of loading is taken and transient analysis is carried out while output is also expressed in time domain. On the other hand, for the frequency

domain analysis, input is taken as PSD and the structure is modeled by a linear transfer function relating to input loading to obtain a stress output which is also in frequency domain.

MSC Nastran is used for the FEM analysis. Random response analysis is treated as a data reduction procedure that is applied to the results of frequency response analysis. Loading condition is taken as unity regardless of the form of the input type (pressure or acceleration) so the output response gives transfer function directly. Acoustic load is defined by its spectral density function. Random analysis uses the frequency response function result as a transfer function and coupled with the given input PSD to calculate stress values needed [32]. Stress results under given PSD pressure input is essential to be used in fatigue calculations as used in analytical procedure with Miner's cumulative damage rule which is expressed in the coming section.

In [31], conversion of root mean square pressure to spectral density of acoustic pressure is expressed as;

$$G_p(f) = \frac{P_{rms}^2}{Bandwidth} \quad (3.3)$$

3.4. Life Assessment under Random Acoustic Loading

Dynamic characteristics of the structure, description of acoustic field and determination of resultant stresses in the structure are explained as the route map of the acoustic fatigue consideration. In this section life assessment will be given in detail. Each of these steps have difficulties since it is not easy to understand the necessary interrelation among concepts in acoustics, dynamics stress analysis and fatigue of materials.

Failure time is predicted by Minor's Cumulative Damage Theory, but it should be prescribed that life estimates have not been particularly accurate. Ignorance of the presence of other loads acting on the structure, use of RMS stress level in the damage

calculations etc. are speculated as the probable reasons of discrepancies for the fatigue life calculations procedure used in this thesis.

3.5. Random Vibration Fatigue and Cumulative Damage Prediction

In real life, all the external effects are of dynamic nature. All fatigue type failure is dynamically induced. For the estimation of the life of the structure from an estimated RMS stress value against acoustic loading, random vibration fatigue endurance data are needed. The most reasonable and meaningful approach is likely to be the use of a random S-N curve. If such a curve is available for the material under consideration obtained from tests as close as the actual loading configuration; then, the probable life is given directly from a knowledge of the RMS stress in the component [27].

It is important to express that the material properties used in random vibration fatigue endurance $S_{\text{rms}}-N$ data differ from Wöhler curve used in conventional fatigue life calculations since the amplitude of the applied loading is random rather than the constant amplitude load arising from the sinusoidal loading of typical fatigue coupon tests as can be seen in Figure 3.5. In order to simulate the stress response of the structure exposed to acoustic load, representative test coupons are excited by load of random amplitude with zero mean. Calculated RMS stress is employed to generate $S_{\text{rms}}-N$ curve, where N is the effective number of reversals used in calculations of life under random loads and can be assumed to be given by half number of zero crossing [33].

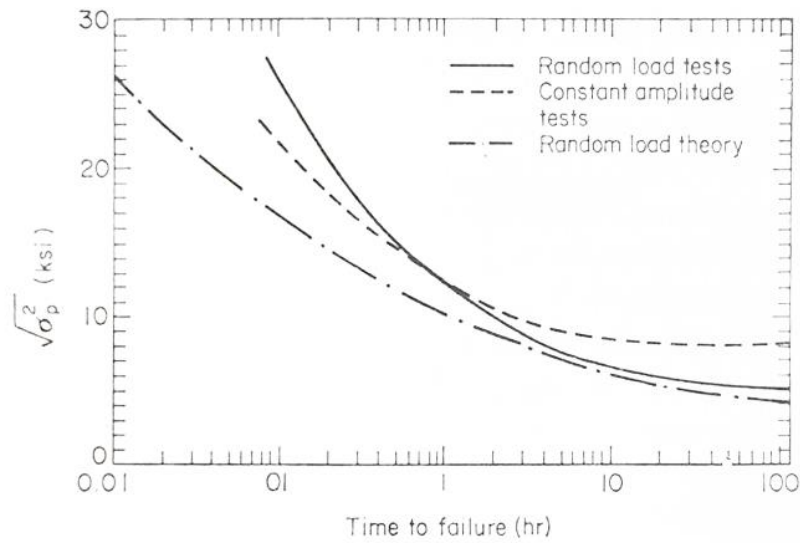


Figure 3.4. Comparative Fatigue Data for Sinusoidal and Random Loading [33]

Employment of logarithmic scale facilitates the calculations. The random vibration S_{rms} - N data are plotted on a logarithmic basis; thus, the best fit-least square fitting- to data is typically straight line with a slope given by $-1/n$ where n is known as a power index as illustrated in Figure 3.6.

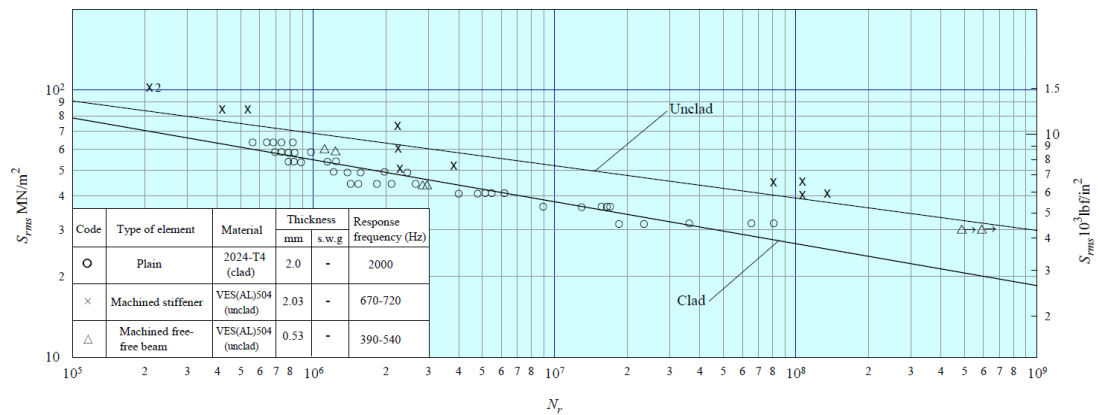


Figure 3.5. Available Data for Plain and Integrally Machined Specimen [34]

ESDU Data item 72015 [34] gives endurance limit characteristics of aluminum alloy 2024-T4 structural elements subjected to simulated acoustic loading as shown in Figure 3.6. This material data provides the estimation of structural-element life to failure $-N_f-$ (or crack initiation) in cycles at calculated RMS value of stress. It is unfortunate that, the material S_{rms} - N information available only for a limited number of materials.

Effects of complex acoustic loading histories are combined by Miner cumulative damage hypothesis.

$$Damage = \frac{n_1}{N_1} + \frac{n_2}{N_2} + \frac{n_3}{N_3} \dots \quad (3.4)$$

more generally,

$$D = \sum_{i=1} \frac{n_i}{N_i}$$

where damage caused by N_i cycles under the condition of load σ_i , N_i is the number of fatigue cycles corresponding to the current load level σ_i and D is the cumulative damage. Failure occurs when summation of damage increments gets equal to unity.

Miner's rule has been widely applied in endurance estimation because it is simple in principle. However, it may be inadequate in some respects and the reasons for these inadequacies should be recognized and allowed in design stages [35].

It is known that demonstration of the structure resistivity against sonic fatigue is all related with low amplitude cycling loading at high frequency excitation. Safe life and damage tolerance are two different design approaches for typical aeronautical structures that can be followed to guarantee the absence of catastrophic failures.

Damage tolerance concept tolerates the presence of a probable reason of failure and tries to contain the damage that can involve safe on the structure until a planned maintenance operation can find and repair it [36]. This concept requires inspection to find the damage before it becomes critical. Due to high number of cycles that should be applied on the element between inspections, no inspection program can ensure that a damage due to sonic fatigue will be detected. Therefore, structures under acoustic fatigue needs to use a safe-life approach but not damage tolerance. Safe-life methodology is designed in such a way to remain free from defects for its whole life.

CHAPTER 4

VALIDATION STUDIES ON FLAT PLATE

This chapter contains both analytical and FEM procedures for sonic fatigue calculations; however, it should be noted that sonic fatigue testing is still required to substantiate the estimated fatigue life. Engineering Science Data Unit and AGARD editions are taken as the references for the analytical and empirical procedures. For FEM analysis, stress analysis results due to random acoustic loading are used and then compared to the relevant random vibration fatigue endurance data in order to establish the component life, as performed in analytical procedure.

Prior to the statement of the route map, exclusive conditions should be given, where the procedure cannot be applied. Firstly, this study is valid only for the structures exposed to acoustic loading that are stationary random, so cannot be used for the time varying(transient) noise sources. For indirectly exposed structures, levels of excitations should be taken as the acoustic pressure itself, after levels of attenuation are taken into consideration. It should be expressed that, the analytical procedure given in this thesis is valid only for metallic structures. There exist other procedures given in ESDU and AGARD documents for composites where RMS strain values are used instead of stress. For the FEM consideration, modeling of composite and sandwich panels are totally different from metallic structures. Moreover, the process applied for analytical calculations is applicable on simple geometries such as a rectangular, flat or single-curved plate, but cannot be applied to more complex geometries (couple-curvature panels, non-rectangular plate etc.). However, sonic fatigue life calculations through FEM method can be used for complex geometries.

4.1. General Assumptions Regarding the Analysis

- It is assumed that the material properties are working within their elastic range and materials fully behave elastically.
- Modes of the structures are considered separately and results may be summed at a later stage if required.
- All the sound pressure levels taken into consideration are converted to a consistent single value which is chosen as 1-Hz bandwidth within the tolerance or range of each natural frequency.
- The calculated root mean square of the acoustic stress variations is assumed to be independent of and not interactive with any other stress state in the component as static, thermal or low frequency fatigue stresses.
- For a conservative estimate of RMS stress (σ_{rms}) a low value of damping ratio ($\xi_{\text{mat}}=0.017$) is used as referenced by ESDU item 72005 [31] and [8].
- The maximum RMS stress amplitudes together with the appropriate stress correction factors are compared with $S_{\text{rms}}\text{-}N$ random vibration fatigue properties for the material to predict damage done on the component for each case. All damage contribution should be summed at a later stage.
- A quasi-safe-life approach is preferred instead of damage tolerance philosophy as stated in the methodology section. Due to the very high number of cycles that could be applied on the element between inspections, a crack that would initiate could grow till failure of the element without being spotted. It is thus not possible to use a crack propagation approach against sonic fatigue; so, damage tolerance is not required.

With the provision of all these conditions, details related to analytical and finite element method are expressed in the following sections.

4.2. Analytical Method and Design Guideline

Considering all locations of acoustic sources (control surface movements, Auxiliary Power Unit (APU) intake and exhausts, aerodynamic flow, cavities and imperfections, engine etc.) the airspeed for each flight case may change the potential critical locations. In the domain of this thesis, flow over cavity is taken as the only acoustic source; however, effects of additional noise sources will be presented to be used if such a need arises. Generic clean cavity models will be used for the Mach number, spoiler and rear wall slope effects on cavity acoustic in Chapter 5; whereas, a simplified flat plate given in Figure 4.1 will be used for both analytical and finite element method for comparison/validation purposes.

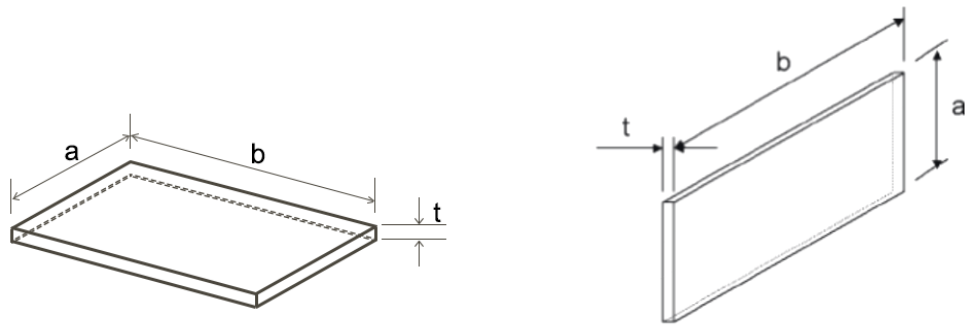


Figure 4.1. Simplified Flat Plate Geometrical Representation

Sonic fatigue can be defined as an accumulative damage on the structure resulted from changes in stress against varying sound pressure acting on it. The damage occurs when available energy overlap with the natural frequency of the structure. In the light of this definition, natural frequencies have to be determined for the extraction of acoustic energy in terms of sound pressure level by simple logarithmic manipulation. Then, the resultant variations in stress response of the structure for each natural frequency should be found depending on ESDU items. “*The estimation of RMS stress in stiffened skin panels subjected to random acoustic loading*” [31] gives a method of estimating RMS stress in rectangular skin panels subjected to random acoustic loading as;

$$\sigma_{rms} = \sqrt{\frac{\pi f_{n2} G_p(f)}{4 \xi_{mat}}} \sigma_{unitload} \quad (4.1)$$

where σ_{rms} represent stress at rivet line for the loading on one side.

Life expectancy calculations for natural frequencies are obtained manually using material random vibration fatigue properties. Total damage can be found by Miner's rule which is simple summation of all damage potential history.

The procedure given in Table 4.1 can be followed for the analytical calculation procedure based on simplified theory of response for stresses in rectangular plates under random acoustic loading.

Table 4.1. Analytical Guideline of Acoustic Fatigue Process

Acoustically Critical Location Determination	Location
Dynamic characteristics, Natural Frequency Calculation	f_1, f_2
Spectral Levels of Acoustic Sources for the Predetermined Location	SPL
Spectral Density Calculation for Relevant Natural Frequency	$G_p(f_n)$
Assess Structural Damping at f_n	ξ_{mat}
Stress Response at The Location of Probable Failure and Relevant Stress Correction Factors Is Necessary	σ_{rms}
Calculate Life and Damage	N_f
Interpret and Assess Results Against Assumptions	Result

Simplified rectangular flat plate is used for validation studies. Determination of the lowest natural frequency of the plate can be found via ESDU items. It can be checked with modal analysis response of FEM. ESDU item 87002 called “*Natural Frequencies of Rectangular Singly Curved Plates*” gives the lower natural frequencies of initial unstressed, thin, isotropic plates having either all edges simply supported or all edges fixed in both translation and rotation [37].

Representation of exact edge constraints is not possible. The natural frequency range is found by assuming that edges of the skin field are held in some way between all edges simply supported and all edges fixed. ESDU 87002 [37] clarifies this assumption depending on aerospace structures’ construction design as can be seen in Figure 4.2. It is typically constructed by stiffening members such as ribs, frames, stringers that divide the panel into plates. These plates vibrate together due to mechanical coupling and the natural frequency range has a number of intermediate modes.

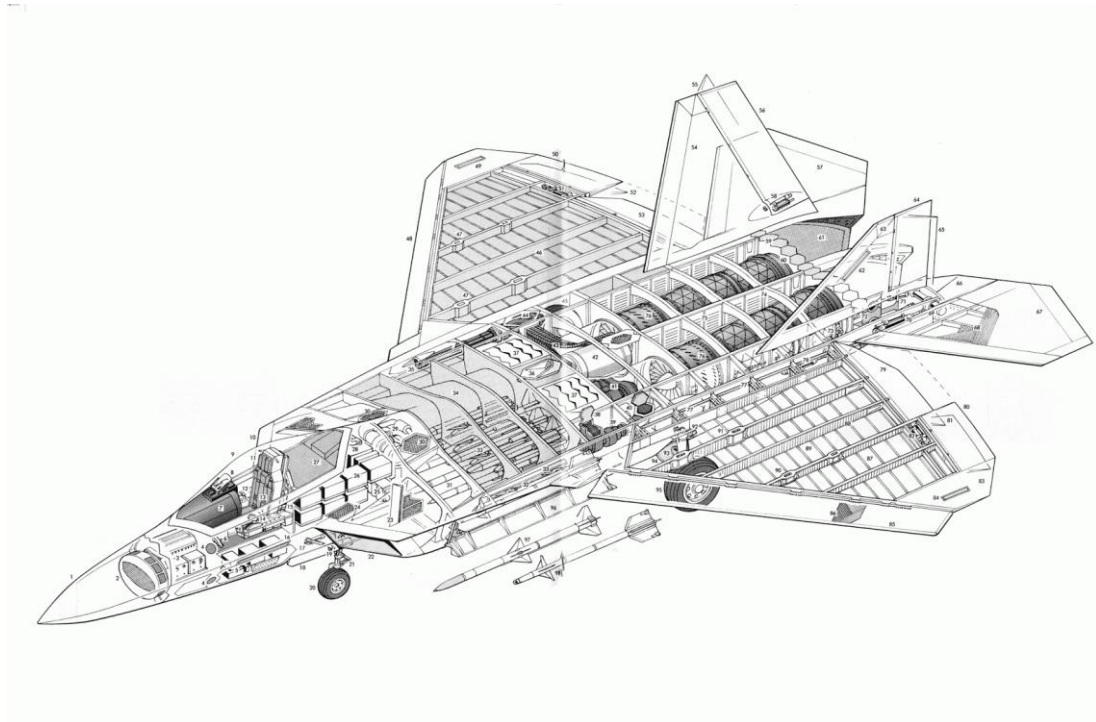


Figure 4.2. Aerospace Structures’ Construction Design Representation [38]

The lowest natural frequency in a frequency group is generally associated with a mode of vibration in which the response of plates is such that half waves across the plates on the two sides of a stringer are out of phase. If the stringers are of low torsional stiffness the lowest frequency for the panel will be close to the value given by [37] for a single plate with simply supported edges. The highest natural frequency in a frequency group is associated with a mode of vibration in which the half waves across the plates on the two sides of a stringer are in phase. This latter behavior corresponds to that resulting from fixed-edge conditions. Therefore, [37] provides upper and lower boundary values for the individual frequency groups.

For the extraction of dynamic characteristic of the structure, material description and fundamental properties (Density (ρ), Young's Modulus (E), and Poisson ratio (ν)) should be determined and Al2024 is chosen with E= 70600 MPa, $\rho=2780 \text{ kg/m}^3$ for the rest of the calculations. Fixed Poisson's ratio of 0.3 to calculate the natural frequencies of a rectangular plate and this value gives sufficiently accurate frequencies for all common structural metallic materials [37].

Analytical procedure starts with the determination of natural frequencies to be used for the noise levels extraction. The analytical calculation for the simply supported edge condition is given as;

$$f = V_s K_{mn} \frac{n^2 t}{b^2} \quad (4.2)$$

and for fully fixed-edge conditions as;

$$f = V_s K \frac{t}{b^2} \quad (4.3)$$

to be used for the upper and lower frequency range determination. V_s is the velocity parameter for plate material, K_{mn} is the natural frequency parameter for simply supported plate in (m, n)th mode, n and m are the mode number in y and x directions,

a and b are the length of plate in x and y directions, t is the thickness of the plate and K is the natural frequency parameter for fixed edge plates.

It should be noted that the fundamental natural frequency for the component being considered lies somewhere between the lowest natural frequencies for all edges simply supported (f_{n1}) and lowest natural frequency for all edges fixed (f_{n2}).

After determination of natural frequency range of the system, acoustic loading, which matches with significant energies in the acoustic environment covering the whole frequency domain, should be obtained. Acoustic spectrum of an aircraft may be broadband or discrete. It can be obtained directly from measurements or aerodynamic analysis. Energy level of the acoustic sources should be expressed in terms of sound pressure level. Each acoustic loading spectrum has to be converted into consistent bandwidth level before addition of contributions by each source to the total SPL value. 1-Hz bandwidth (SPL_{1HzBW}), measure of the energy available at a single frequency based around a bandwidth of 1-Hz, is used as a consistent level for the calculation process. Acoustic spectrum can be taken as directly in 1-Hz bandwidth- narrow band- or 1/3 octave band which needs conversion. ESDU 66016 [30] is referenced for simple conversion as;

$$\Delta SPL = 10 \log(\Delta f) \quad (4.4)$$

where

$$\Delta SPL = SPL_{total} - SPL_{1HzBW_{total}} \quad (4.5)$$

Discrete sources are not considered in the domain of this thesis; however, it can be expressed that narrow band analysis with 1-Hz bandwidth can be directly used without conversion. On the other hand, 1/3-octave bandwidth discrete sources are not as the same in broadband calculation process because the energy level within 1/3 octave range could have been shared over the whole bandwidth. It is why 1/3 discrete source values should not be used directly in the analysis of acoustic fatigue unless the process for deriving these values is fully understood.

In the scope of this thesis, generic SPL values will be used for the simplified flat plate calculations. Wind tunnel measurements from literature, converted in the form of PSD envelopes, are used for cavity wall calculations in Chapter 5. SPL values at the natural frequency of the structure by all the sources should be extracted and converted into consistent unit to be summed up to single value as placed in ESDU66017 [39];

$$\begin{aligned} \text{SPL}_{1\text{HzBW}_{total}} = & \text{SPL}_{1\text{HzBW}_1} \\ & + 10 \log \left(1 + 10^{\frac{\text{SPL}_{1\text{HzBW}_2} - \text{SPL}_{1\text{HzBW}_1}}{10}} \right) [dB] \end{aligned} \quad (4.6)$$

Next step is the conversion of the $\text{SPL}_{1\text{HzBW}_{total}}$ values to the equivalent pressure in terms of RMS from the summed total $\text{SPL}_{1\text{HzBW}_{total}}$ is given by ESDU 66018 [40];

$$P_{rms} = 10^{\frac{\text{SPL}_{1\text{HzBW}_{total}} - 4.69897}{20}} [Pa] \quad (4.7)$$

and then, power spectral density can be calculated as;

$$G_p(f) = \frac{P_{rms}^2}{\text{Bandwidth}} \left[\frac{Pa^2}{Hz} \right] \quad (4.8)$$

After calculation of excitation PSD values which is assumed to be applied at the fundamental natural frequency of the structure, sonic fatigue stress on the element has to be considered. ESDU 72005 [31] is used for the calculation of RMS stress for the all edges fixed condition (using f_{n2}) as;

$$\sigma_{rms} = \sqrt{\frac{\pi f_{n2} G_p(f)}{4 \xi_{mat}}} \sigma_{unitload} [Pa] \quad (4.9)$$

ξ_{mat} is the damping ratio which is taken constant 0.017 [8], [31] as referenced before and σ_{unitload} is the maximum unit load stress is which calculated using the method is given in *Roark's Formulas for Stress and Strain* [41]. For the simplified rectangular all edge fixed plate with uniform pressure load case, the stress amplitude at the fixings or edge of the skin field is given as;

$$\sigma_{\text{unitload}} = \beta_1 p \frac{b^2}{t^2} \quad (4.10)$$

where β_1 is derived from a linear interpolation, b is the length of the longest side of the skin field and t is its thickness. This stress value will be used for the fatigue life estimation by using $S_{\text{rms}} - N$ data (for metals) curve which gives life of failure in cycles for the structure against random stress variations.

In addition to this method, “*The Estimation of RMS Stress in Stiffened Skin Panels Subjected to Random Acoustic Loading*” [31] provides a graphical representation for estimating σ_{rms} . Details can be found in Section 4.4.1, Figure 4.5.

Analytically calculated stress value, found by using “*Roark's Formulas for Stress and Strain*” [41] expressed in equation (4.9), is validated by the stress value found by nomograph available in [31] as can be seen Figure 4.5.

In order to take the effect of geometrical and some other factors on estimated stress value, additional stress correction factors can be used. That is to say, such as counter sunk holes in a row at an edge distance should be calculated separately and must be considered when determining the value and location of maximum stress.

$$\sigma_{\text{rms}_{\text{corrected}}} = \sigma_{\text{rms}} k_{\text{total}} \quad (4.11)$$

where k_{total} is total stress factor as;

$$k_{\text{total}} = k_1 k_2 k_3 \dots \quad (4.12)$$

In order to estimate life expectancy of panel the estimated RMS stress will be compared with the relevant fatigue strength. ESDU 72015 “*Endurance of Aluminum Alloy Structural Elements Subjected to Simulated Acoustic Loading*” [34] supplies data on endurance of various type of joints in Aluminum subjected to acoustic loading.

The cycles to failure at each of the natural frequencies and flight phases concerned are the number of stress that would cause failure in a specific percentage of any samples tested at a particular RMS of stress. The percentage value is called the confidence limit value and can be 50%, 90 % or 99%, depending on the data supplier.

The equation of the graphical representation of $S_{rms} N$ (for metallic material) data is used in the analysis of acoustic fatigue and takes the form.

$$N_f = (k_{rms})^{b_{rms}} (\sigma_{rms\ corrected})^{-b_{rms}} \quad (4.13)$$

or

$$\sigma_{rms\ corrected} = k_{rms} (N_f)^{\left(-\frac{1}{b_{rms}}\right)} \quad (4.14)$$

where k_{rms} and b_{rms} are constants for the type of material, test specimen type and temperature and N_f is the safe life number of cycles to failure at the calculated RMS of stress found by $S_{rms}N$ curve. These data are available for limited number of materials and ESDU 72015 [34] will be used for the Al2024 material properties throughout the calculations in this thesis. If no data can be found available, then properties of a similar material, which is conservative in its random fatigue performance should be used.

After determination of number of cycles to failure, it is needed to find total amount of cycles required in order to calculate acoustic fatigue life margin. Required life calculation procedure employs the knowledge of predetermined design service goal (DSG) and scatter factor (SF) which is taken as 5 [16]. Scatter factor is directly related with confidence level used to obtained allowable curve; so, required life in cycles can be calculated as [16],

$$n_{total_{life_{cycle}}} = (DSG)(60)(60) (f_{n2})(SF) \quad (4.15)$$

DSG is represented in terms of hours and it shows the number of cycles that will be applied to the element studied during its life. Upper frequency, f_{n2} , is used for the fatigue life calculations for conservative approximation.

The damage is the value characterizing the degree of fatigue before a failure and is defined as follows;

$$Damage = \frac{n_{total_{life_{cycle}}}}{N_f} \quad (4.16)$$

If more than one flight phase is being considered or more than one natural frequency is being excited in the component at the same time, then the damage should be accumulated by a linear cumulative Miner's Law and then the resultant damage is expected to be less than unity.

$$\begin{aligned} Overall\ Damage &= \left(\frac{n_{total_{life_{cycle1}}}}{N_{f1}} + \frac{n_{total_{life_{cycle2}}}}{N_{f2}} + \frac{n_{total_{life_{cycle3}}}}{N_{f3}} \right. \\ &\quad \left. + \dots \right) \end{aligned} \quad (4.17)$$

$$Overall\ Damage = (Damage_1 + Damage_2 + Damage_3 \dots) \quad (4.18)$$

when the total damage reaches unity, then the component is expected to have failed.

4.3. Finite Element Method and Design Guideline

The objective of this part is to describe implementation of finite element analysis (FEA) process of the component in attempt to investigate its sonic fatigue life.

The user of finite element does not need to be aware of the details of intricacies of matrix inversion, eigenvalue calculation, Gaussian quadrature principles etc. in order to formulate the problem. However, a basic understanding of the engineering principles involved will help in the formulation of a model and interpretation of the results. This section provides a brief introduction to the basic considerations behind the FEM.

In a steady-state condition where applied forces can be defined as a function of frequency, the problem can be solved directly to produce the frequency response function. In addition, if the loading is applied in the form of random loading spectra, the results of a frequency response analysis can be statistically analyzed to yield results which can be interpreted in problems such as acoustic fatigue.

The representation of the real structure in FEM should include the load path and realistic loading distributions. Idealization of the real structure is converted into a model which involves an acceptable geometrical grid, set of elements, sizes, constraints or boundary conditions, material and loading. Structural loads, stresses, and deflections are then calculated based on this representative model. Accuracy of results are closely related to the source and quality of the information provided to FEM. Modelling, loading and constraint errors should be critically checked and eliminated, but may still be present. Thus, one should be on guard for unexpected results.

Within the scope of this thesis, the total maxima of the acoustic energy available from sources are used in the form of sound pressure level data as performed in the analytical method. Surface pressures can be specified as block pressures on the surface of elements or as pressure distributions by specifying the pressure at a grid point of an element. In the selected commercial FEM code, Nastran for analysis, random response analysis is used to calculate the stress response of the structure under acoustic loading. Through manual application of material fatigue properties, damage

and endurance life is calculated with found stress levels under predetermined conditions.

Finite element analysis methods enable the analysis of more complex structures with detailed acoustic loading characteristics in comparison to analytical methods. In addition, the analysis process provides contributions of higher-order modes and assessment of the frequency response of the structure across the relevant frequency range. Power spectral densities of RMS stress response levels are obtained as the outcomes of the analysis.

4.3.1. FEM Relevant Parameters

4.3.1.1. Mesh Size

The first step in the modeling process is to estimate the overall finite element (FE) mesh size and the level of details needed in the geometric approximations. Ideally, the mesh should be refined to a point where further refinement produces negligible change. It is important to focus on the critical sections to determine the proper mesh size; whereas, for noncritical sections the only expectation is the transfer of loads correctly to the other/critical areas.

As a general rule, mesh size for dynamic considerations is determined with respect to the maximum frequency of interest and its corresponding wavelength in the medium of wave propagation. The rule of thumb to estimate required mesh size in solids is to take six elements per wavelength corresponding to the maximum frequency of interest [32].

4.3.1.2. Material Definitions

The material used for the model is metallic and there exist different definitions of material as linear isotropic material, orthotropic or anisotropic material for 2D elements, and anisotropic material for solid elements in Nastran.

Material characteristic are expressed in terms of Young's modulus, Poisson ratio and density. An assumption can be made for material damping. In the scope of this thesis, damping will be added to the global damping applied to the complete model as 0.017 [8] [31] and isotropic, 2D shell elements are used.

It is further assumed that the material is a continuum and all material properties remain constant with respect to frequency although they are function of temperature in real life applications.

4.3.1.3. Properties

Properties defined for the model are the properties assigned to elements in order to introduce the behavior of the element under loading. Each element is associated through its property with the corresponding material characteristics.

4.3.1.4. Boundary Conditions

Representation of real physical boundary conditions is almost impossible in finite element analysis with the exception of the free-free case. The flexibility of attachment provides additional uncertainties for the clamped, fixed or simply-supported boundary conditions.

Representation of boundary conditions as accurate as possible enhances the reliability of the analysis since an accurate representation of the real element degrees of freedom allows an accurate frequency response and modal behavior of the finite element model.

4.3.1.5. Loading Conditions

Prediction and representation of the loads in real life is not easy due to the randomness of the nature. Therefore, theory of random process is preferred for complete description of acoustic loading. Nastran random analysis is treated as a data reduction procedure that is applied to the results of a frequency response analysis; as definition of dynamic loads is complicated due to their frequency varying nature. [32]

$$S_j(\omega) = |H_{ja}(\omega)|^2 S_a(\omega) \quad (4.19)$$

$S_j(\omega)$ is the power spectral density of the response, $H_{ja}(\omega)$ is the frequency response function similar to transfer function in terms of physically relevant variables and $S_a(\omega)$ is the power spectral density of the input source.

The relation in equation (4.19) is essential since it allows the statistical properties of the response of a system to random excitation to be evaluated via the frequency response technique [32]. MSC Nastran random analysis requires a preliminary frequency analysis to generate the proper transfer functions that define output input ratios. Spectral density of actual loads is multiplied with the squared magnitudes of results as given by equation (4.19) and ideally the inputs are unit loads as unit pressure on the surface.

Extraction of spectrum loading for the FEM analysis procedure is the same as the one used in analytical procedure. Conversion of 1-Hz bandwidth has to be performed if sound pressure levels are quoted in terms of 1/3-octave bandwidth. It is necessary to extract 1-Hz bandwidth contribution from the total SPL at its center frequency by the bandwidth correction technique imported from ESDU 66016 [30] as computed in the analytical method.

4.3.1.6. Frequency Range of Interest

In order to ensure no mode has been overlooked, the definition frequency range of interest is important in FEM analysis. Summation of the effective masses in the predetermined frequency interval is a way of verification which can be executed through modal analysis. If the effective mass computation is not representing the reasonable value of total mass, it may indicate errors in the analysis. Frequency range must be extended to cover all frequencies relevant to these analyses.

Moreover, validity of the applicable frequency band can be verified by cumulative RMS value on the critical elements. This value has to be ended toward an asymptote in the frequency band. Application of these validations are executed for flat plate and the results are provided in Figure 4.9 in Section 4.4.2.

Output frequency extraction is one of the most important parameters since each type of output extraction gives a typical response in RMS stress. The extraction should include the limits of frequency range and the natural frequency values in order to obtain accurate RMS stress values.

Determination of frequency increment can be associated with the damping value. Response at resonance is inversely proportional with damping; whereas half-power bandwidth is directly proportional to the amount of damping [32]. If the RMS stress response curves are not smooth, selection of frequency increment is too large and has to be redefined as proved in Appendix B Figures 0.1 and 0.2. It is known that for lightly damped structures ($\xi_{mat} < 0.1$) half-power bandwidth can be represented directly as $f_2 - f_1$ so;

$$f_2 - f_1 = (m - 1) \Delta f \quad (4.20)$$

$$\xi_{mat} \approx ((f_2 - f_1)/2)f_n \quad (4.21)$$

$$\Delta f = \frac{2 f_n \xi_{mat}}{m - 1} \quad (4.22)$$

m , f_n and ξ_{mat} are the number of frequencies within the half-power bandwidth, resonant frequency and damping ratio, respectively.

Sensitivity studies on frequency extraction are represented in Section 4.4.2 and the detailed explanation about frequency cards of Nastran can be found in Appendix B. It can be obviously seen from Figure 0.1 the stress response of the structure is directly related to output frequency extraction determination.

4.3.1.7. Monitoring Results

Frequency range has to include sufficient number of modes and frequency output extraction has to include important frequencies for the analysis as expressed before. Nastran random vibration “XY plots” and “RMS stress” analysis results are used for the response of the structure exposed to acoustic loading.

Principal RMS stress values can be calculated by using RMS values of critical elements' σ_x, σ_y and τ_{xy} stress components. Obtained principal RMS stress is a conservative estimation of RMS principal stress. Principal RMS stress is not the same thing as the RMS value of principal stress over the frequency range. Stress principal direction changes with frequency; therefore, it is not possible to determine principal orientation of the stress on the whole frequency range. Although principal RMS stress bring delamination of principal orientation which is involved in principal RMS stress, it is a good and safe way of fatigue calculations. Stress matrix for each element can be expressed as;

$$\begin{bmatrix} \sigma_x & \tau_{xy} \\ \tau_{xy} & \sigma_y \end{bmatrix}_{RMS} \quad (4.23)$$

The principal RMS stress corresponds the maximum eigenvalue of this RMS matrix and can be formulated as;

$$\sigma_{principal\ rms\ stress} = \frac{\sigma_x + \sigma_y}{2} + \sqrt{\left(\frac{\sigma_x - \sigma_y}{2}\right)^2 + \tau_{xy}^2} \quad (4.24)$$

Obtained principal RMS stress value may need some correction factors due to the quality of mesh or geometry effects. The overall stress factor is defined by multiplication of all correction factors as given in analytical procedure equation (4.11). The same fatigue life calculation in analytical procedure is applied after analysis of principal RMS stress.

4.3.2. Frequency Response Analysis

Frequency response analysis gives relationship between an arbitrary unit loading input and the response at a point for a linear time-invariant system. It is used to assess how the structure would respond in a linear manner. The effect of the

‘randomness’ of the loading input on the response is introduced by the input power spectral density [32].

The number of retained modes, the frequency increment and damping are the main influential factors that should be determined for an accurate frequency response analysis. Excitation force is another important parameter for involving the range of excitation frequency. Two or three times the range of excitation frequency is expected to be covered in order to have accurate results at the high end of the frequency range [32]. For example, if the excitation applied is about 500 Hz, modes with frequency up to 1000 to 1500 Hz should be analyzed.

4.3.3. Random Vibration Analysis

Random response analysis is widely used in automotive, aerospace, construction and defense industries for engine vibration, turbulence, and acoustic pressure analysis. Classification of dynamic environment is summarized in Figure 4.3. Structures are exposed to random loading or prescribed base excitations which are characterized in the frequency domain by a matrix of PSD functions. This function is statistical representation of time history loads and results are expected to be expressed as root mean square values or power spectral density result of displacements, velocities and stresses. MSC Nastran is preferred for the analysis in the scope of this thesis as mentioned before.

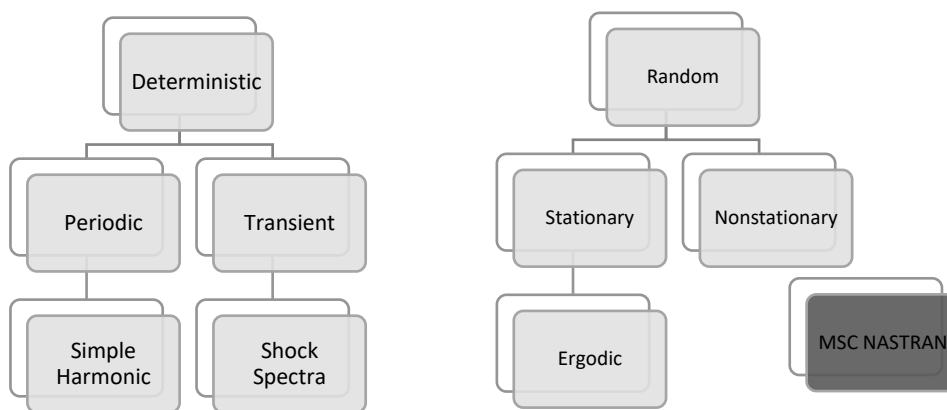


Figure 4.3. Classification of Dynamic Environment

FEM random response analysis for the structure exposed to acoustic pressure loading in MSC Nastran follows below procedure;

- ✓ Create model as normally developed in MSC Patran (Mesh generation, attachment of large mass nodes with RBE2's if there is any in the real model, material definition, property assignment, boundary condition etc.)
- ✓ Create time dependent load case which will involve unit pressure loading and boundary conditions.
- ✓ Non-tabular field is produced for the generation of frequency-dependent unit load.
 - Frequency-range determination is explained in detail before.
- ✓ With the formation of unity field, pressure load can be defined as unity time-dependent pressure load.
 - Time-dependent load case ought to be checked. Both boundary conditions and modeled pressure load should be involved in this time-dependent load case.
- ✓ MSC random-response toolbar has to be selected and change to frequency response applied loads analysis.
- ✓ Modal-damping and advanced-frequency output (FREQ cards) should be defined in this step, which affect the output results directly. Detailed explanations can be found in Appendix B.
- ✓ Frequency-response analysis basis is developed. Full run can be achieved.
 - Before full run of frequency response analysis, subcase selection should be checked for predefined time dependent load case selection. Output request can be selected in this toolbox also.
- ✓ Once the above steps are done, click apply to bring up the analysis form. Frequency response analysis is then completed.

The real power of MSC random will be apparent in the following steps;

- ✓ Inputs include the results of frequency response analysis performed and loading conditions in the form of PSD which should be defined under field as “non-spatial tabular input”.
- ✓ Return to MSC random and select XY plots this time to generate results by attachment of frequency response-.xdb file and assignment of PSD.
- ✓ Moreover, return to MSC Random and select RMS Analysis. Attach frequency response and input PSD as in XY plots. In addition, change the result type to obtain stress output results directly. Random response analysis is completed.

4.4. Flat Plate Application by both Analytical and FEM Method

4.4.1. Analytical Method of Flat Plate Application

It is expressed that analytical method is applicable not for the complex geometries but for the simple geometries such as flat or singly curved plates. Predominant form of skin vibration is the one in which individual plates within the stiffened panel vibrate independently in their fundamental fixed-edge mode. For flat plates, the thickness requirement is the ratio $b/t < 200$, for curved plates the ratio is greater depending on the curvature.

The process of analytical process can be divided into 4 steps as;

1st Step) Geometry of the component is established and ESDU library is used to calculate natural frequencies.

2nd Step) Maximum value of acoustic energy in accordance with the known natural frequencies is extracted to be used as acoustic loading.

3rd Step) Two different ways, ESDU 72005 [31] and “*Roark’s Formulas for Stress and Strain*” [41], are expressed for the stress response of the structure under acoustic loading.

4th Step) Manual application of material random vibration fatigue properties are used to determine the damage done on the structure.

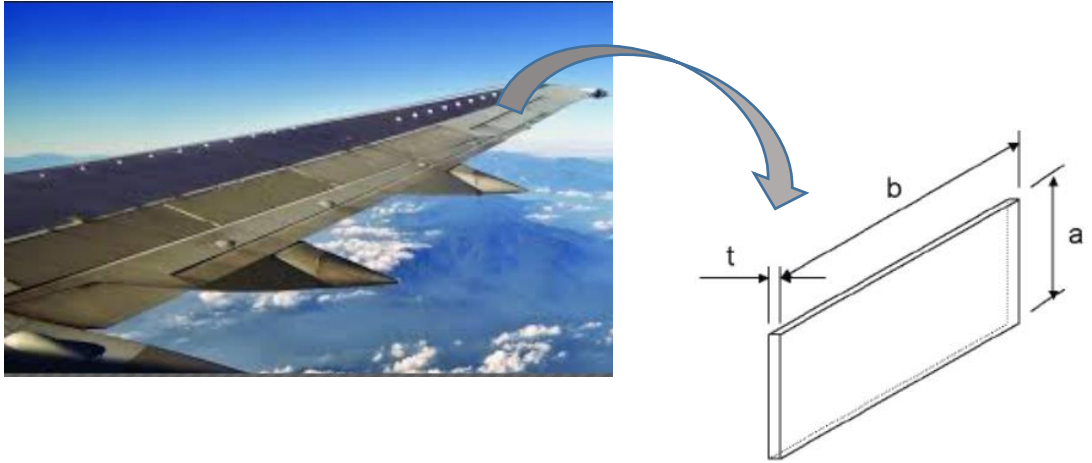


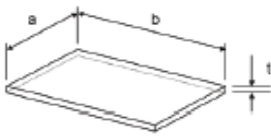
Figure 4.4. Panel of Wing Trailing Edge Simplified Representation

The flat plate analytical application may be used for a metallic skin of wing or any wetted substructure of the aircraft as shown in Figure 4.4.

Different bandwidth sources are chosen in order to show the conversion and contribution calculations of different sources to single 1-Hz bandwidth value. The analytical procedure, expressed by 4 steps before, is given in detailed as follows.

1st Step) Natural frequencies of the structure are calculated by ESDU 87002 [37].

Table 4.2. Geometrical Properties and Dimensions

Flat Plate	
Geometrical Properties & Dimensions	
Longer Length, a [m]	0.36
Smaller Length, b [m]	0.12
Thickness, t [m]	0.003
Radius of Curvature for Flat Plate, R [m]	100

Material information for Al2024;

Table 4.3. Material Properties

Al2024 Material Properties SI unit	
Density - ρ [kg/m ³]	2780
Elastic Modulus - E [Pa]	70.6e9
Rigidity - G [Pa]	27.2e9
Poisson Ratio, ν	0.3

Simply supported-edge conditions, calculation procedure needs the information given in Table 4.4 as [37];

Table 4.4. Natural Frequency of Simply Supported Edge Condition (ESDU 87002 Figure 1 [37])

Natural Frequency for Simply Supported Edge Condition				
m & n mode number in x & y directions	m, n=1,1	m, n=1,2	m, n=2,1	m, n=2,2
$\frac{a n}{b m}$	3	6	1.5	3
$\frac{b^2}{n^2 R t}$	0.048	0.012	0.048	0.012
K_{mn}	2700	2450	3500	2700
$V_s = \frac{\sqrt{E}}{5080 \sqrt{\rho}}$	0.99	0.99	0.99	0.99
$f = V_s K_{mn} n^2 \frac{t}{b^2}$ [Hz]	556	2021	721	2228

Lowest frequency from above 4 values $f_{n1} = 556$ Hz represents the lower limit of the natural frequency range. 552 Hz found by Nastran will be shown under Appendix C Figure 0.2.

Table 4.5. Natural Frequency for Fixed Edge Condition (ESDU 87002 Figure 2,4,6,8 [37])

Natural Frequency for Fixed Edge Condition				
m & n mode number in x & y directions	m, n=1,1	m, n=1,2	m, n=2,1	m, n=2,2
$\frac{a}{b}$	3	3	3	3
$\frac{b^2}{R} t$	0.048	0.048	0.048	0.048
K_{mn}	5750	15500	6600	16000
$f_n = V_s K \frac{t}{b^2}$	1186	3197	1361	3300

The lowest frequency in Table 4.5, $f_{n2} = 1186$ Hz represents the upper limit of the natural frequency range. 1166 Hz found by Nastran will be shown in Section 4.4.2 Figure 4.7.

Note that Appendix D can be checked for the values of frequency parameters K and K_{mn} values [37].

Edge constrain condition for the skin field cannot be known using a simple calculation technique; therefore, natural frequency is considered to lie between f_{n1} and f_{n2} , namely, 556 Hz and 1186 Hz [37]. The lowest 1/3-octave bandwidth containing the natural frequency range of 556 Hz and 1186 Hz has the center frequency f_c of 500 Hz and all these values are summarized in Table 4.6.

$$\Delta f = 0.23156 f_c = (0.23156)(500) = 115.78 \text{ Hz} \quad (4.25)$$

Table 4.6. Frequency Information of the Structure

Lower Limit_ f_1 [Hz]	556
Upper Limit_ f_2 [Hz]	1186
Lowest Centre Frequency_ f_c [Hz]	500
Bandwidth frequency_ Δf [Hz]	115.78

As the upper and lower frequency limits for the natural frequencies are known, total pressure spectrum level in the domain of frequency range can be extracted. If the natural frequency range is found to exceed the bandwidth, then note the lowest center frequency and the value of the highest SPL within the range to be conservative.

2nd Step) Assumed acoustic loading data is used for the flat plate calculations. Data is supplied in a different way to ensemble the summation and conversion to common bandwidth values and calculation procedure involving summation of contributions by different acoustic sources calculation procedure. The SPL values used are chosen as 120 dB in 1/3-octave bandwidth and 2 separate 110 dB discrete 1-Hz bandwidth sound pressure level, casually.

120 dB 1/3-octave band SPL is spread across a bandwidth of 115.78 Hz. The average of each 1-Hz bandwidth contribution using equations (4.4) and (4.5) is given by,

$$SPL_{1HzBW_{sub1}} = 120 - 10 \log(115.78) = 99.369 \text{ dB} \quad (4.26)$$

Two discrete sources in 1-Hz octave bandwidth needs no conversion but has to be summed up according to [39] as given in equation (4.6);

$$SPL_{1HzBW_{sub2}} = 110 + 10 \log\left(1 + 10^{\frac{110-110}{10}}\right) = 113.01 \text{ dB} \quad (4.27)$$

Addition of all consistent unit SPL values summation provides a single excitation level as;

$$SPL_{1HzBW_{total}} = 113.01 + 10 \log \left(1 + 10^{\frac{113.01-99.369}{10}} \right) = 113.194 \text{ dB} \quad (4.28)$$

Final SPL value can be converted to RMS pressure as given in equation (4.7) according to ESDU 66018 [40];

$$P_{rms} = 10^{\frac{113.194}{20} - 4.69897} = 9.136 \text{ Pa} \quad (4.29)$$

Related power spectral density by equation (4.8);

$$G_p(f) = 83.459 \text{ Pa}^2/\text{Hz} \quad (4.30)$$

It is assumed that there is only one natural frequency being excited. Therefore, no further extraction is required. If so, the same procedure should be applied for each case and each damage has to be summed up at the end of calculation.

3rd Step) Stress response calculation is investigated in two different ways.

1st alternative employs Roark's Formulas for Stress and Strain [41], to determine the maximum stress factor under unit pressure load acting over the skin field.

Table 4.7. Rectangular Plate All Edges Fixed, Uniform Pressure Over Entire Plate [41]

Rectangular plate, all edges fixed	Uniform over entire plate							(at center of long edge) $\sigma_{unitload} = -\beta_1 p \frac{b^2}{t^2}$
	$\frac{a}{b}$	1.0	1.2	1.4	1.6	1.8	2.0	∞
β_1	0.3078	0.3834	0.4356	0.4680	0.4872	0.4974	0.5	

$$\beta_1 \cong 0.498 \text{ for } \frac{a}{b} = 3$$

$$\sigma_{unitload} = \beta_1 p \frac{b^2}{t^2} = (0.498)(1)\left(\frac{0.12^2}{0.003^2}\right) = 796.8 Pa \quad (4.31)$$

Mile's equation given in equation (4.9) in ESDU 72005 [31] performs overall stress using $\sigma_{unitload}$ stress factor as follows;

$$\sigma_{rms} = \sqrt{\frac{\pi (1186)(83.459)}{4(0.017)}} (796.8) = 1.704 \cdot 10^6 Pa \quad (4.32)$$

The second alternative method doesn't need any pre-calculated unit load stress factor. It is obtained directly from the nomograph shown in Figure 4.5 from ESDU 72005 [31] for the determination of RMS stress of the structure.

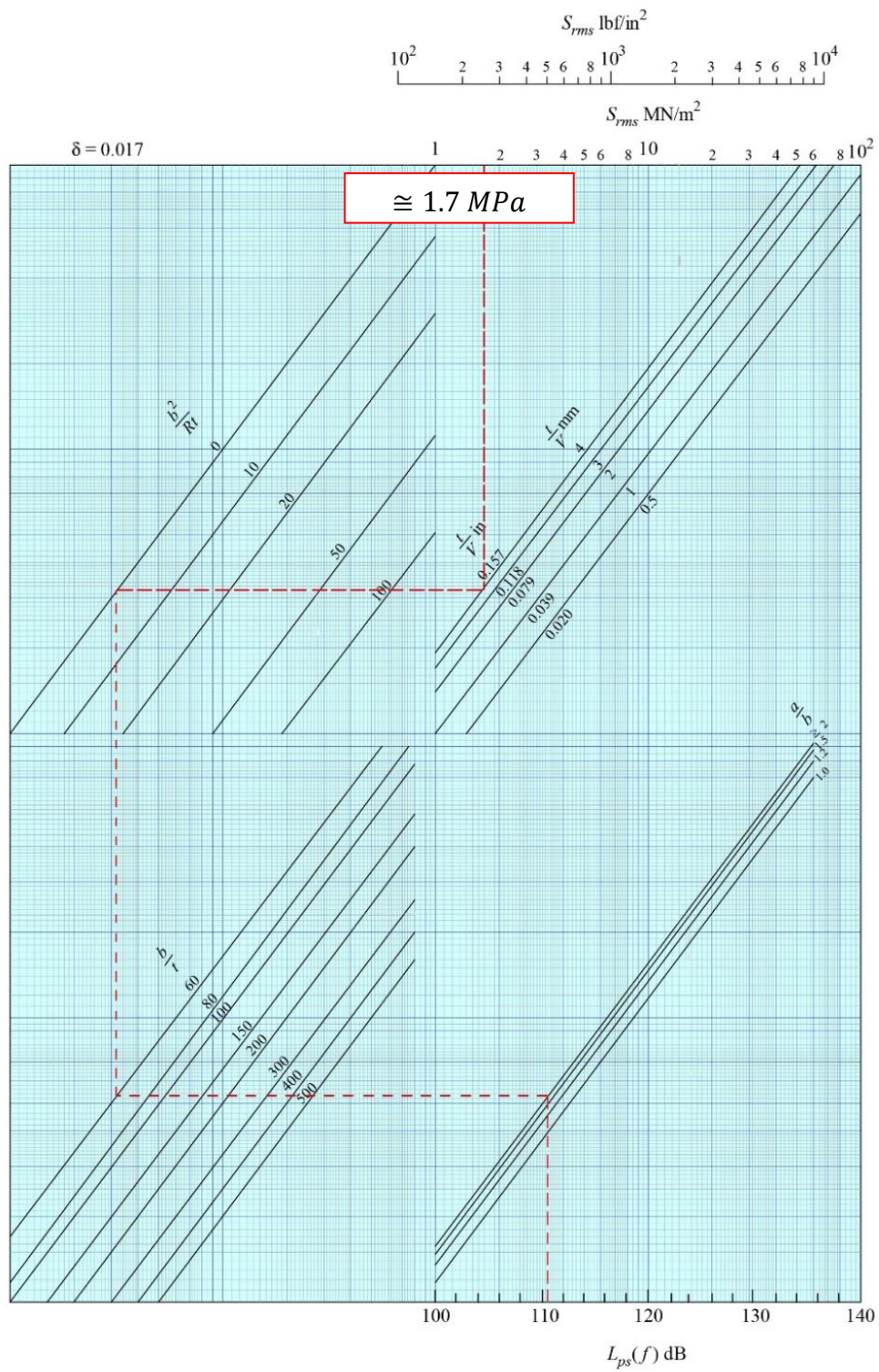


Figure 4.5 Low Range Stress Nomograph [31]

Table 4.8. Parameters needed for nomograph 1 in ESDU 72005 [31]

$\frac{a}{b}$	$\frac{t}{V_s}$	$\frac{b}{t}$	$\frac{b^2}{Rt}$	L_{ps}
3	0.003	40	0.0048	113.194

S_{rms} is read approximately as 1.7 MN/m² as found from Mile's equation (4.32).

Calculated stress may need correction stress factors due to the assumptions made. According to [42] all the assumptions contributed to significant stress difference by as much as factor of 2 between stress predictions and measurements. Therefore, equation (4.11) results in equation (4.33) as follows,

$$k_{total} = 2$$

$$\sigma_{rms_{corrected}} = 1.704 (10^6)(2) = 3.408 \cdot 10^6 Pa = 3.408 Mpa \quad (4.33)$$

4th Step) The safe life number of cycles to failure is calculated from random vibration $S_{rms}N$ data curve. Al2024-T4 is used from ESDU 72015 [34] and equation (4.13) yields as;

$$N_f = (485)^{6.33}(3.408)^{-6.33} = 4.266 \cdot 10^{13} \text{cycles} \quad (4.34)$$

The failure number of cycles that is fatigue life, has to be greater than required total life cycle of the structure to ensure safe life of the structure.

Total life cycle needs exposure time information. It can be taken as a generic value as 20000 hours arbitrarily for flat plate considerations.

According to the article “Acoustic Fatigue Analysis of Composite Outboard and Inboard Flap of a Commercial Aircraft” [16], scatter factor is taken as 5 and total life cycle equation (4.15) becomes,

The required condition can be checked to understand whether the structure could withstand to sonic fatigue.

$$n_{total\,lifecycle} = (t_{exposure})(60)(60)f_{n2} SF = 20000(3600)(1186)(5) = 4.27 \cdot 10^{11} \text{ cycles} \quad (4.35)$$

$$N_f \geq n_{total\,lifecycle} \quad (4.36)$$

$4.266 \cdot 10^{13} \geq 4.27 \cdot 10^{11}$ as required.

Damage can be calculated with the natural frequency, scatter factor and generic exposure time data information by equation (4.16) as follows;

$$Damage = \frac{n_{total\,lifecycle}}{N_f} = \frac{4.27 \cdot 10^{11}}{4.266 \cdot 10^{13}} = 0.01 \quad (4.37)$$

10^4 micro damage value characterizes the degree of fatigue before failure.

If different natural frequencies and exposure conditions are taken into consideration at the same time apply equation (4.17) or (4.18) for total damage occurred.

4.4.2. Finite Element Method Flat Plate Application

This section may be used to predict issues that arise from acoustic loading only in order to validate the results found in the analytical procedure. It does not provide any assessment of the combination with any other stress condition. Prediction of structural responses could be employed to:

- Predict environmental requirements,
- Predict acoustic fatigue,
- Predict the effect of structure design changes.

Finite element approach of fatigue performance under acoustic loading will be expressed step by step in this chapter. This method can be implemented on any part, but usually for parts with complex geometries, shapes or loading for which analytical methods cannot be applied.

Firstly, finite element model is built to calculate its natural frequencies through modal analysis. The energy in the environment at a frequency matching that of any natural frequency must be extracted. Finally, random pressure fields are applied to the finite element model to calculate response in terms of stress.

The same geometrical and material properties are applied with the same excitation values used in the analytical procedure. These values are directly taken from Table 4.2, Table 4.3 and equation (4.30) in analytical calculations, Section 4.4.1 for verification purposes.

$$\text{SPL}_{1\text{HzBW}_{total}} = 113.194 \text{ dB}$$

$$P_{rms} = 9.136 \text{ Pa}$$

$$G_p(f) = 83.459 \text{ Pa}^2/\text{Hz}$$

It is assumed that the structure is excited only at its fundamental natural frequency of 1166.8 Hz found by modal analysis. Power spectral density, 83.459 Pa²/Hz, is applied to the lower and upper limit range of the natural frequency. Center frequency shared in Appendix B can be checked for the frequency range, (1122.3 Hz -1412.5 Hz), that the structure's fundamental frequency lies on.

➤ **Mesh Checking's**

Mesh size criteria for dynamic models is directly related to wavelength size. A wavelength can be estimated by the frequency and speed of sound. Six elements per wave for approximately 10% accuracy is a general rule-of-thumb for solids in the maximum frequency range of interest [32]. Also, this method may be used to evaluate the quality of the calculated eigenvectors.

$$meshsize \leq \frac{\lambda}{6} \quad (4.38)$$

$$\lambda = \frac{v}{f} \quad (4.39)$$

where λ , v and f are wavelength, speed of sound and frequency of interest, respectively.

For the frequency range 0-5000 Hz and speed of sound (in dry air at 20 °C) 343 m/s, minimum required mesh size can be calculated as follows:

$$\lambda = \frac{343}{5000} = 0.0686 \text{ m}$$

$$meshsize \leq \frac{0.0686}{6}$$

$$meshsize \leq 0.01143 \text{ m}$$

Required minimum mesh size is found as 0.01m approximately, for the frequency range up to 5000 Hz. Although minimum required mesh size is obtained, mesh convergence check is done for varying mesh sizes and shown in Table 4.9. The following basic steps are required for manual mesh convergence analysis:

- Create a mesh using the fewest, reasonable number of elements and analyze the model.
- Recreate the mesh with a denser element distribution, re-analyze it, and compare the results to those of the previous mesh. Notice where high deformations or high stresses occur, perhaps it is worth to refine mesh in those regions.
- Keep increasing the mesh density and re-analyzing the model until the results converge satisfactorily.

Table 4.9 Mesh Size Comparison

Mesh size	1 st Natural Frequency [Hz]	2 nd Natural Frequency [Hz]	3 rd Natural Frequency [Hz]
0.06	1267.9	1838.2	2464.1
0.03	1157.5	1266.7	1466.1
0.01	1164.7	1290.2	1523.1
0.005	1166.8	1298.2	1539.9
0.003	1167.3	1300.1	1573.7
0.001	1167.8	1300.5	1574.1

 Minimum required mesh size

 Determined to be used throughout the thesis mesh size

It is obviously validated that minimum 0.01 m of mesh size should be used to represent structure's dynamic characteristics as increase mesh results are highly close to values obtained for 0.01m. In order to ensure accuracy of results 0.005 mesh size given in Figure 4.6 will be used for the rest of the calculations.

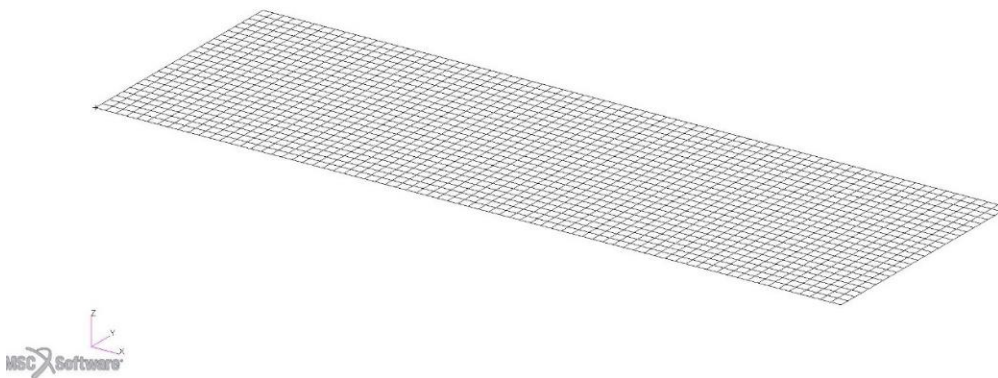


Figure 4.6. Finite Element Model Mesh of Flat Plate

First 3 mode shapes of flat plate for selected mesh size of 0.005 m are shown in Figure 4.7 just to ensample the mode shape of the flat plate.

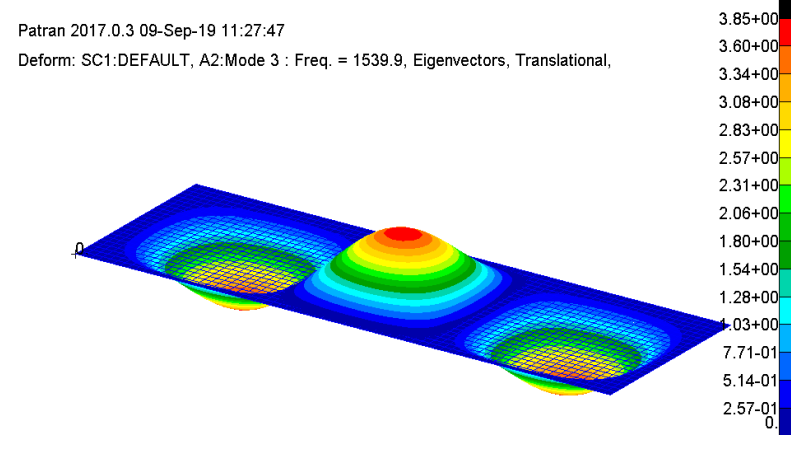
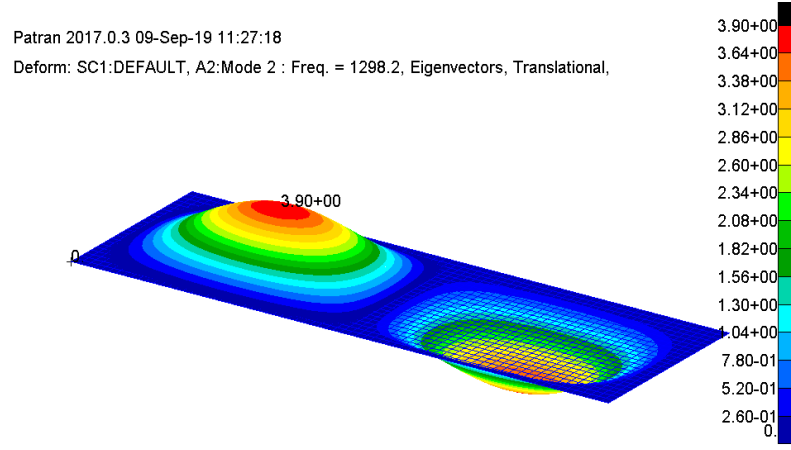
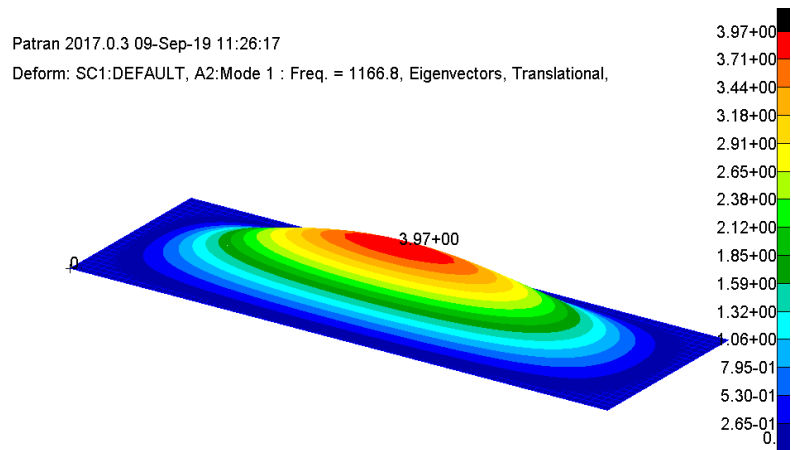


Figure 4.7. First 3 Modes of the Flat Plate

Table 4.10. Conformity of the items for meshing

	Status	Notes
Respect of Mesh Size	✓	
Respect for Element Normal Orientation	✓	
Zero Element Duplicated	✓	
Zero Free Edge Unjustified	✓	
Set unit system	✓	Model unit system is N/m/Hz/kg

The model used for validation purposes is simple flat plate; therefore, it does not require complicated mesh checking. However, for more complex structures, percentage of number of triangle elements, free edge elements' quality, zero free edges justification, aspect ratio/wrap angle/skewness/distortion of the elements etc. should be checked.

➤ **Material Definition, Properties and Damping**

Needed material characteristics is Young Modulus, Poisson coefficient and density. The damping ratio is set to 0.017 [8], [31].

Table 4.11. Damping Definition .bdf file of NASTRAN

TABDMP1 1 CRIT
.1 .017 5000. .017 ENDT

➤ **Validity of Natural Frequency Band and Modal Frequency Extraction**

Verification of cumulative RMS stress (CRMS) value is checked on the elements estimated critical. Element 865 is selected as critical which is at the center of long edge as is expected [41] and proved by maximum 2D principal stress results as can be seen in Figure 4.8.

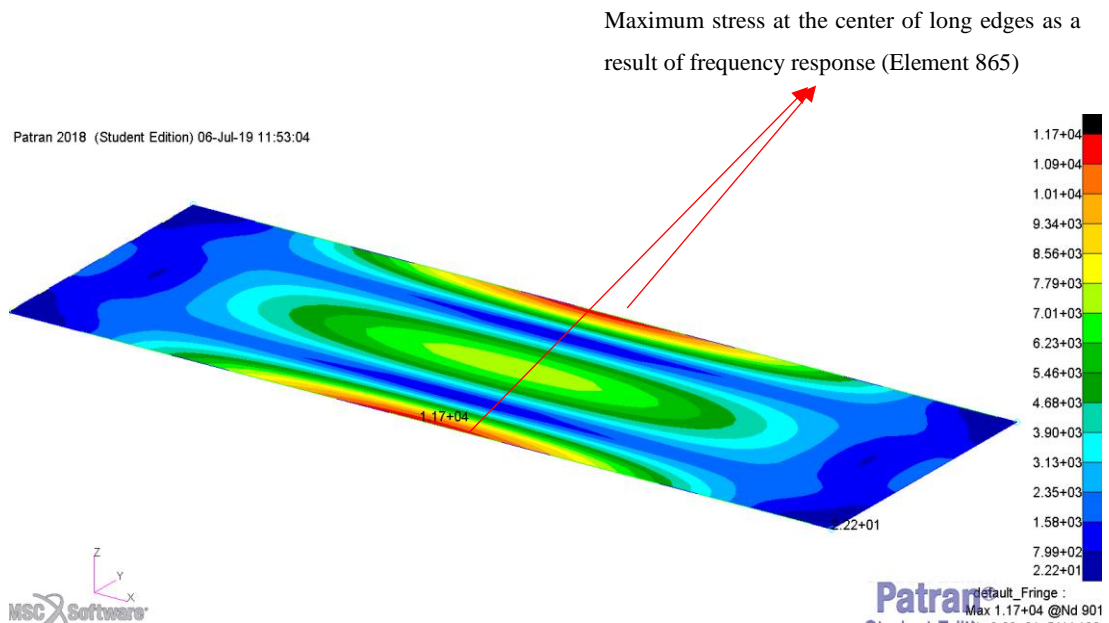


Figure 4.8. Frequency Response - Maximum Stress Location and Critical Element

CRMS curves tend toward an asymptote on the frequencies band 0-5000 Hz (along X, Y and XY) which can be thought as the evidence of the reliability of frequency range.

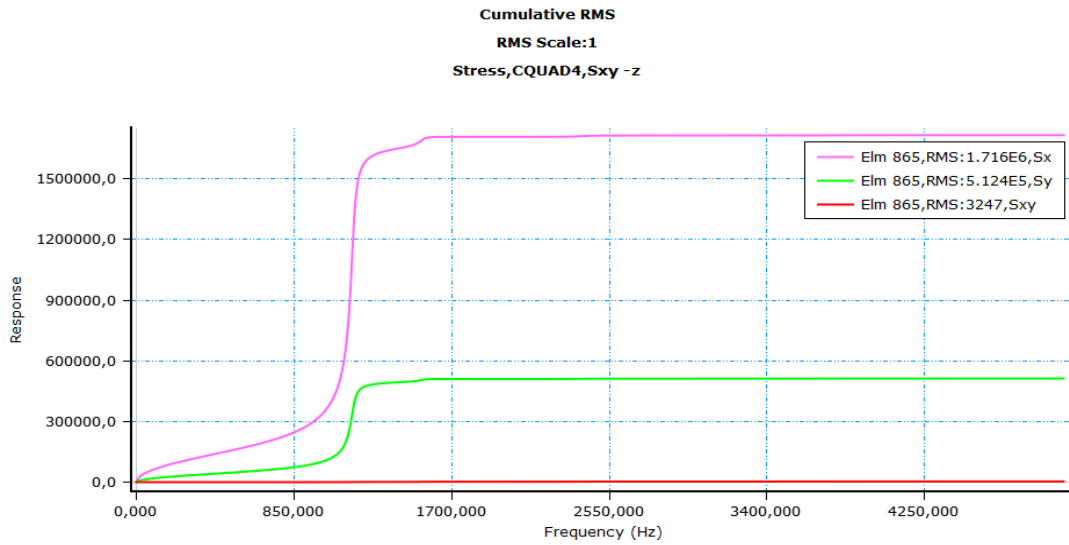


Figure 4.9. Cumulative RMS stress -Element 865

The modal base calculation provides modal frequencies and their associated effective modal masses. This calculation has been performed on the 0-5000 Hz frequency range. The self-consistency of this range for given item is deemed appropriate for this particular case.

Total effective mass fractions are checked whether sufficient modes have been retained or not. It directly shows how much of total possible rigid body mass is represented by the extracted modes. Modal effective mass fractions, on the other hand, shown the mass fractions for each mode. It helps to predict what the important modes are.

Table 4.12. Total Effective Mass Fraction

Total Effective Mass Fraction					
Reference Point at Origin of Basic Coordinate System					
T1	T2	T3	R1	R2	R3
1.42E-17	3.22E-20	6.67E-01	6.17E-01	6.47E-01	5.37E-19

The model represents 66.7% of total mass by 0-5000 Hz range with 14 modes extraction. If more complex geometries are excited with random acoustic loading that includes more than one mode contribution, total effective mass fraction is expected to be higher than % 80-90. However, the sum of total effective mass on all frequency range contains at least % 50 of global mass is almost acceptable for the simplified flat plate.

Table 4.13. Modal Effective Mass Fraction

Modal Effective Mass Fraction							
For Translational Degrees of Freedom							
Mode	Frequency	T1		T2		T3	
NO.		Fraction	Sum	Fraction	Sum	Fraction	Sum
1	1.17e+03	7.21e-36	7.21e-36	5.22e-37	5.22e-37	5.39e-01	5.39e-01
2	1.30e+03	2.47e-35	3.19e-35	1.30e-36	1.82e-36	6.58e-19	5.39e-01
3	1.54e+03	7.13e-36	3.90e-35	1.05e-36	2.87e-36	7.59e-02	6.15e-01
4	1.90e+03	2.20e-34	2.60e-34	1.55e-35	1.84e-35	1.70e-17	6.15e-01
5	2.39e+03	2.85e-35	2.88e-34	1.80e-34	1.98e-34	3.33e-02	6.48e-01
6	3.01e+03	5.12e-27	5.12e-27	3.26e-29	3.26e-29	3.37e-17	6.48e-01
7	3.13e+03	3.80e-28	5.50e-27	6.93e-31	3.33e-29	4.30e-18	6.48e-01
8	3.27e+03	3.81e-26	4.36e-26	2.61e-28	2.95e-28	1.15e-19	6.48e-01
9	3.51e+03	2.57e-27	4.62e-26	6.69e-28	9.63e-28	6.62e-19	6.48e-01
10	3.74e+03	2.04e-23	2.04e-23	1.73e-25	1.74e-25	1.92e-02	6.67e-01
11	3.85e+03	3.58e-23	5.62e-23	6.60e-26	2.40e-25	2.06e-19	6.67e-01
12	4.30e+03	2.15e-24	5.84e-23	1.42e-24	1.67e-24	2.49e-19	6.67e-01
13	4.58e+03	9.61e-20	9.61e-20	5.27e-22	5.28e-22	6.70e-17	6.67e-01
14	4.86e+03	1.41e-17	1.42e-17	3.16e-20	3.22e-20	4.16e-18	6.67e-01

Dominant modes are selected by reviewing the effective modal masses in only the excitation axis (T3). 1st mode, 3rd mode and 5th mode contributions to overall mass fractions are 53.9%, 7.6% and 3.3 %, respectively. Summation of first 5 modes represents 64.8% of total mass whereas 14 modes represent 66.7 %. It can be concluded that considering first 5 modes only (0 -2500 Hz frequency range approximately) instead of 14 modes (0 – 5000 Hz frequency range) makes almost no difference if mass fractions are considered only. However, as the acoustic excitation frequency used is high, the analysis ranges up to 5000 Hz is preferred for this particular case.

➤ **Acoustic Loading and Boundary Conditions**

The loading condition used for this method is unit pressure applied on lower panel of the surface as illustrated in Figure 4.10. Fully fixed edge conditions shown in Figure 4.11 is considered as used in the analytical procedure for conservatism.

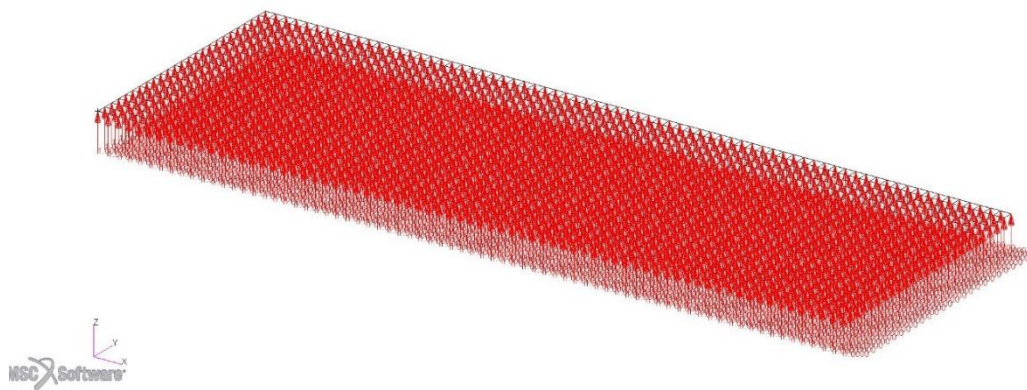


Figure 4.10. Unit Pressure Excitation for Frequency Response Analysis

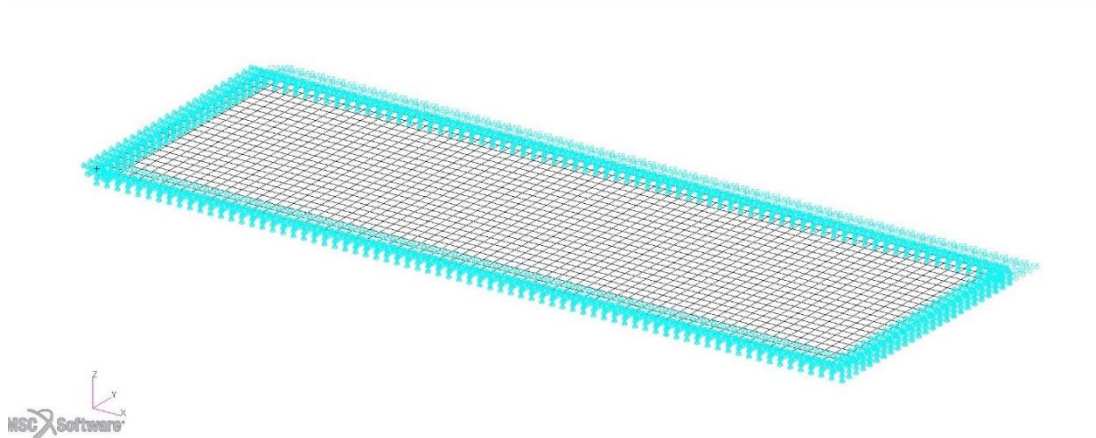


Figure 4.11. Fully Fixed Boundary Condition

The acoustic loading spectrum for known SPL values were calculated in analytical method. For validation purposes, the same assumptions are tried to be provided to the finite element model of the flat plate. As it is assumed that the structure is excited at its fundamental natural frequency only, calculated PSD is applied to the frequency range of center frequency table (Appendix A) that the fundamental frequency lies on. However, for real life applications to be shown for cavity analysis in Chapter 5, the acoustic loading spectrum has to be obtained for each flight case and applied to the structure as a spectrum. An example of real loading for different 2 flight conditions can be found with representative SPL values in Table 4.14.

Table 4.14. Example of Generic SPL Spectrum for 2 Different Flight Cases

<i>1/3-Octave Band Center Frequencies</i>													
Phase [Hz]	50	63	80	100	125	160	200	315	400	500	630	800	1000
Take off [dB]	140	141	137	139	135	132	132	130	129	129	129	124	122
Cruise [dB]	115	117	118	118	121	122	124	125	126	127	127	128	128

Table 4.15 is taken from the RANDPS chart of the Nastran for flat plate analysis which is the probabilistic magnitude of each load source defined by spectral density functions by definition [32].

Table 4.15. Spectra $G_p(f)$ for Validation Analysis - .bdf file of NASTRAN

```
RANDPS,101,1,1,1,0.,300022
$
$ From Patran Field: psd
TABRND1, 300022,log,log,,,,,+
+, 1122.30, 83.4590, 1412.50, 83.4590,endt
```

➤ **Frequency Extraction and RMS Stress**

Almost the most important section of the random vibration analysis in Nastran is the determination of output frequency extraction. Each type of output extraction gives a typical response in RMS stress. Of course, the “finer” the output extraction, including boundaries of frequency range and the natural frequency values, the closer the RMS value is to the reference value. **FREQ**, **FREQ5** and **FREQ3** cards are used for the analysis and detailed information about **FREQi** cards of Nastran are provided in Appendix B.

Sensitivity analysis is carried out for the determination of frequency extraction and the results can be found in Appendix B Figure 0.1.

Table 4.16. Frequency Extraction **FREQi** Card

```
FREQ 1 .1 5000.
FREQ5 1 .1 5000. 1.
FREQ3 1 .1 5000. LINEAR 100 1.
```

The random response analysis results are shown in Table 4.17.

Table 4.17. Stress Value for Element 865

@ Element 865	RMS stress [Pa]	Frequency [Hz]
σ_x at Z1	$1.72 \cdot 10^6$	@1185
σ_y at Z1	$5.12 \cdot 10^5$	
τ_{xy} at Z1	$3.25 \cdot 10^3$	
σ_x at Z2	$1.72 \cdot 10^6$	
σ_y at Z2	$5.12 \cdot 10^5$	
τ_{xy} at Z2	$3.25 \cdot 10^3$	

All these values are checked and matched with RMS stress results of Nastran random vibration analysis.

All RMS response results and XY plot graphs of stress response of the structure are shown on Figures 4.12, 4.13 and 4.14.

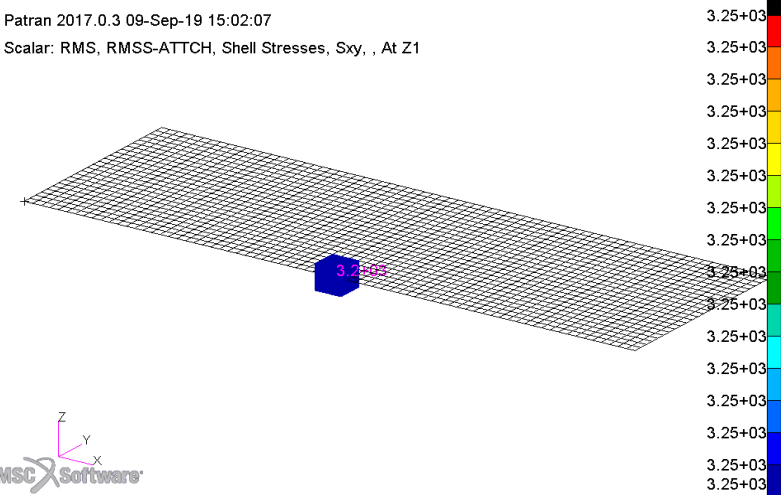
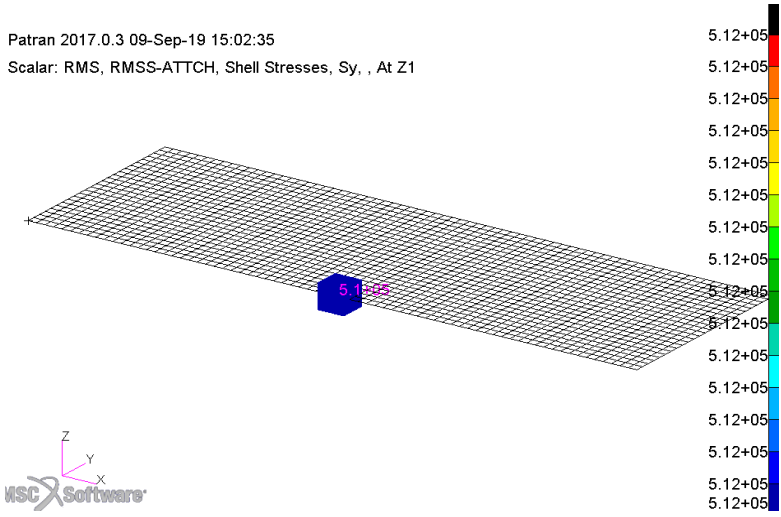
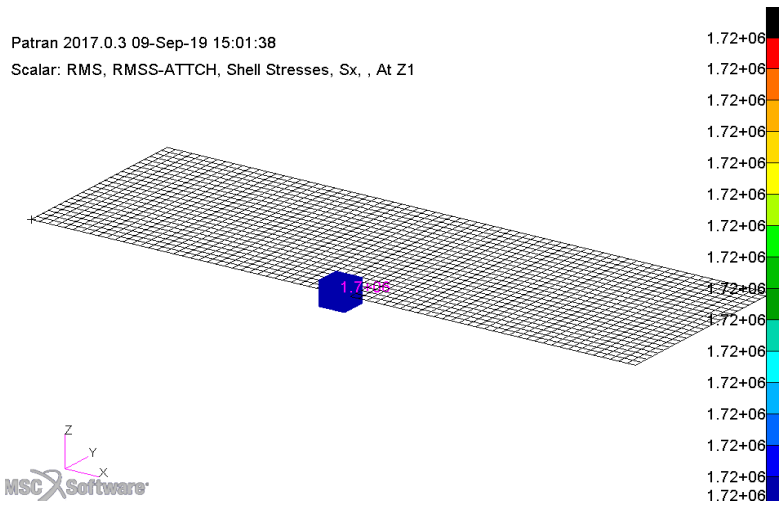


Figure 4.12. RMS Stress Results of Elements 865 @ Z1

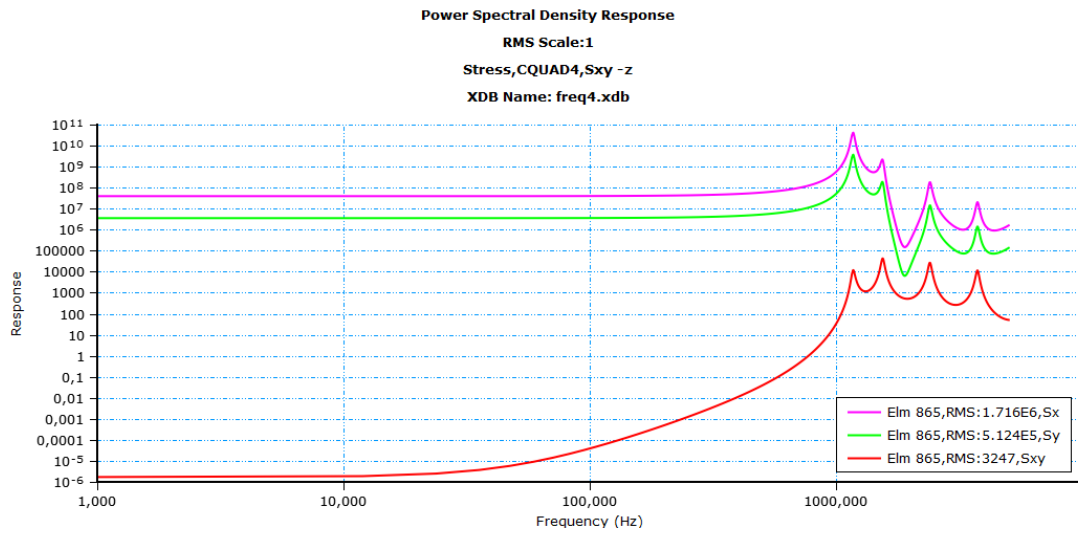


Figure 4.13. XY Plot log-log Scale Results of Stress Response

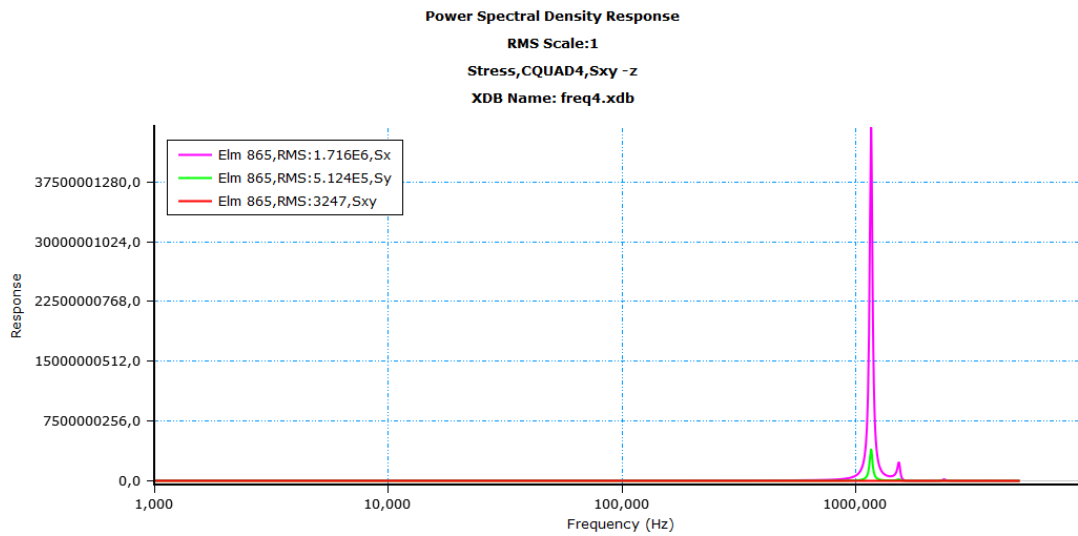


Figure 4.14. XY plot in lin-log Scale Results of Stress Response

Maximum value of Z1 or Z2 directions has to be taken for principal stress calculation; however, in this particular case both Z1 and Z2 results of stress values for element 865 are the same and obtained as follows;

$$\sigma_x = 1.72e6 Pa$$

$$\sigma_y = 5.12e5 Pa$$

$$\tau_{xy} = 3.25e3 Pa$$

Principal RMS stress is calculated by equation (4.24) as;

$$\sigma_{principal\ rms\ stress} = \frac{\sigma_x + \sigma_y}{2} + \sqrt{\left(\left(\frac{\sigma_x - \sigma_y}{2}\right)^2 + \tau_{xy}^2\right)} = 1.72e6\ Pa$$

➤ **Establishment of Material Data and Life Expectancy**

Expected stress levels are obtained and verified with the analytical method under section 4.4.1 equation (4.32) and the low range stress nomograph Figure 4.5.

After this stage, the 4th step can be followed in section 4.4.1 for life expectancy calculations.

4.5. Comparison of Analytical and Finite Element Method

Table 4.18. Comparison of Analytical Method with FEM

	<i>Analytical Method</i>		<i>Finite Element Method</i>	
Natural Frequency Comparison (Simply supported / Fully Fixed)	556 Hz	1186 Hz	552 Hz	1166 Hz
Stress Level Comparison	Roark's Formulas for Stress and Strain [3]	Low Range Stress Nomograph ESDU 72005[2]	1.72e6[Pa]	
	1.704e6 [Pa]	1.7e6 [Pa]		

For the interpretation of results, cumulative damage must be less than unity where all conservative measures have been provided.

In case the results are not found acceptable then further work is needed: the inputs to the analysis should be considered and questioned as to their validity and other mitigating factors must be considered. When all these parameters are checked and

acceptable results cannot be obtained, then changes to the material damping characteristics, changes in geometry (thickness or distance between stiffeners) or stiffness of the component or the supporting structure may be considered.

Simplified flat plate geometry does not yield any significant difference between FEM and analytical process under SDOF assumption; however, for more complex geometries a poor level of accuracy of the analysis may need to be raised to give a more detailed analysis than the analytical procedure. In other words, forced response analysis is required where natural frequency and stress arising from the pressure variations have to be found accurately for complex geometries and real case loading applications.

CHAPTER 5

CAVITY STUDIES

This chapter of the thesis is devoted to the structural response of critical wall of the cavity that represents internal weapon bay of the high-performance aircraft. From the structural point of view, inclusion of a component in design process is critical for the successful operation of the designed component. Therefore, investigation of the critical section of the component and focusing on this part is needed. Weapon bay is one of the most critical section of the combat.

Flow characteristics over the cavity was dealt earlier with a reference to Figure 1.1. Top of the rear wall is the location that the shear layer impacts onto the rear of the cavity leading to high fluctuating pressure levels [23]. That's the reason behind that most experimental measurements and CFD analysis presented in the literature reach a common conclusion that rear wall is the most critical section of the cavity. Many papers presented in the review of literature mentioned in Chapter 2 as [19], [23] [25], [26] etc. support significance of the high levels of pressure on the rear wall of the cavity.

One of the most relevant papers to be used in the scope of this thesis is issued by Defence Science and Technology Laboratory [23]. The main objective of this paper is the comparison of the experimental data for the baseline weapons bay and computational fluid dynamics results obtained using Detached Eddy Simulation (DES). Boeing/AFRL 1303, 1:10.8 scale generic wind tunnel model is used in this research. Two comprehensive wind tunnel experiments (in November 2002 and March 2012) and high fidelity CFD methods conclude that, internal weapon bay flow field is highly complex both for prediction and measurements.

Likewise, all the sources mentioned before, [23] indicates the rear wall's importance with the comparison of Figure 5.1 and 5.2, obviously.

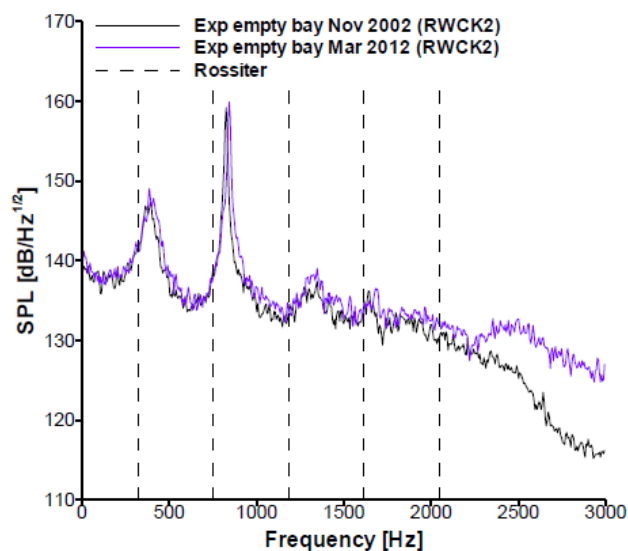


Figure 5.1. Measured local SPL spectra on the cavity rear wall for the empty bay case. Rossiter mode predictions are also known: $M=0.85$ $\alpha = \beta = 0$ [23]

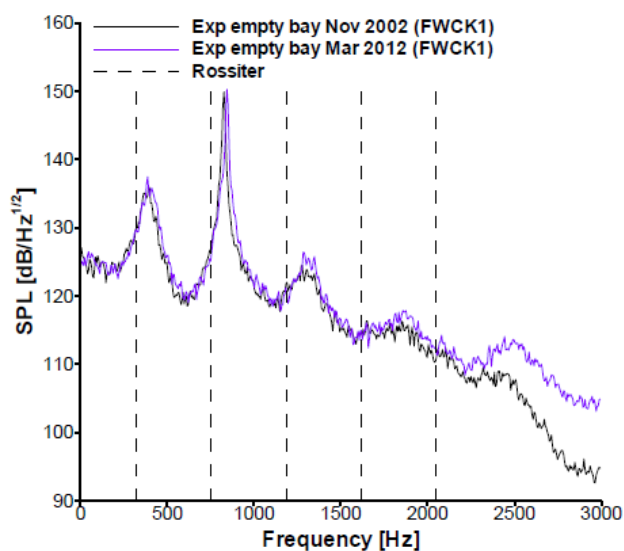


Figure 5.2. Measured local SPL spectra on the cavity front wall for the empty bay case. Rossiter mode predictions are also known: $M=0.85$ $\alpha = \beta = 0$ [23]

Maximum ceiling length of 251.8 mm with depth of 46.629 mm and width of 60.8 mm cavity shape is used for the measurement. $L/D = 5.4$ is classified as open type cavity flows. The cavity, 1303 Unmanned Combat Aerial Vehicle (UCAV), empty bay rear wall measurement (at a Mach number 0.85, zero angle of attack and side slip) raise up to 175 dB, Figure 5.3, with the combination of high level of broadband and narrowband, Rossiter tones (OASPL) [23]. This value is likely to cause damage of the structure of the airframe and the equipment within the weapon bay.

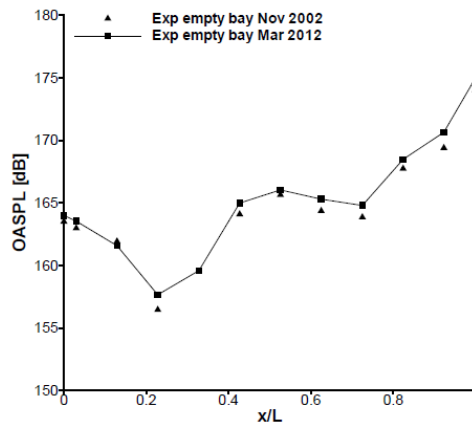


Figure 5.3. Measured OASPL as a function of Cavity Location (x/L) for the empty bay case: $M=0.85$
 $\alpha = \beta = 0$ [23]

In order to reduce the fluctuating pressure levels of this magnitude, palliative methods are developed such as spoiler at the leading edge and swept rear wall. Mach number's effect, in the structural point of view will be investigated in addition to these most favorable two controlling methods.

5.1. Cavity Rear Wall Analysis

Depending on the common conclusion of the experimental and measurement results of the sources in the literature, only critical rear wall is modeled with different boundary conditions. The rear wall of the cavity with 3 different boundary conditions is analyzed to investigate the Mach number, spoiler and swept rear wall effect on structural response in terms of stress. The main goal is to feed the design process for the determination of ribs and spars on the aircraft by means of different boundary conditions.

In order to determine the structural design in acoustic aspects, main sources should be defined generically as shown in Figure 5.4. All the Figures 5.4, 5.5 and 5.6 are constructed with the pattern technical drawing found in [43]. All these figures are generically drawn in order to show how rib and spar location may affect the boundary condition of the critic components. Note that scaling is not used.

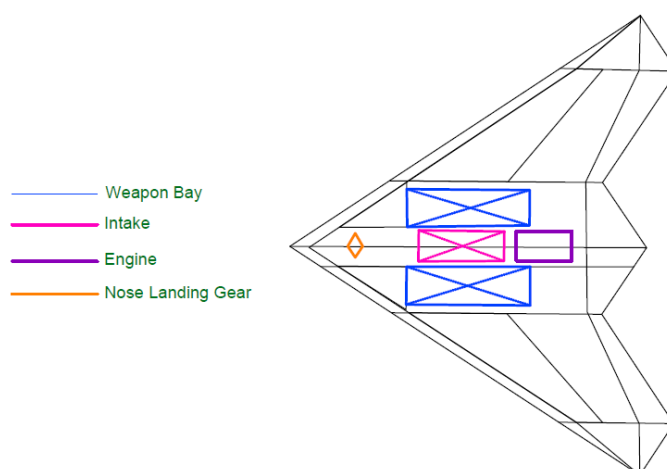


Figure 5.4. Generically constructed layout – main noise sources location generically

Noise levels are dependent on the detailed design and location of internal members and equipment of the aircraft. Figure 5.5 and 5.6, are simulated according to [43] and represent the probable rib and spar location, with red and green lines, of the genericUCAV used in [23]. The selection of these rib and spar location given in Figures 5.5 and 5.6 may result with three different boundary conditions. The red point

indicates the critical stress location where given stress results are measured from the wall in Figures 5.7, 5.8 and 5.9.

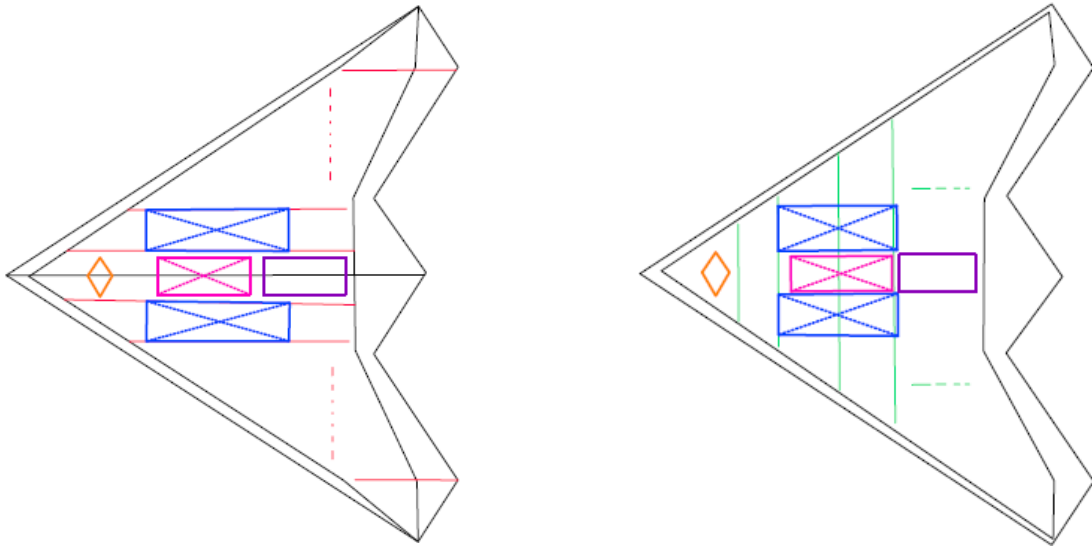


Figure 5.5. Probable rib and spar location of generic UCAV

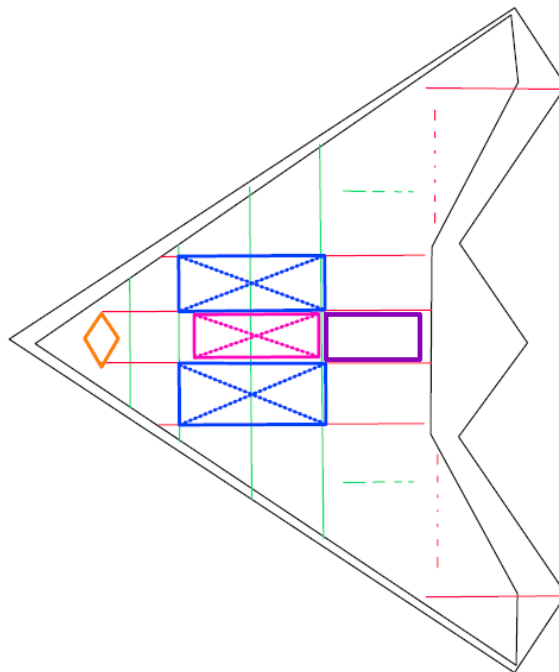


Figure 5.6. Probable rib and spar locations of generic UCAV

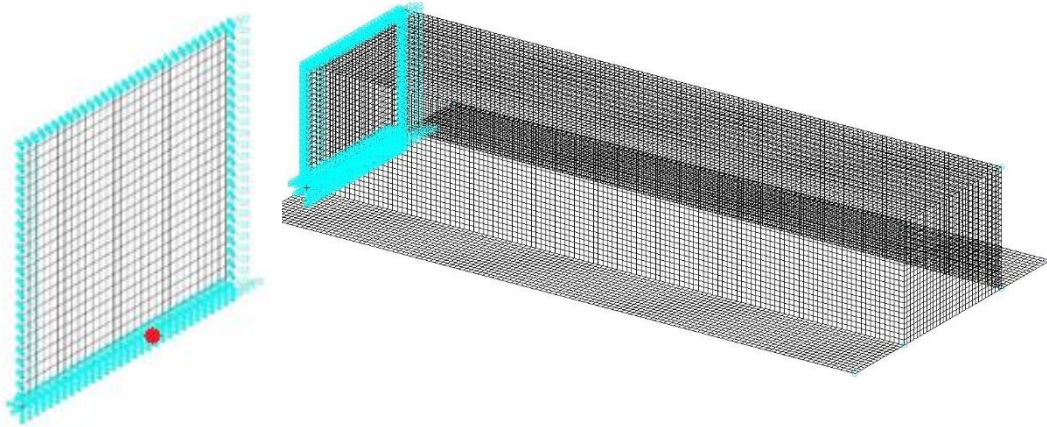


Figure 5.7. Selected Boundary Condition 1

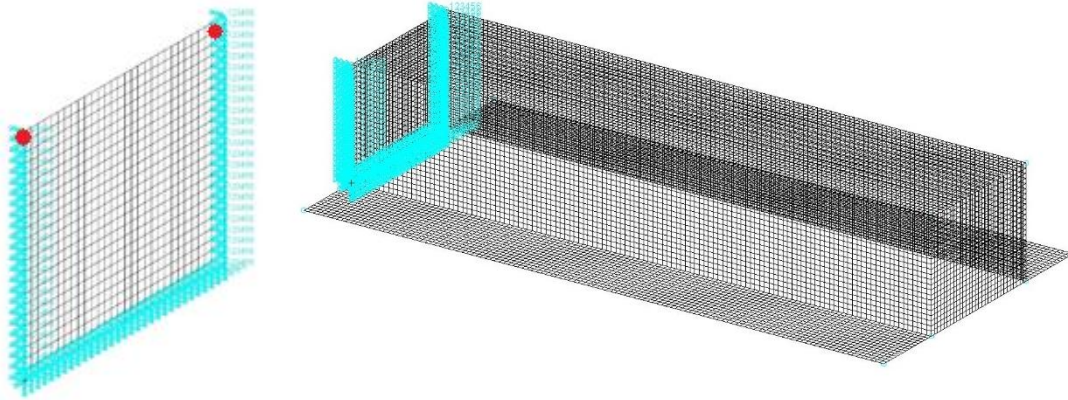


Figure 5.8. Selected Boundary Condition 2

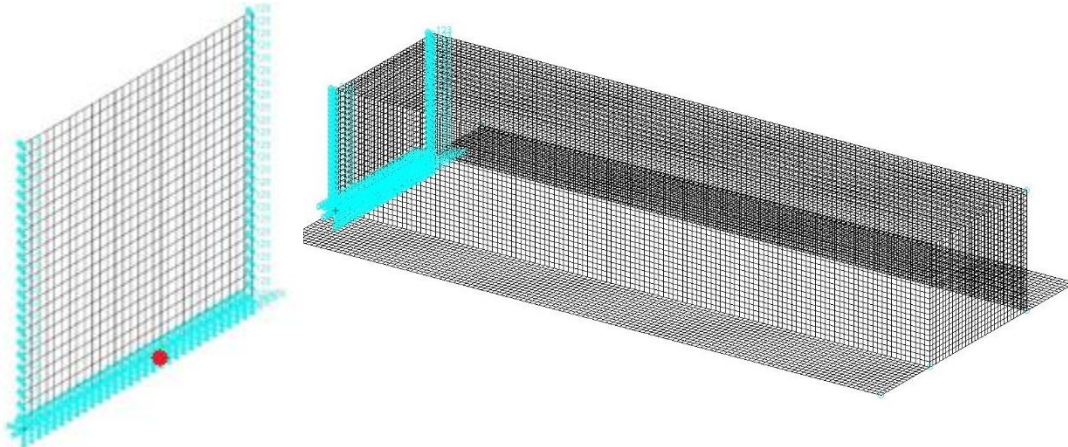


Figure 5.9. Selected Boundary Condition 3

The input loading taken from [23] which presents the sound pressure level measurements for a weapon bay mounted within the airframe of a generic UCAV which is based on the Boeing /AFRL 1303. This wind tunnel model shown in Figure 5.10 is 1:10.8 scaled, blended wing-body with a lambda planform and leading-edge sweep of 47° [23].



Figure 5.10. Parent and store models installed in the TWT working section on the TSR during the March 2012 tunnel entry [23]

SPL measurements for the Mach number and spoiler are taken from the critical upper section of rear wall; however, for the swept rear wall, measurements are taken from front wall to ensure the results reliability. The logic behind is keep the measurement point stationary. Stress comparison and critical location determination directly feed the design loop and may be used for the fatigue life expectancy for preliminary design process of the projects.

Mach number, spoiler and swept rear wall local SPL spectra are taken to be digitized and re-plotted to check the reliability. Validation of the digitized values can be compared by Figures 5.11, 5.12 and 5.13 for Mach number, swept rear wall and spoiler, respectively.

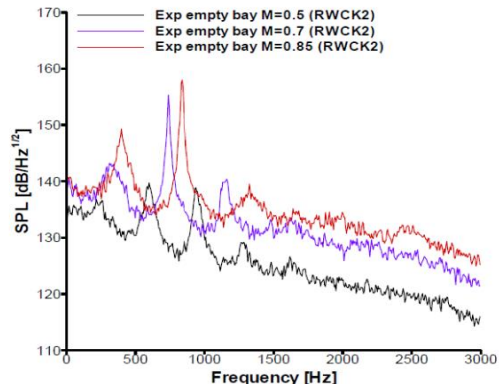
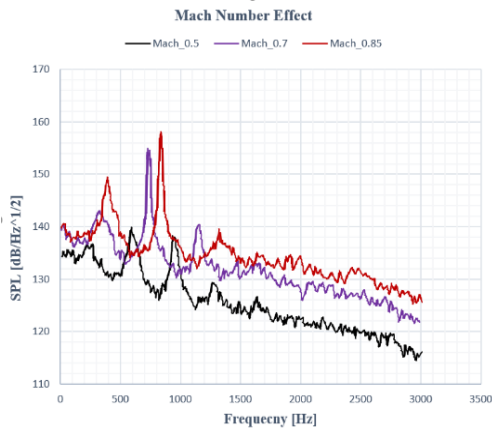


Figure 5.11. Digitized Mach Number vs Literature Mach Number [23] SPL Plot at Rear Wall

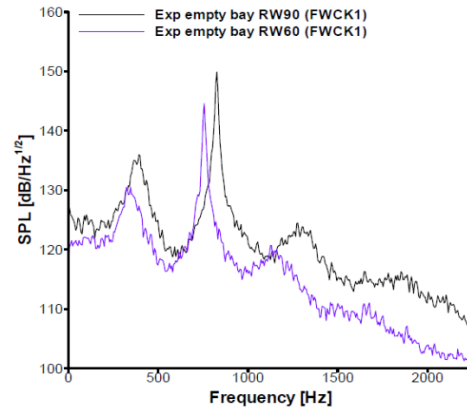
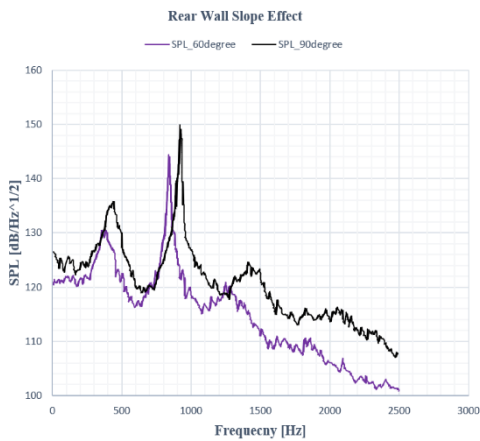


Figure 5.12. Digitized Rear Wall Slope Effect vs Literature Rear Wall Slope Effect [23] SPL Plot at Front Wall at 0.85 Mach Number

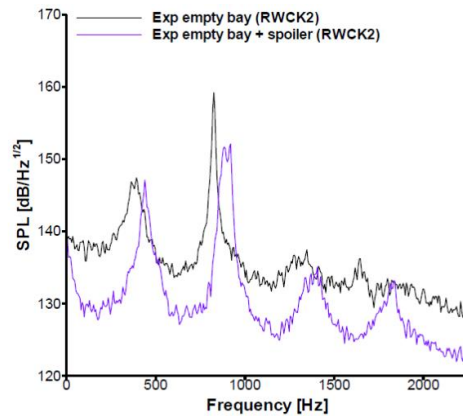
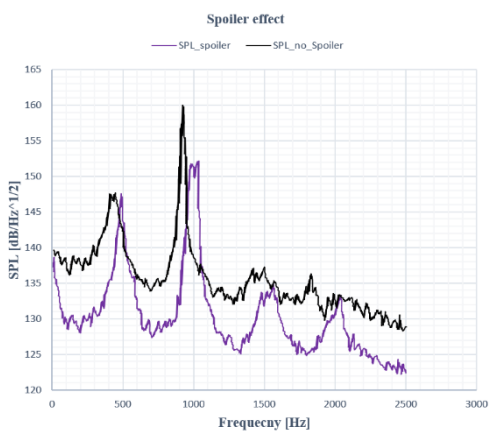


Figure 5.13. Digitized Spoiler Effect vs Literature Spoiler Effect [23] SPL Plot at Rear Wall at 0.85 Mach Number

All digitized sound pressure level values are converted to RMS pressure and power spectral density values with equation (3.1) and (3.3) respectively.

Obtained PSD values are exposed to the structure as random acoustic loading; however, it is not feasible to apply the loading per frequency. The goal is deriving a data set that represents the loading in the most sufficient way which is chosen as generation of an envelope. This goal is achieved by center frequency sound pressure levels extraction and calculation of related power spectral densities individually. These values are applied to the frequency range of relevant center frequency. The validation of this enveloping process is provided by overlapping of the PSD curves obtained per frequency and PSD envelopes obtained by centered frequency as shown in Figures 5.14 and 5.15 for 0.5 Mach number condition. Calculated values are shared more clearly in table 5.1 for Mach number 0.5 only.

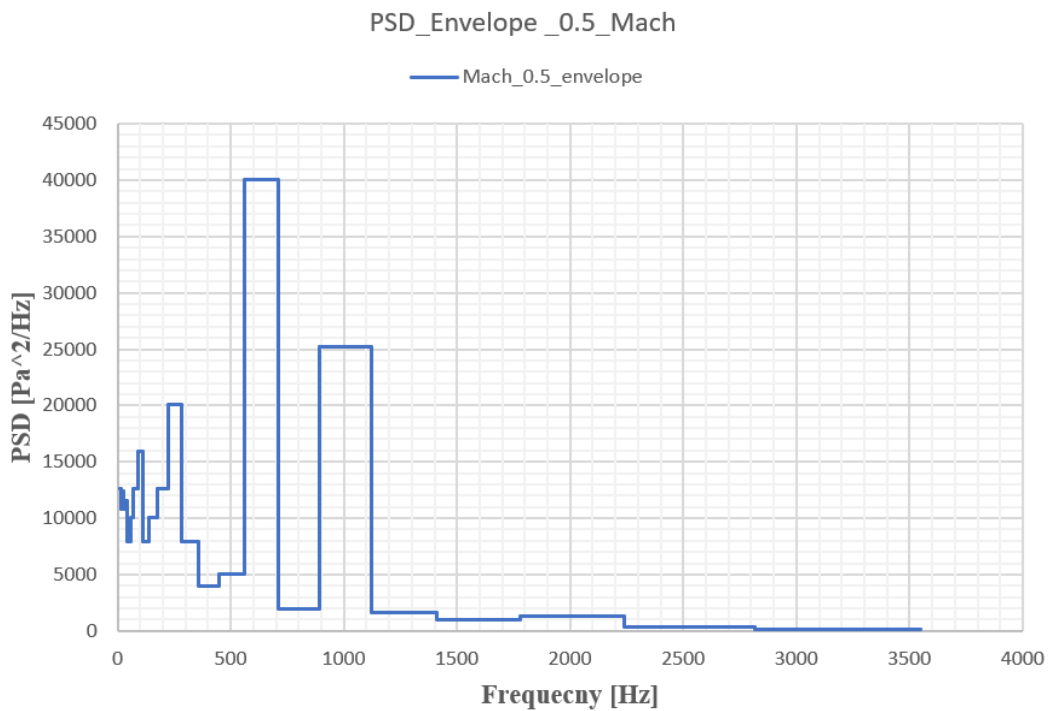


Figure 5.14. PSD Envelope Extracted by Center Frequencies M=0.5

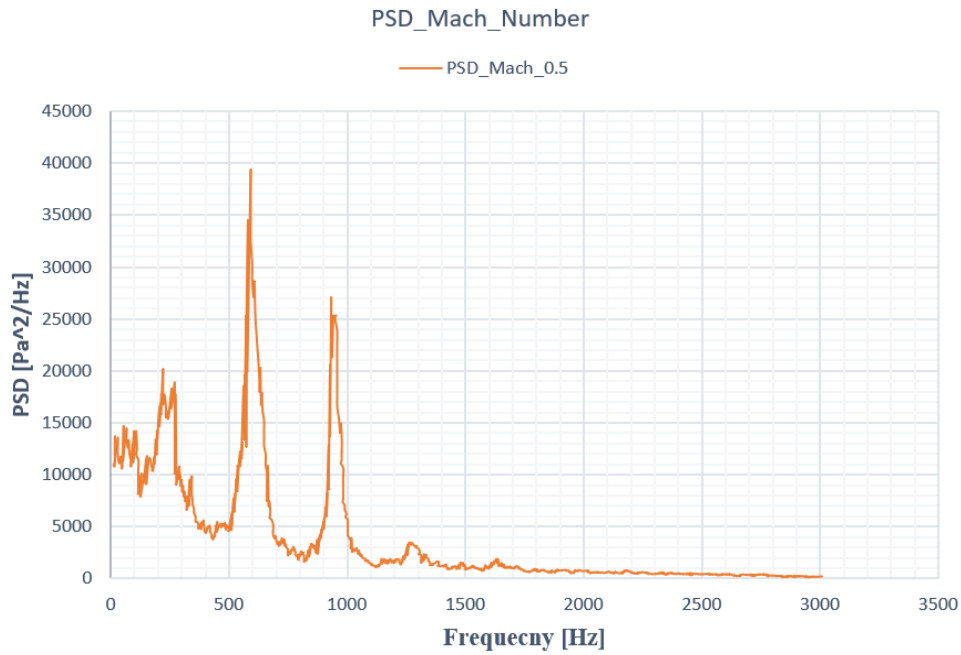


Figure 5.15. PSD Extracted per Frequency by Using Digitized Frequencies M=0.5

Table 5.1. Mach Number 0.5 PSD values for Envelope

<i>Mach Number 0.5 PSD Envelope</i>				
Freq_range [Hz]	Center Freq.[Hz]	SPL [dB]	P _{rms} [Pa]	PSD[Pa ² /Hz]
11.2	12.5	135.0	112.47	12649.11
14.1	12.5	135.0	112.47	12649.11
14.1	16.0	134.3	103.76	10766.14
17.8	16.0	134.3	103.76	10766.14
17.8	20.0	134.4	104.96	11016.91
22.4	20.0	134.4	104.96	11016.91
22.4	25.0	134.9	111.18	12361.18
28.2	25.0	134.9	111.18	12361.18
28.2	31.5	134.3	103.76	10766.14
35.5	31.5	134.3	103.76	10766.14
35.5	40.0	134.6	107.41	11536.13
44.7	40.0	134.6	107.41	11536.13
44.7	50.0	133.0	89.34	7981.05
56.2	50.0	133.0	89.34	7981.05

56.2	63.0	134.0	100.24	10047.55
70.8	63.0	134.0	100.24	10047.55
70.8	80.0	135.0	112.47	12649.11
89.1	80.0	135.0	112.47	12649.11
89.1	100.0	136.0	126.19	15924.29
112.0	100.0	136.0	126.19	15924.29
112.0	125.0	133.0	89.34	7981.05
141.0	125.0	133.0	89.34	7981.05
141.0	160.0	134.0	100.24	10047.55
178.0	160.0	134.0	100.24	10047.55
178.0	200.0	135.0	112.47	12649.11
224.0	200.0	135.0	112.47	12649.11
224.0	250.0	137.0	141.59	20047.49
282.0	250.0	137.0	141.59	20047.49
282.0	315.0	133.0	89.34	7981.05
355.0	315.0	133.0	89.34	7981.05
355.0	400.0	130.0	63.25	4000.00
447.0	400.0	130.0	63.25	4000.00
447.0	500.0	131.0	70.96	5035.70
562.0	500.0	131.0	70.96	5035.70
562.0	630.0	140.0	200.00	40000.00
708.0	630.0	140.0	200.00	40000.00
708.0	800.0	127.0	44.77	2004.75
891.0	800.0	127.0	44.77	2004.75
891.0	1000.0	138.0	158.87	25238.29
1122.0	1000.0	138.0	158.87	25238.29
1122.0	1250.0	126.0	39.91	1592.43
1413.0	1250.0	126.0	39.91	1592.43
1413.0	1600.0	124.0	31.70	1004.75
1778.0	1600.0	124.0	31.70	1004.75
1778.0	2000.0	125.0	35.57	1264.91
2239.0	2000.0	125.0	35.57	1264.91
2239.0	2500.0	120.0	20.00	400.00
2818.0	2500.0	120.0	20.00	400.00
2818.0	3150.0	116.0	12.62	159.24
3548.0	3150.0	116.0	12.62	159.24

At the end of the above calculation process, for each Mach number and palliative method combination, input loading data has been prepared for the comparative evaluation of the following cases;

Case 1: Effect of Mach number at Rear Wall

- Case 1.1: Mach number 0.5, empty cavity, SPL spectra on the cavity rear wall, $\alpha, \beta = 0$
- Case 1.2: Mach number 0.7, empty cavity, SPL spectra on the cavity rear wall, $\alpha, \beta = 0$
- Case 1.3: Mach number 0.85, empty cavity, SPL spectra on the cavity rear wall, $\alpha, \beta = 0$

Case 2: Effect of Swept Rear Wall at Front Wall

- Case 2.1: Mach number 0.85, empty cavity, SPL spectra on the cavity front wall, $\alpha, \beta = 0$, rear wall 60°
- Case 2.2: Mach number 0.85, empty cavity, SPL spectra on the cavity front wall, $\alpha, \beta = 0$, rear wall 90°

Case 3: Effect of Spoiler at Rear Wall

- Case 3.1: Mach number 0.85, empty cavity, SPL spectra on the cavity rear wall, $\alpha, \beta = 0$, with spoiler
- Case 3.2: Mach number 0.85, empty cavity, SPL spectra on the cavity rear wall, $\alpha, \beta = 0$, without spoiler (same with case 1.3)

After determination of boundary condition and extraction of acoustic loading, frequency extraction should be determined with caution. It was emphasized in Chapter 4 that frequency extraction has a great importance on the results obtained. The frequency cards' features were given in detail in Appendix B. Definition of the frequency range and natural frequencies of the structure, proper "frequency card selection", should be exercised on Nastran.

For the representative cavity rear wall analysis, Rossiter modes should be extracted apart from the border of the frequency range and natural frequencies of the structure. Rossiter modes are directly related with the flow feedback mechanism of flow over cavity and is needed to be expressed in detail.

In 1964 Rossiter developed a model, depending on the experiments carried out for the subsonic and transonic regimes, to predict frequencies of the cavity oscillation modes. The acoustic radiation triggers the vortex shedding at the upstream lip of the cavity and the vorticities generated is the reason of the acoustic radiation as a loop mechanism between [44]. This feedback mechanism takes fluid frequency equal to the acoustic resonance frequency which resulted with Rossiter frequencies of the cavity as follows;

$$f_m = \frac{U_\infty}{L} \frac{m - \alpha}{M_\infty + \frac{1}{\kappa}} \quad (5.1)$$

where m is the mode number of interests, U_∞ is the freestream velocity, L is the length of the cavity, M_∞ is the Mach number, α and κ are taken as 0.25 and 0.57 for the Mach number range from 0.1 to 0.9 [44]. These most commonly used values are determined empirically. α represents the phase difference between two vortices shedding from front wall of the cavity and κ is the ratio of convective velocity in the cavity to freestream velocity [44].

Rossiter modes are included in Figure 5.1 and 5.2 [23] as vertical dash lines and it can be obviously seen that the Rossiter basic formula predictions are greatly close to the peak values of the cavity, by approximately 10% underpredicted.

First 3 Rossiter modes for $M_\infty = 0.85$, $U_\infty = 295.55 \text{ m/s}$ $L = 0.251 \text{ m}$ can be calculated as follows;

$$f_1 = \frac{295.55}{0.251} \frac{1 - 0.25}{0.85 + \frac{1}{0.57}} = 339.08 \text{ Hz}$$

$$f_2 = \frac{295.55}{0.251} \frac{2 - 0.25}{0.85 + \frac{1}{0.57}} = 791.20 \text{ Hz}$$

$$f_3 = \frac{295.55}{0.251} \frac{3 - 0.25}{0.85 + \frac{1}{0.57}} = 1243.32 \text{ Hz}$$

where real values are $f_1=395 \text{ Hz}$ $f_2=840 \text{ Hz}$ and $f_3=1340 \text{ Hz}$ [23].

The frequency extraction by the “frequency card” is selected as shown below to analyze the frequency range as fine as required. The “frequency cards selections” are presented as determined by sensitivity analysis shared in Appendix E.

FREQ	1	.1	3000.	395.	840.	1340.
FREQ5	1	.1	3000.	1.		
FREQ3	1	.1	3000.	LINEAR	100	1.
FREQ1	1	.1	2.9999	1000		

The material property selection is kept as generic aluminum as used in Chapter 4. The real-life material properties are unknown for the weapon bay design; however, Al2024 is commonly used aluminum alloy in aviation industry. As a matter of fact, the main goal of this chapter is to compare effects of boundary conditions to feed the design in terms of ribs and spar location selection together with the effect of Mach number. Another area of interest is assigned study serviceability of controlling methods. On that account, aluminum selection is favorable in terms of convenience sampling. In addition, thickness information is not given and 1 mm thickness is used throughout the analysis. As required material properties and thickness information are not available, generic material and thickness values are preferred for the purposes of risk assessment only.

Cumulative RMS stress values are checked on the critical element, determined by stress results of the frequency response analysis shown in Figure 5.16. Figure 5.17 proves that the frequency range used is sufficiently wide that the curves tend to move toward an asymptote. This verification is noted for the analysis in all combinations; however, only for 0.5 Mach number and boundary condition case 1 combination is shared in 5.18 for demonstration of the results.

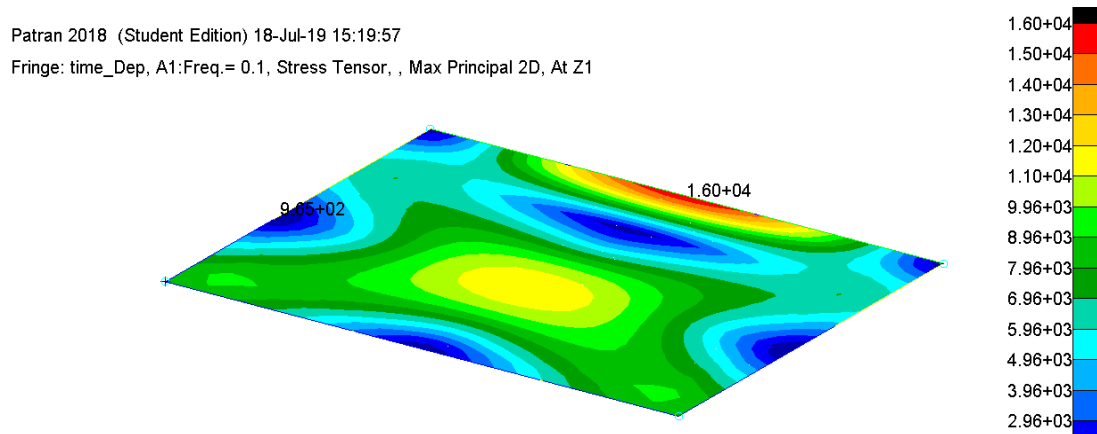


Figure 5.16. Frequency response of the representative rear wall under unit loading and determination of the critical element – Element 323 for Boundary Condition 1

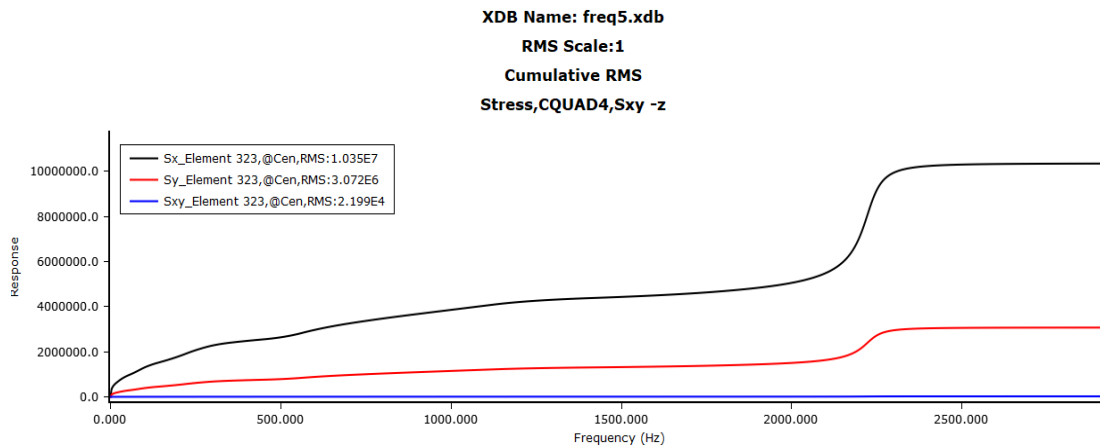


Figure 5.17. CRMS on Element 323 for 0.5 Mach number and Boundary Condition 1

Moreover, modal effective mass and modal fractions are also investigated. Total effective mass fractions represent 82.3%, 75.6% and 82.5% of total mass for boundary condition cases 1,2 and 3 respectively. Modal effective mass fractions reveal that first mode contribution highly dominates with the percentages 61.5 % 48.1% and 55.8% respectively. All these fractions are assessed adequate enough for the stress result under acoustic loading.

The calculation procedure of the acoustic loading was presented in Table 5.1 for 0.5 Mach number case. Loading information for the rest of the cases calculated as the same procedure used in 5.1 which provides the SPL values, 1/3-Octave band center frequencies and related power spectral densities for each case. By this way, all PSD envelopes are generated and given as an input to the model developed in Patran. Figure 5.18 is shown as an example $G_p(f)$ plot obtained by Nastran for the 0.5, 0.7 and 0.85 Mach number cases only.

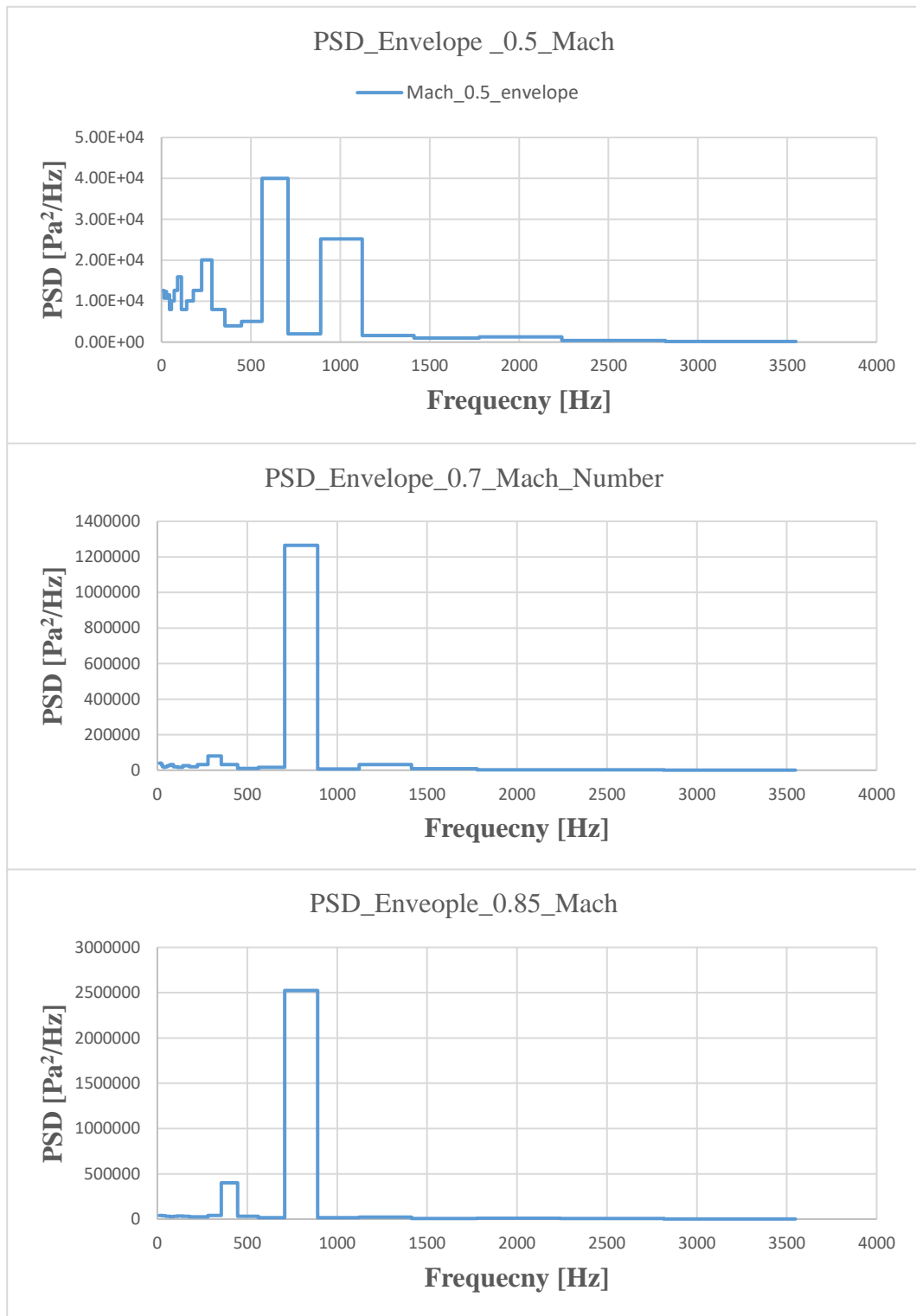


Figure 5.18. PSD envelopes obtained by Nastran for 0.5, 0.7 and 0.85 Mach number cases

RMS stress results for each case is represented in Table 5.2 for the specified boundary conditions and loading cases expressed before.

Table 5.2. Mach Number Effect Analysis Result Summary at Rear Wall at 0.85 Mach Number

Rear Wall RMS Stress Results [Pa]	BC1			BC2			BC3		
	S _x	S _y	S _{xy}	S _x	S _y	S _{xy}	S _x	S _y	S _{xy}
Mach Number 0.5	1.03 5E+ 07	3.07 0E+ 06	2.19 9E+ 04	3.38 0E+ 06	1.74 0E+ 07	8.15 0E+ 05	1.05 0E+ 06	2.98 0E+ 07	5.86 0E+ 05
Mach Number 0.7	1.92 7E+ 07	5.72 0E+ 06	3.95 0E+ 04	7.92 0E+ 06	4.07 0E+ 07	1.19 0E+ 06	2.74 0E+ 06	7.79 0E+ 07	5.86 0E+ 05
Mach Number 0.85	3.36 0E+ 07	9.98 0E+ 06	7.20 0E+ 04	1.00 8E+ 07	5.18 0E+ 07	2.43 0E+ 06	3.73 0E+ 06	1.06 0E+ 08	2.08 0E+ 06

Table 5.3. Spoiler Effect Analysis Result Summary at Rear Wall at 0.85 Mach Number

Rear Wall RMS Stress Results [Pa]	BC1			BC2			BC3		
	S _x	S _y	S _{xy}	S _x	S _y	S _{xy}	S _x	S _y	S _{xy}
w/ spoiler	1.92 6E+ 07	5.71 6E+ 06	4.08 9E+ 04	8.33 0E+ 06	4.28 6E+ 07	1.97 4E+ 06	2.66 5E+ 06	7.55 8E+ 07	1.48 8E+ 06
w/o spoiler	3.36 0E+ 07	9.98 0E+ 06	7.20 0E+ 04	1.00 8E+ 07	5.18 0E+ 07	2.43 0E+ 06	3.73 0E+ 06	1.06 0E+ 08	2.08 0E+ 06

Table 5.4. Swept Rear Wall Effect Analysis Result Summary at Front Wall at 0.85 Mach Number

Front Wall RMS Stress Results [Pa]	BC1			BC2			BC3		
	S _x	S _y	S _{xy}	S _x	S _y	S _{xy}	S _x	S _y	S _{xy}
60-degree RW	2.43 0E+ 06	7.22 9E+ 05	4.18 4E+ 03	9.25 0E+ 05	4.75 4E+ 06	2.39 1E+ 05	6.42 4E+ 05	1.82 8E+ 07	3.57 7E+ 05
90-degree RW	4.64 4E+ 06	1.38 1E+ 06	8.40 4E+ 03	1.72 8E+ 06	8.88 0E+ 06	4.44 1E+ 05	1.62 1E+ 06	4.59 7E+ 07	9.04 2E+ 05

Principal RMS stress is calculated, using above values for critical elements, by equation (4.24). The overall results are tabulated in Tables 5.5, 5.6 and 5.7 as follows:

Table 5.5. Principal RMS Stress Values for Mach Number at Rear Wall

Rear Wall Stress [Pa]	BC1	BC2	BC3
Mach Number 0.5	1.035E+07	1.745E+07	2.981E+07
Mach Number 0.7	1.927E+07	4.074E+07	7.790E+07
Mach Number 0.85	3.360E+07	5.194E+07	1.060E+08

Table 5.6. Principal RMS Stress Values for Spoiler at Rear Wall at 0.85 Mach Number

Rear Wall Stress [Pa]	BC1	BC2	BC3
w/ spoiler	1.926E+07	4.297E+07	7.561E+07
w/o spoiler	3.360E+07	5.194E+07	1.060E+08

Table 5.7. Principal RMS Stress Values for Swept Rear Wall at Front Wall at 0.85 Mach Number

Front Wall Stress [Pa]	BC1	BC2	BC3
60-degree RW	2.430E+06	4.769E+06	1.829E+07
90-degree RW	4.644E+06	8.907E+06	4.599E+07

Mach number and spoiler effect studies are carried out for the rear wall measurements. However, swept rear wall studies are realized for the front wall. The varying parameter is the rear wall itself for the case of swept wall; therefore, a front wall measurement is opted to see the effect of 30-degree angle of gradient. It can be obviously seen from stress values, shown in Table 5.7. These are much lower than the values listed in Tables 5.5 and 5.6. This proves the importance of the rear wall from structural point of view once more. Although the front wall is not the right wall to look after, the front wall measurement will be analyzed for the spoiler case in order to provide comparison between two controlling methods. The comparative evaluation of discretized SPL curves is given in Figure 5.19 and PSD enveloping procedure is carried out for front wall measurements with spoiler in accordance with this purpose.

Case 4: Effect of Spoiler at Front Wall

- Case 4.1: Mach Number 0.85, empty cavity, SPL spectra on the cavity front wall, $\alpha, \beta = 0$, with spoiler
- Case 4.2: Mach Number 0.85, empty cavity, SPL spectra on the cavity front wall, $\alpha, \beta = 0$, without spoiler (same with case 2.2)

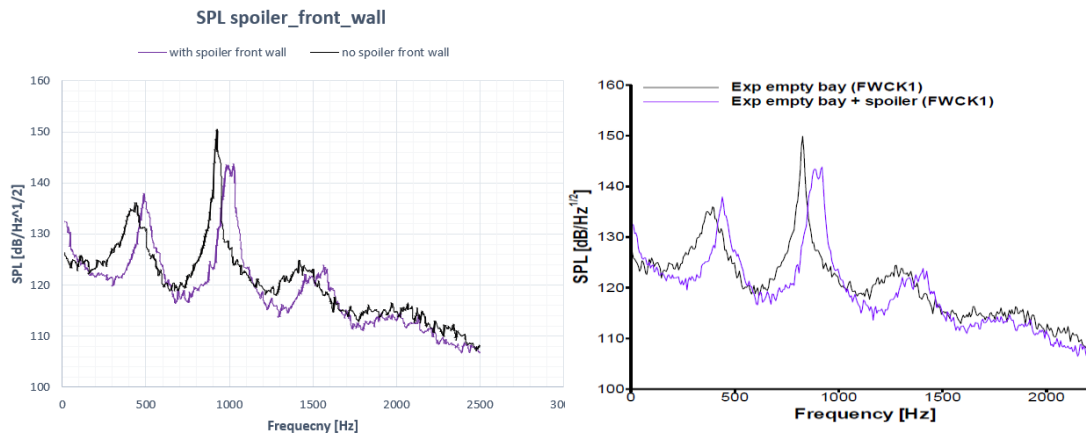


Figure 5.19. Digitized Spoiler Effect vs Literature Spoiler Effect [23] SPL Plot at Front Wall at 0.85 Mach Number

Stress results are shown in Table 5.8 for the front wall acoustic loading measurements with spoiler.

Table 5.8. Summary of RMS Stress Results for Spoiler Effect at Front Wall at 0.85 Mach Number

Front Wall RMS Stress Results [Pa]	BC1			BC2			BC3		
	Sx	Sy	Sxy	Sx	Sy	Sxy	Sx	Sy	Sxy
w/ spoiler	3.17 8E+ 06	9.44 8E+ 05	5.83 5E+ 03	1.35 1E+ 06	6.94 3E+ 06	3.38 0E+ 05	8.76 0E+ 05	2.48 6E+ 07	4.89 1E+ 05
w/o spoiler	4.64 E+0 6	1.38 E+0 6	8.40 E+0 3	1.73 E+0 6	8.88 E+0 6	4.44 E+0 5	1.62 E+0 6	4.60 E+0 7	9.04 E+0 5

and principal RMS stress are as follows;

Table 5.9. Principal RMS Stress Values for Swept Rear Wall at Front Wall at 0.85 Mach Number

Front Wall Stress [Pa]	BC1		BC2		BC3
w/ spoiler	3.18E+06		6.96E+06		2.49E+07
w/o spoiler	4.64E+06		8.91E+06		4.60E+07

Investigation of spoiler effect depending on front wall measurements provide an opportunity to compare two palliative methods effectivities. It can be obviously seen that swept rear wall is highly effective method when compared to spoiler. Predicted stress levels at front wall for swept rear wall reduces the stress from 4.6e+7 Pa to 1.83e+7 Pa; whereas, spoiler decrease it up to 2.49e+7 Pa. Although both of them has a great influence, swept rear wall is much preferable design variation. Reduction rates of controlling methods will be given in Chapter 6 to show the difference clearer.

When it comes to Mach number effect, increasing Mach number directly raise principal RMS stress levels as expected. Increasing Mach number tend to nonlinear interactions and higher order harmonics. That's why controlling methods are highly needed for reasonable attenuation levels across aircraft's flight envelope at higher Mach numbers.

CHAPTER 6

CONCLUDING REMARKS AND FUTURE WORK

6.1. Concluding Remarks

This thesis aimed to develop an acoustic fatigue analysis method for use in preliminary design phase of components such as Weapon's Bay. In addition, mitigation efforts concerning rear wall of cavity structure are carried out on series of analysis for different Mach-numbers, controlling methods and boundary conditions.

Analytical procedure is developed for the simple structures, exposed to acoustic loading, based on the assumptions expressed in Section 4.1. As can be deduced from the results presented in Chapter 4, the outcomes of analytical procedure are sufficiently accurate for simple geometries at preliminary design phase. The results are verified via finite element method for a generic flat plate model. Verification is achieved by providing the same conditions that analytical methods are based on to the FEM model.

Analytical procedure relies on single-degree-of-freedom theory which simplifies the calculation procedure with a reservation that it retains the most significant aspect of analysis. Only predominant mode, the lowest one in general, is excited by acoustic pressure as shown in Figure 3.3. Single degree of freedom assumption is supplied to the FEM model for validation purposes in Chapter 4. However, it should be noted that, acoustical transmitted power may have importance as resonant frequencies for interconnected structures. More comprehensive investigation is needed for such cases. In addition, the excitation force is assumed to be uniformly distributed. Values of maximum sound pressure level are converted in the form of PSD and are then applied to the structure. These maximum SPL values provide conservative approximations for design purposes.

Experimental acoustic loading taken from [23], excites the structure with presumably different boundary conditions for FEM analysis of cavity rear wall to see the effect of internal members' housing on the stress response of the structure. Rear wall has been analyzed as it is considered critical for acoustic vibration as proved in literature and underlined in Chapter 5.

Only principal stress values are compared in Chapter 5, although acoustic fatigue procedure takes it a step further, that is, the prediction of endurance life by random S-N curve. RMS stress against S-N curve comparison would result with fatigue life prediction directly. It should be noted that, the stress results obtained via random vibration analysis has the same trend that would have been obtained from fatigue calculations. This is because acoustic loading exposure time and used material properties are the same for both analyses carried out in Chapter 5. RMS stresses are the only values that bring difference on fatigue life.

Three different boundary conditions are chosen as given in Figures 5.7, 5.8 and 5.9. One extra condition is also tried which has all edged fixed model but the results are not given in this thesis. This is due to the structure become too stiff that the acoustic loading does not excite the wall crucially. In other words, the panel with four edges fixed possesses the lowest natural frequency higher than the excitation frequency. Therefore, there is no need for investigation in the scope of the thesis. Besides, all edges-fixed condition requires four internal members which introduce extra weight and never preferred in aviation industry.

When it comes to stress response of the critical wall with selected three boundary conditions, results are presented in Tables 5.5, 5.6, 5.7 and 5.9. Excitation pressure based on maximum SPL values of wind tunnel experiments [23].

It is concluded from the principal stresses, shown in Table 5.5, that the higher the Mach number the higher the stress response as expected from measured SPL values. Primary concern here is the comparison of boundary conditions. It should be noted that the highest stress location is changed with boundary conditions as shown in

Figures 5.7, 5.8 and 5.9 with red points. Even this is a conclusion to supply information on the design as thicken critical location of the wall if necessary. It may be reasonable to design the wall as a tapered structure.

In addition, comparison of two different controlling methods stress levels values and reduction rate comparison is presented in Table 6.1 and 6.2, respectively. Taking 0.85 Mach clean cavity configuration, i.e. cavity without any palliative methods applied at 0.85 Mach number, swept rear wall reduce the stress values about % 55-60 whereas spoiler effect is up to % 35-45 only.

Table 6.1. Principal RMS Stress Values Comparison at Front Wall

	BC1	BC2	BC3
Reference Case FW	4.64E+06	8.91E+06	4.60E+07
w/ spoiler	3.18E+06	6.96E+06	2.49E+07
60-degree RW	2.43E+06	4.77E+06	1.83E+07

Table 6.2. % Reduction Rate Values at Front Wall

	% Reduction Rate for BC1	% Reduction Rate for BC2	% Reduction Rate for BC3
w/ spoiler	40.56074766	35.55555556	46.56652361
60-degree RW	54.57943925	55.84259259	60.75107296

Effect of spoiler and swept rear wall is compared through front wall measurement as explained earlier. It is obviously seen that front wall stress values are considerably lower than rear wall stress values. Moreover, it is concluded that 30° swept wall is more efficient controlling method when compared to spoiler at leading edge. Swept rear wall is more preferable design variation in terms of observability and

drag concern of the high-performance aircraft also. The only handicap may be about sizing, integration of munition and hydraulic like cables housing challenges.

Last consideration that should be added about cavity wall analysis is the Rossiter frequencies that have a place in the analysis as natural frequencies of the cavity structure of interest. Rossiter frequencies may excite the structure when they couple with the excitation frequencies. Therefore, special interest is needed for determination of frequency extraction. This consideration is given in detail in Chapter 5.

6.2. Future Work

It is known that dynamic response of aircraft structures subjected to high intensity acoustic loading is focus of interest. There are many relevant studies presented. In the light of all these studies, there are suggested avenues that provide further improvements to this thesis.

Linearity assumptions are used throughout the thesis; however, including nonlinear effect would be a great development. Moreover, any other stress considerations are not taken into consideration aside from the acoustic stress variations calculated. Other stresses exposed to structure can be added to the calculation procedure to improve the results' utility. Combining these two enhancements would provide the prediction of nonlinear response of the structures exposed to combined loading at high intensity acoustic loading. It would be great development to be used in the industry.

In addition, comprehensive investigations are needed for interconnected structures where transmitted power has influence on the response of the structure. More examination is needed to obtain power transmission from the connection elements to the skin elements. Proposed method in this thesis can be modified in terms of the formulation of the ribbed panels and more complex structures.

Apart from all these, the fatigue calculation presented in this thesis provides very basic level of consideration that is developed for preliminary design stage of the projects as a pre-assessment of sonic fatigue. There is a need for more accurate endurance life prediction methods for the later stages of the projects.

Another issue is about the damping value used as constant 0.017 which is recommended in [8] and [31]. Typical value of damping for conventional aircraft structures without special treatment is determined as 0.017 in literature. This value represents as default value for flexural waves. It would be better if damping values can be determined by wind tunnel experiments for both extensional and torsional waves to provide a complete picture. It should be noted that complete picture will affects the results about %10 as % 90 of failures is caused by bending. Therefore, it does not affect the results considerably.

REFERENCES

- [1] ESDU, Item 000001. 'Aerodynamics series organisation', 2001.
- [2] J. Walter Hykytow, 'Sonic Fatigue Design Guide For Military Aircraft', Air Force Flight Dynamic Laboratory Technical Report, May 1978, 1977.
- [3] T.-H. Le, I. Mary, and M. Terracol, 'LES of Pressure Loads Suppression in Weapons Bay Flow', January 2005.
- [4] G. A. Flandro, H. R. Jacobs, University of Utah, 'Vortex Generated Sound in Cavities', AIAA, 1973.
- [5] P.R. Cunningham, R.G White, 'A review of analytical methods for aircraft structures subjected to high-intensity random acoustic loads', Proceedings of the Institution of Mechanical Engineers, Part G: Journal of Aerospace Engineering, 218(3) , pp. 231-242, 2004.
- [6] ESDU, Item 74037, 'Introduction and guide to ESDU Data On Acoustic Fatigue The Royal Aeronautical Society', 1974.
- [7] R. C. W. van der Heyde and A. W. Kolb, 'Sonic Fatigue Resistance of Lightweight Aircraft Structures', in *Symposium on Acoustic Fatigue*, 1972.
- [8] A. G. R. Thomson and R. F. Lambert, 'Design Data for Acoustic Fatigue', in *Symposium on Acoustic Fatigue*, 1972.
- [9] B. L. Clarkson, 'Estimates of the Response of Box Type Structures to Acoustic Loading', in *Symposium on Acoustic Fatigue*, 1972.
- [10] ESDU, Item 86025, 'Design against fatigue: vibration of structures under acoustic or aerodynamic excitation', 1986.
- [11] D. Tougard, 'Brite-Euram Programme: Acoufat Acoustic Fatigue and Related Damage Tolerance of Advanced Composite and Metallic Structures', in *Impact of Acoustic Loads on Aircraft Structures*, 1994.
- [12] H. F. Wolfe, 'Nonlinear Dynamic Response of Aircraft Structures to Acoustic Excitation', in *Impact of Acoustic Loads on Aircraft Structures*, 1994.
- [13] D. C. G. Eaton, 'Response and Fatigue Characteristics of Light Alloy Machined Plank Structures', in *Symposium on Acoustic Fatigue*, 1972.
- [14] I. Holehouse, 'Sonic Fatigue of Diffusion Bonded Titanium Sandwich Structure', in *Symposium on Acoustic Fatigue*, 1972.
- [15] W. Kirkby, 'Some Considerations of the Fatigue Behaviour of Aluminium Alloy Structures Under Acoustic Loading', in *Symposium on Acoustic Fatigue*,

1972.

- [16] I. Salvatore, D. Orlando, and G. Di Spirito, 'Acoustic fatigue analysis of composite outboard and inboard ap of a commercial aircraft Relatore Correlatore', no. August, 2015.
- [17] M. H. Morton *et al.*, 'Cycle and Sonic Fatigue', no. April, pp. 1–15, 2007.
- [18] S. Aradag and D. Knight, 'Simulation of Supersonic Flow over a Cavity', no. January, pp. 1–17, 2012.
- [19] S. L. Gai, H. Kleine, and A. J. Neely, 'Supersonic Flow over a Shallow Open Rectangular Cavity', *J. Aircr.*, vol. 52, no. 2, pp. 609–616, 2014.
- [20] D. Parkhi, 'Aeroacoustics of Cavity Flow using Time-Resolved Particle Image Velocimetry', pp. 1–90, 2009.
- [21] K. K. Ahuja and J. Mendoza, 'Effects of cavity dimensions, boundary layer, and temperature on cavity noise with emphasis on benchmark data to validate computational aeroacoustic codes', *NASA Contract. Rep. 4653*, no. NASA Contract. Rep. 4653, p. 284, 1995.
- [22] N. Murray and L. Ukeiley, 'Flow Field Dynamics in Open Cavity Flows', no. May, pp. 8–10, 2012.
- [23] R. A. Chaplin, T. J. Birch, 'The aero-acoustic environment within the weapons bay of a generic UCAV', June 2012.
- [24] D. Williams and C. Rowley, 'Recent Progress in Closed-Loop Control of Cavity Tones', no. January, 2012.
- [25] D. Roberts, 'Analysis and Control of Resonant Cavity Flows School of Engineering Academic year : 2012 – 2013 Supervisor : Dr D G MacManus Submitted for the degree of PhD', pp. 2012–2013, 2013.
- [26] A. Cenko, R. Deslandes, M. Dillenius, and M. Stanek, 'Unsteady Weapon Bay Aerodynamics - Urban Legend or Flight Clearance Nightmare', no. January, pp. 1–13, 2013.
- [27] J. Nilsson, *Numerical Methods for Load and Response Prediction for Use in Acoustic Fatigue*. 2016.
- [28] D.C.G. Eaton, 'An Overview of Structural Acoustics and Related High-Frequency-Vibration Activities', 1997.
- [29] ESDU, Item 73011, 'Damping in Acoustically Excited Structures', 1974.
- [30] ESDU, Item 66016, 'Bandwidth correction', 1978.
- [31] ESDU, Item 72005, 'The Estimation of RMS Stress in Stiffened Skin Panels Subjected to Random Acoustic Loading', 1996.

- [32] MSC Nastran 2013. 'Dynamic Analysis User's Guide', 2013.
- [33] E. J. Richards and D. J. Mead, Eds., *Noise and Acoustic Fatigue in Aeronautics*.
- [34] ESDU, Item 72015, 'Endurance of Aluminium Alloy Structural Elements Subjected to Simulated Acoustic Loading', 1972
- [35] ESDU, Item 95006, 'Fatigue life estimation under variable amplitude loading using cumulative damage calculations', 1995.
- [36] R. Lazzeri, 'A Comparison between Safe Life, Damage Tolerance and probabilistic approaches to aircraft structure fatigue design', no. July, 2015.
- [37] ESDU, Item 87002, 'Natural frequencies of rectangular singly-curved plates', 1996.
- [38] 'Cutaway Raptor F22 Lockheed Martin', Available: <https://cellcode.us/quotes/cutaway-raptor-f-22-lockheed-martin.html>, [Access, June 2019]
- [39] ESDU, Item 66017, 'Combination of Levels in dB', 1978.
- [40] ESDU, Item 66018, 'Relation Between Sound Pressure Level and RMS Fluctuating Pressure', 1966.
- [41] W. C. Young, *Roark's Formulas for Stress and Strain*, 6th Editio. 1989.
- [42] Brian L. Clarkson, 'Stress in Skin Panels Subjected to Random Acoustic Loading', Air Force Materials Laboratory Research and Technology Division Technical Report, June 1967.
- [43] E. Sepulveda, H. Smith, and D. Sziroczak, 'Multidisciplinary analysis of subsonic stealth unmanned combat aerial vehicles', *CEAS Aeronaut. J.*, vol. 10, no. 2, pp. 431–442, 2019.
- [44] Ö. H. Ünalms, N. T. Clemens, and D. S. Dolling, 'Cavity Oscillation Mechanisms in High-Speed Flows The University of Texas at Austin', *AIAA J.*, 2004.

APPENDICES

A. Frequency Ranges Corresponding to Center Frequency for a 1/3-Octave Bandwidth

Table 0.1. Frequency Ranges Corresponding to Center Frequency for a 1/3-Octave Bandwidth

<i>Lower Frequency [Hz]</i>	<i>Center Frequency [Hz]</i>	<i>Upper Frequency [Hz]</i>
44.7	50	56.2
56.2	63	70.8
70.8	80	89.1
89.1	100	112.2
112.2	125	141.3
141.3	160	177.8
177.8	200	223.9
223.9	250	281.8
281.8	315	354.8
354.8	400	446.7
446.7	500	562.3
562.3	630	707.9
707.9	800	891.3
891.3	1000	1122.0
1122.0	1250	1412.5
1412.5	1600	1778.3
1778.3	2000	2238.7
2238.7	2500	2818.4
2818.4	3150	3548.1
3548.1	4000	4466.8
4466.8	5000	5623.4
5623.4	6300	7079.5
7079.5	8000	8912.5
8912.5	10000	11220.2

B. Frequency Extraction FREQ_i Cards of Nastran

This presents the influence of various output extraction frequency and the FREQ_i cards to be recommended for a calculation of RMS stress with MSC Nastran

Output extractions accounting for PSD peaks, i.e. including the natural frequencies values, assess RMS stress in a conservative way.

The interpolation case of decreasing PSD peak values (at the natural frequencies), logarithmic curve interpolation is closer to the reference value for the system.

Type of Cards to Use

To date, there are six cards of output extraction.

FREQ gives frequencies at which extractions are made (as many as wanted).

FREQ1 gives 1st frequency, frequency increment and number of increments.

FREQ2 gives 1st frequency, last frequency and number of logarithmic increments.

FREQ3 gives 1st frequency, last frequency, type of interpolation between frequencies and number of frequencies to include between boundaries along with clustering of frequencies (more extractions along boundaries or central frequency).

FREQ4 gives 1st frequency, last frequency, frequency spread near resonance frequency and number of frequencies per spread.

FREQ5 gives 1st frequency, last frequency and fractions of natural frequencies.

Sensitivity Analysis

Reference Case – Used to obtain all results throughout the validation analysis

FREQ	1	.1	5000.		
FREQ5	1	.1	5000.	1.	
FREQ3	1	.1	5000.	LINEAR 100	1.

Case 1

FREQ	1	.1	5000.		
FREQ5	1	.1	5000.	1.	

Case2

FREQ1	1	.1	499.99	10	
-------	---	----	--------	----	--

Case 3

FREQ2	1	.1	5000.	500	
FREQ	1	.1	5000.		

Case 4

FREQ3	1	.1	5000.	LINEAR 5	2.
FREQ	1	.1	5000.		

Case 5

FREQ1	1	.1	4.9999	1000	
-------	---	----	--------	------	--

Table 0.2. Comparison of FREQi Selection Sensitivity Analysis Number of Frequency Extracted

	<i>Reference Case</i>	<i>Case 1</i>	<i>Case 2</i>	<i>Case 3</i>	<i>Case 4</i>	<i>Case 5</i>
Number of Frequency Extracted	1486	16	11	390	61	1001

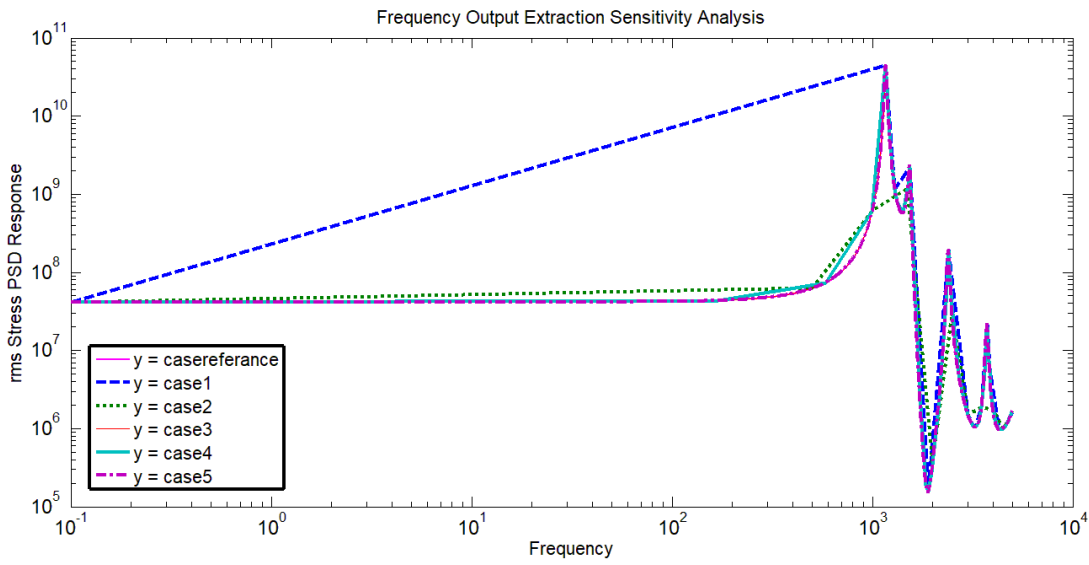


Figure 0.1. PSD response of system with different output extraction log-log scale

C. Simply Supported Edge Condition Dynamic Characteristic of Flat Plate

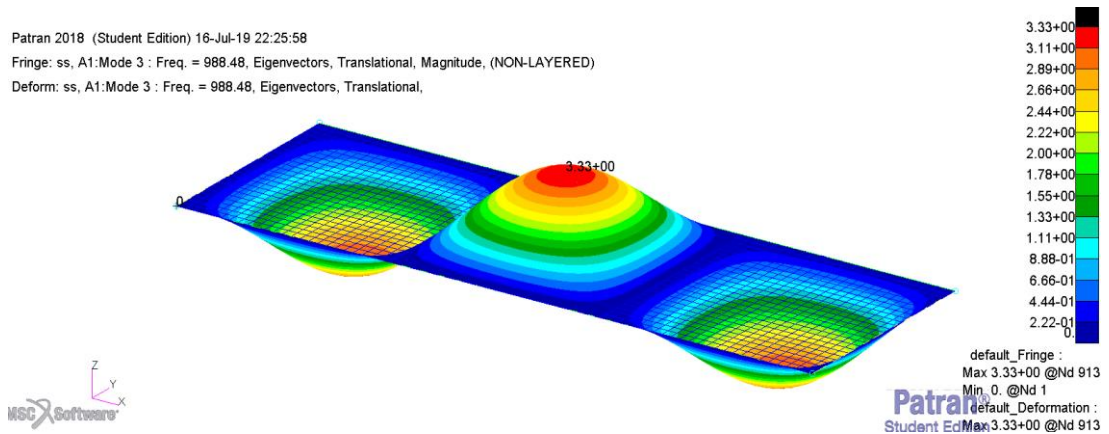
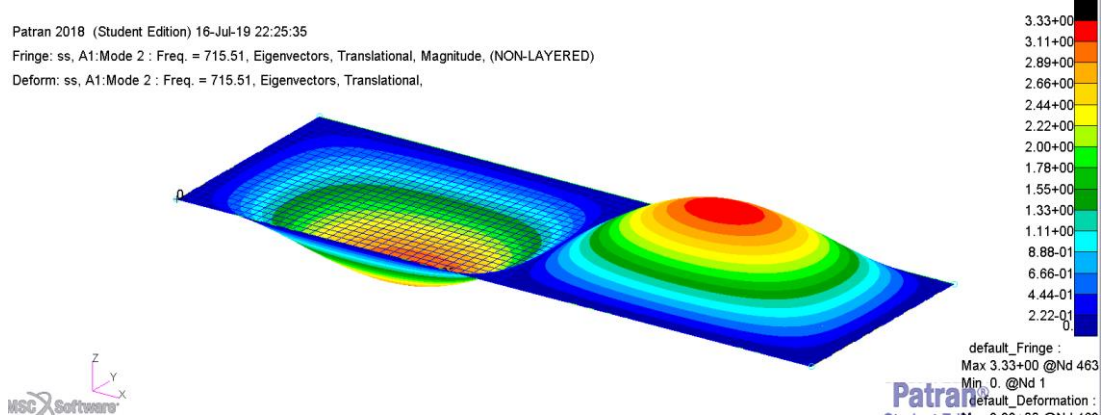
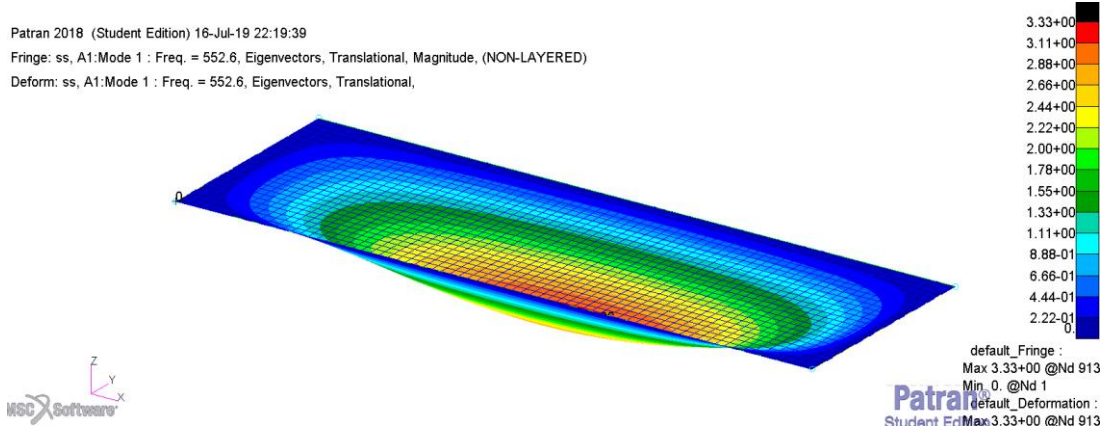


Figure 0.2. First 3 Mode of Simply Supported Flat Plate (552.6 Hz first mode)

D. Frequency Parameters K and K_{mn} for Natural Frequency Calculation in Analytical Procedure

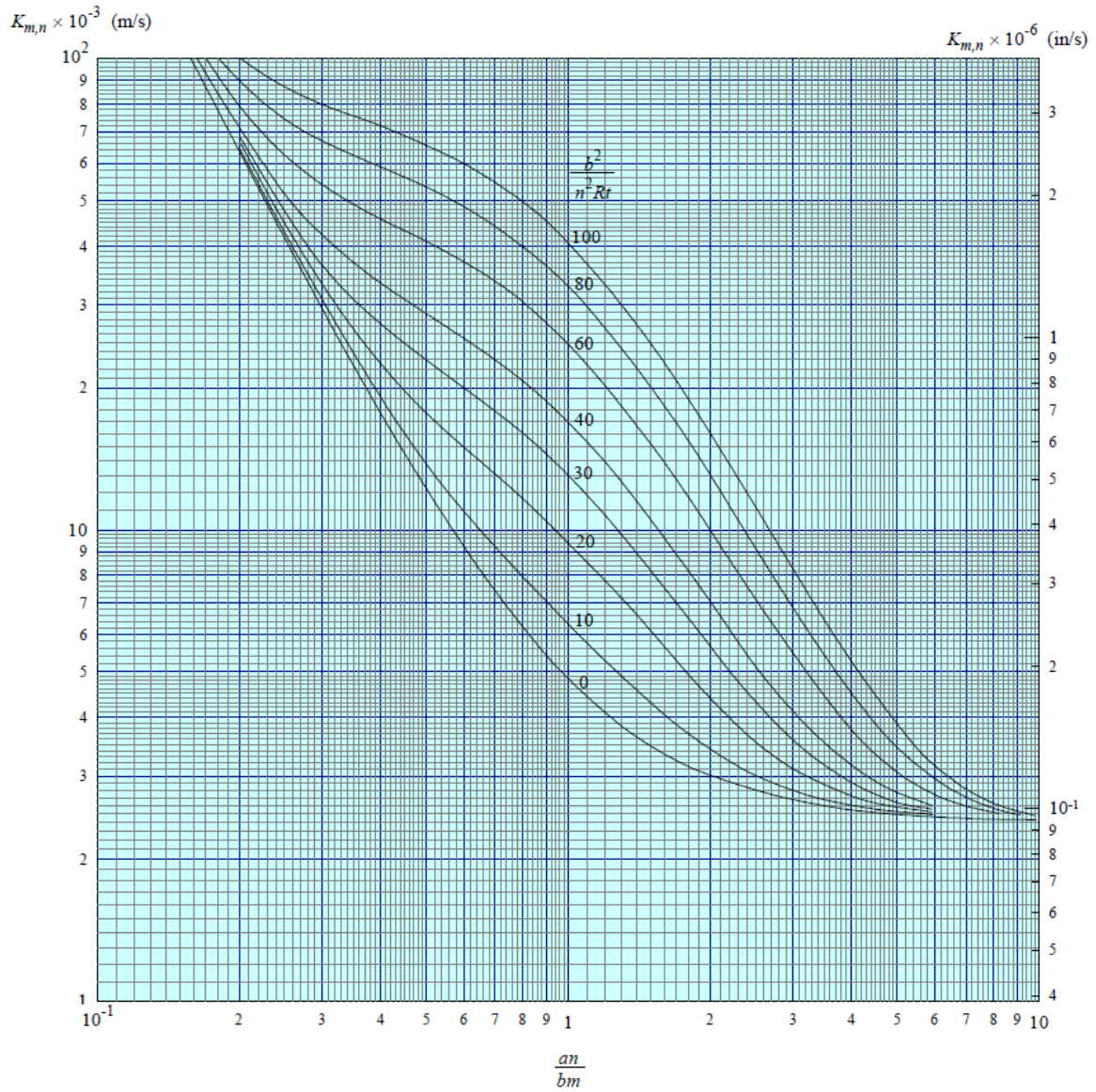


Figure 0.3. Frequency Parameter for Plates with all Edges Simply Supported [37]

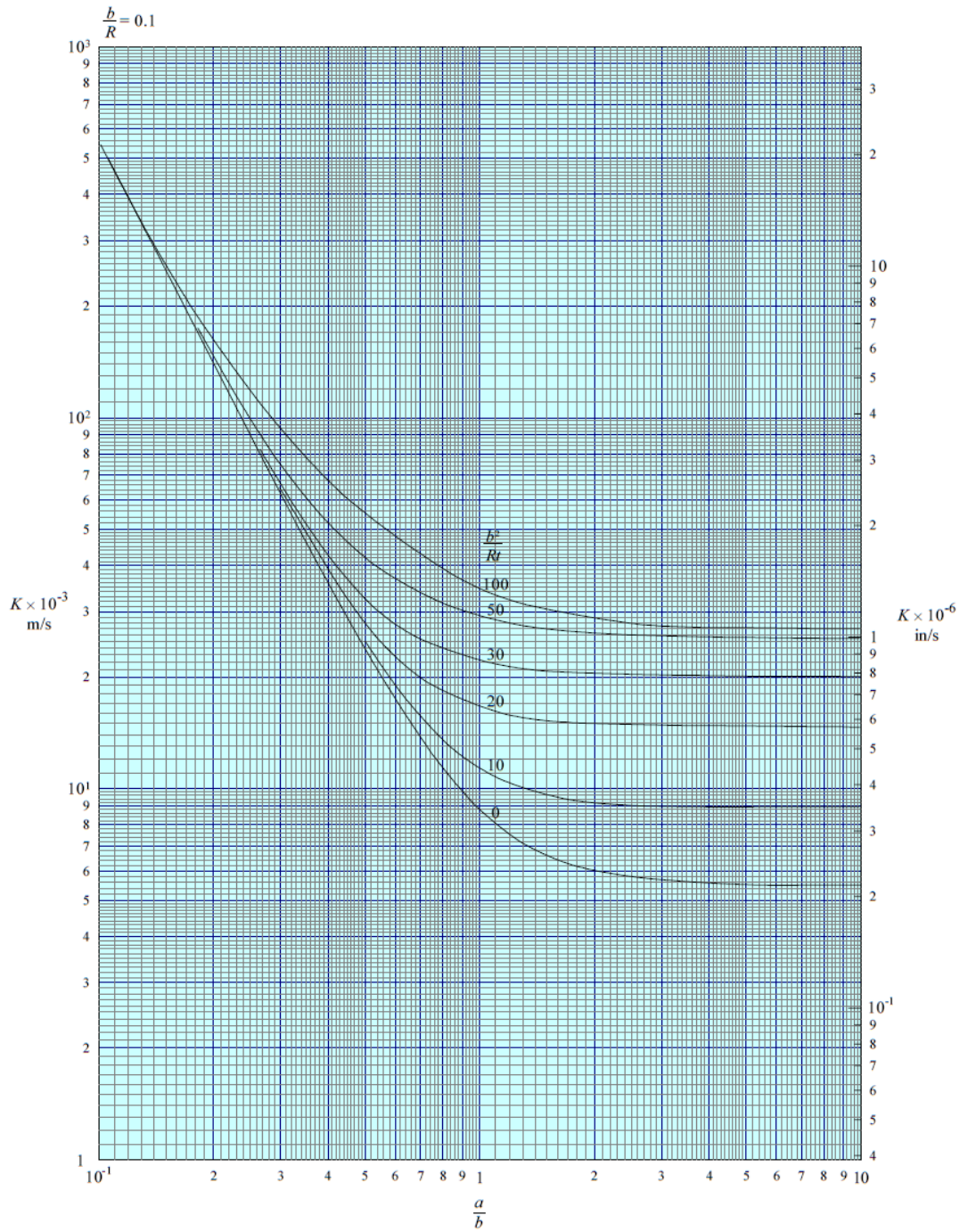


Figure 0.4. Frequency Parameter for First Symmetric – Symmetric Mode (Plates with all Edges Simply Fixed) [37]

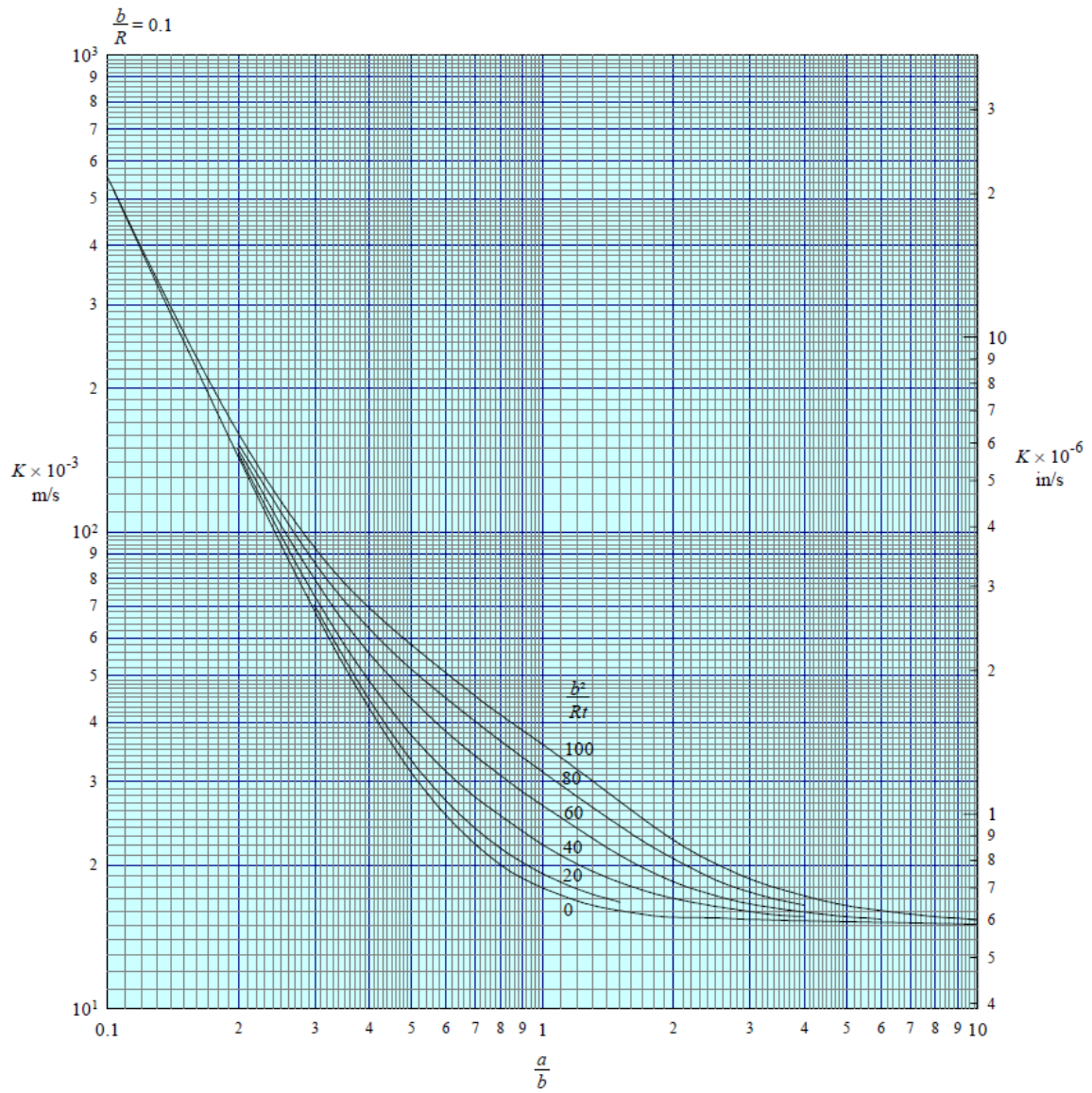


Figure 0.5. Frequency Parameter for First Symmetric – Antisymmetric Mode (Plates with all Edges Simply Fixed) [37]

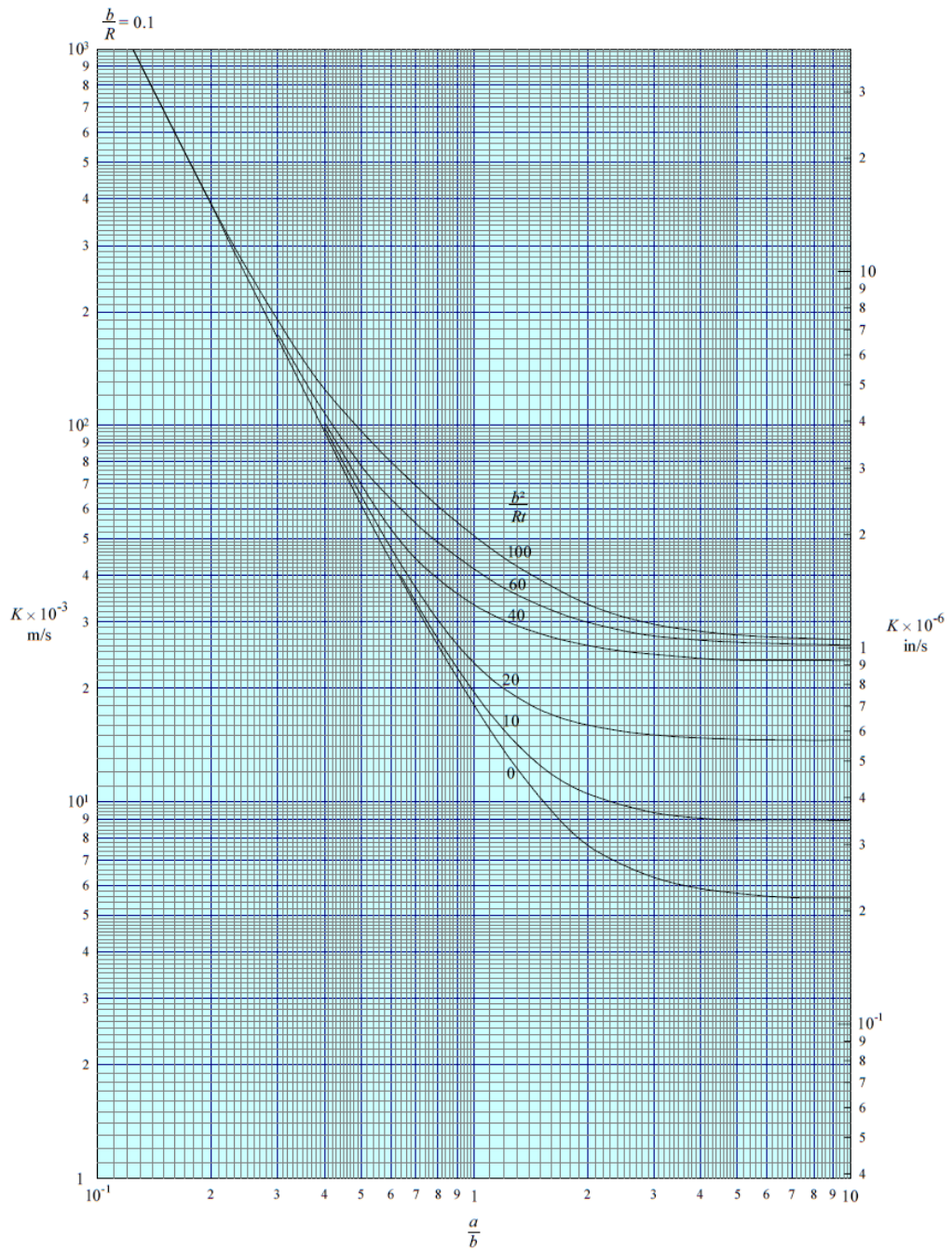


Figure 0.6. Frequency Parameter for First Antisymmetric- Symmetric Mode (Plates with all Edges Simply Fixed) [37]

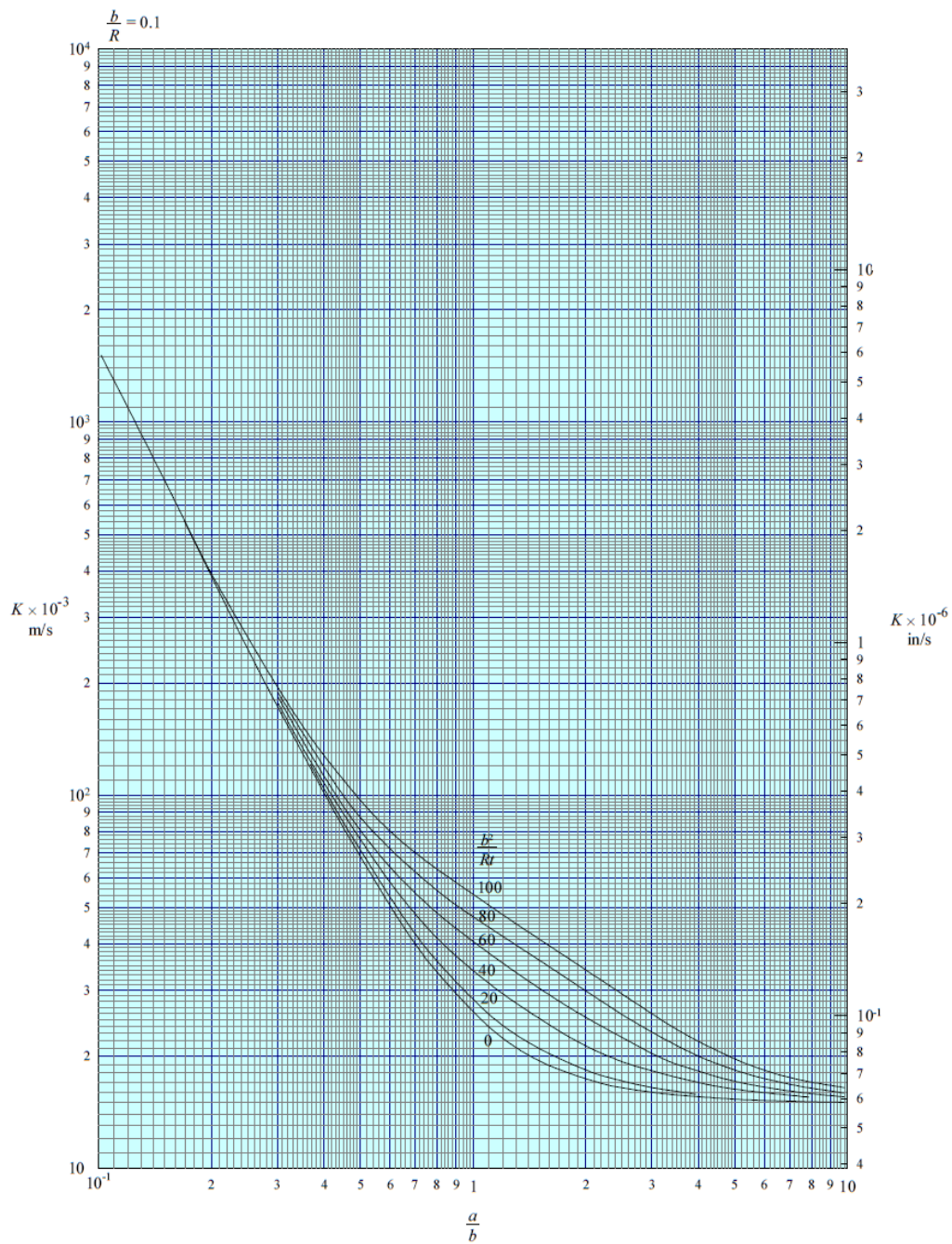


Figure 0.7. Frequency Parameter for First Antisymmetric- Antisymmetric Mode (Plates with all Edges Simply Fixed) [37]

E. Frequency Extraction FREQ*i* Cards of Nastran

Case 1

```
FREQ 1 .1 3000.  
FREQ5 1 .1 3000. 1.
```

Case 2

```
FREQ 1 .1 3000.  
FREQ3 1 .1 3000. LINEAR 5 2.
```

Case 3

```
FREQ 1 .1 3000.  
FREQ5 1 .1 3000. 1.  
FREQ3 1 .1 3000. LINEAR 100 1.
```

Case 4

```
FREQ 1 .1 3000.  
FREQ5 1 .1 3000. 1.  
FREQ3 1 .1 3000. LINEAR 100 1.  
FREQ 1 395. 840. 1340.
```

Case 5

```
FREQ 1 .1 3000. 395. 840. 1340.  
FREQ5 1 .1 3000. 1.  
FREQ3 1 .1 3000. LINEAR 100 1.  
FREQ1 1 .1 2.9999 1000
```